DOXORUBICIN LOADED POLYPHOSPHATE GLASS MICROSPHERES FOR TRANSARTERIAL CHEMOEMBOLIZATION

by

Hayden Peter Nix

Submitted in partial fulfilment of the requirements
for the degree of Master of Applied Science

at

Dalhousie University
Halifax, Nova Scotia
June 2018

DEDICATION

To Papa, Gramma Nix, Granddad, Uncle Paul, and Uncle Earl,

to all patients who have suffered from this devastating disease,

and to the loved ones of these patients.

Table of Contents

List of Tables

List of Figures

Abstract

Polyphosphate glass microspheres (PGM) are currently under development for application in transarterial chemoembolization (TACE), the standard of care treatment for intermediate stage hepatocellular carcinoma. PGMs are radiopaque, hemostatic, and resorbable. This thesis investigates the compatibility of doxorubicin (DOX), a chemotherapeutic, with this PGM system.

A process was developed to synthesize PGMs that were efficiently loaded with DOX, spherical in nature, and in the clinically relevant size range. DOX release and PGM degradation were assessed as a function of elution media pH, PGM composition, and %DOX loading. *In vitro* cytocompatibility of PGM degradation products and the pharmacological activity of released DOX were also evaluated.

Composition, therapeutic loading, and pH minimally affected PGM degradation. DOX release was mediated by eluant pH, and was highly linear while appearing to retain its pharmacological activity. However, PGM degradation products were also found to be cytotoxic. Overall, this PGM system shows promise as a TACE device.

List of Abbreviations Used

ABS	N-(2-acetamido)-2-aminoethanesulfonic acid buffered saline
ACES	N-(2-acetamido)-2-aminoethanesulfonic acid
ANOVA	analysis of variance
BCLC	Barcelona Clinic Liver Cancer
CCN	carboxymethyl chitosan
CMC	carboxymethyl cellulose
cTACE	conventional transarterial chemoembolization
ddH_2O	double deionized water
DEB-TACE	drug eluting bead transarterial chemoembolization
DOX	doxorubicin
D_p	degree of polymerization
EDTA	ethylenediaminetetraacetic acid
HCC	hepatocellular carcinoma
ICP-OES	inductively coupled plasma optical emission spectrometry
M^{2+}	divalent metal cation
MTT	3-(4,5-dimethylthiazol-2-yl)-2,5-diphenyltetrazolium bromide
NaPP	sodium polyphosphate
NMR	nuclear magnetic resonance
PBS	phosphate buffered saline
PCL	polycaprolactone
PDLLA	poly(D,L-lactic acid)
PEG	polyethylene glycol
PEGMA	poly(ethylene glycol) methacrylate
PGM	polyphosphate glass microsphere
PLGA	poly(lactide-co-glycolide)
PVA	polyvinyl alcohol
SEM	scanning electron microscopy
TACE	transarterial chemoembolization
TBS	tris(hydroxymethyl)aminomethane buffered saline

TGA-DSC	thermogravimetry/differential scanning calorimetry
tris	tris(hydroxymethyl)aminomethane
VEGF	vascular endothelial growth factor

Acknowledgements

Thank you, Dr. Mark Filiaggi. You took me on and guided me through these last two years. You gave me the freedom to grow as a student, and were always available when I needed guidance. I resisted for as long as I could, but you have finally succeeded in instilling me with a deep, monstrous craving for coffee, congratulations. Your somewhat begrudging, yet unfailing support of my career goals won't be forgotten. I'm sure that sentence made you roll your eyes.

An extra special thanks to Dr. Arash Momeni and Dr. Dan Chevrier. None of this would have been possible without your combined efforts. Arash, you welcomed me into the lab and introduced me to this wonderful world of PGMs, a world you somehow created. Dan, you helped me along every step of the way, taught me the importance of laughter in science, and made coming into the lab every day an incredibly enjoyable experience. Your 'Left or Right' record will never be broken. Imagine if we could all work on this project at the same time… we would be unstoppable.

To Dr. Alicia Oickle and everyone in the biomaterials lab, thank you for all of the instruction, advice, support, and baked goods you have provided. You made the lab a wonderful place to work.

Thank you Dr. Boyd, Dr. Gratzer, Dr. Abraham for you continued support over the course of this project, and for making committee meetings an enjoyable experience. Also, thank you to Dr. Brillant as well as all the staff, students and faculty of the School of Biomedical Engineering.

To my family, thank you for all the love and support throughout my education. You've given me every opportunity to succeed, and shown boundless belief in me. This would not have been possible without the foundation you provided.

Finally, what has Ellen Parker done for me anyway? Besides the countless double days, the introduction to the miracle of coffee, the large amount of emotional support (by any standard), The Puzzle (a true comedy of errors), the trip to Paradise Falls, convincing me (hypocritically) that breaks are a good thing, finally agreeing to watch Star Wars, the unconditional belief in me, and the provision of limitless inspiration and empathy, what did you really contribute?

Anywho, financial support provided by the Beatrice Hunter Cancer Research Institute, the Terry Fox Research Institute, and the Nova Scotia Health and Research Foundation is gratefully acknowledged for supporting this work

Chapter 1: Introduction

1.1 Hepatocellular Carcinoma

Worldwide, liver cancer is the sixth most common cancer and the second deadliest, accounting for 5.6% of new cancer cases and 9.1% of cancer related deaths in 2012 [1]. In 2012, there were an estimated 782,451 new cases of liver cancer and 745,533 deaths caused by the disease [2]. The disease affects men over twice as often as women and incidence rates vary by geographical region, with the highest rates occurring in Eastern and South-Eastern Asia [1]. The vast majority (75-90%) of primary liver cancer cases are hepatocellular carcinoma (HCC): malignant tumours originating from liver parenchymal cells [3]. The remainder of primary liver tumours originate in the cells lining the bile ducts, and are classified as intrahepatic cholangiocarcinoma [3]. Major risk factors for HCC include chronic hepatitis C virus and hepatitis B virus infections, ingestion of food contaminated with aflatoxin (a common toxin produced by fungi), fatty liver disease and lifestyle related factors (alcohol-induced cirrhosis, smoking, obesity, Type II diabetes) [4-6]. Socioeconomic status is thought to be a critical component of HCC risk, as countries with higher gross domestic products and human development indexes tend to have lower incidence and death rates from HCC [2].

Developed in 1999, the Barcelona Clinic Liver Cancer (BCLC) staging system is the most widely accepted criteria for staging HCC [7, 8]. Tumour staging is a means of ranking the spread of a tumour to predict patient prognosis and determine the best treatment option. This system ranks HCC tumours from ‘very early’ (Stage 0) to ‘terminal’ (Stage D) depending on a number of factors, including the number and size of the tumour nodules, the extent of portal vein invasion, and the impact on liver function [8]. ‘Very early’ stage tumours consist of a single nodule, less than 2cm in diameter; ‘early’ stage tumours are less than 3cm in total diameter and can consist of 1-3 nodules; ‘intermediate’ stage tumours are multinodular, but do not have a negative impact on liver function and have not invaded the portal vein; ‘advanced’ stage tumours are metastatic, negatively impact liver function, and have invaded the portal vein; ‘terminal’ tumours strongly inhibit normal liver function [7].

The treatment of HCC varies depending on the stage of the tumour at the time of diagnosis [9]. Very early and early stage tumours have the potential to be treated curatively. A variety of curative treatment options are available to clinicians, including resection of the tumour, liver transplantation, and radiofrequency ablation [7]. These curative treatment options are not viable for intermediate, advanced, or terminal stage tumours, and so these patients are given palliative care. The first-line treatment option for intermediate stage HCC is transarterial chemoembolization (TACE). The standard of care for advanced stage HCC is systemically administered sorafenib: an anti-angiogenic multikinase inhibitor that acts to inhibit the action of the vascular endothelial growth factor (VEGF) [7]. Terminal HCC treatment options are targeted exclusively at symptom management [7]. At the time of diagnosis, approximately 80% of HCC tumours are at the intermediated or advanced stage, making research into improving treatment options a high priority [10].

1.2 TRANSARTERIAL CHEMOEMBOLIZATION (TACE)

As noted, TACE is the standard of care for patients with intermediate stage HCC [7]. It is a procedure that involves the local delivery of both a chemotherapeutic and an embolic agent directly into the branches of the hepatic artery feeding the tumour. In conventional TACE (cTACE), the chemotherapeutic is delivered in an emulsion. This emulsion is commonly followed by the injection of embolic particles into the tumour's vasculature. More recently, drug-eluting beads have emerged as the preferred delivery vehicle for the chemotherapy; this procedure is known as drug eluting bead TACE (DEB-TACE) [11].

The liver, unlike most organs, has a dual blood supply. Left and right hepatic arteries provide oxygenated blood from the heart, while the portal vein carries blood from the digestive tract to the liver so that freshly absorbed compounds can be metabolized and detoxified as they enter the body. In a healthy liver, approximately 70% of the organ's oxygen is supplied by the arterial blood flow, with the remaining 30% coming from the portal circulation [12]. Interestingly, as HCC tumours progress in the liver, the process of angiogenesis results in the selective recruitment of vasculature from the arteries, meaning that the tumour's vasculature consists almost exclusively of branches of the hepatic artery

[13]. This pathology is exploited by embolic therapies that attempt to selectively block these blood vessels; theoretically, blocking flow to one branch of the hepatic artery will not completely starve the healthy parenchyma supplied by that artery, as it is receiving a supplemental supply of blood from the portal vein and collateral hepatic arteries.

1.2.1 Conventional Transarterial Chemoembolization (cTACE)

The first TACE protocol, now known as cTACE, involves the injection of chemotherapy and a contrast agent, followed by a second injection of embolic particles [14]. Before the procedure, patients undergo a hepatic artery angiogram to identify the branches of the artery that are feeding the tumour [9]. The clinician then guides a catheter to the distal segment of the identified hepatic artery branch and injects a water-in-oil emulsion intra-arterially. The water component is a mixture chemotherapeutic drugs in aqueous solution, while the oil component is lipiodol, an ethyl ester of iodized fatty acids [9]. A variety of chemotherapeutics are used, including doxorubicin (DOX), cisplatin, epirubicin, and mitomycin C, with no one drug showing a significant benefit over the others [15]. Lipiodol is highly viscous, and is sometimes used as the sole temporary embolic in the procedure, while acting as a radiopaque contrast agent [15]. After this injection, clinicians have the option to inject embolic particles to further embolize the artery [16]. Gelfoam, a biodegradable gelatin sponge particle that resorbs 1-3 weeks after injection, is the most commonly used embolic material in cTACE [15]. Evidence indicates that the additional embolic particles significantly increase tumour necrosis [14]. If no contraindications are present, clinicians commonly repeat the procedure 6-8 weeks after the first round [17].

While cTACE has been shown to have a significant benefit on HCC patient survival, is it a sub-optimal technique for a number of reasons. The depth of penetration into the artery and the quality of embolization are highly inconsistent when using the liquid water-in-oil emulsion [16, 18]. Further, lipiodol is very ineffective at trapping DOX within its matrix; an *in vitro* model demonstrated that when loaded with a therapeutic dose of DOX, half of the drug was released from the emulsion one hour after injection [19]. This is supported by clinical evidence indicating that DOX has the same pharmacokinetic profile whether administered via intravenous injection, or intra-arterially in a lipiodol emulsion

[20]. This translates to high levels of DOX in the systemic circulation that can cause serious side effects, the most severe of which is cardiotoxicity [20, 21]. Additionally, blebs of the lipiodol can break off and travel through the hepatopulmonary shunt, resulting in pulmonary embolization in patients [22]. The adverse effects associated with cTACE have motivated others to develop improved TACE treatment platforms.

1.2.2 Drug Eluting Bead Transarterial Chemoembolization (DEB-TACE)

DEB-TACE is a significant improvement over cTACE [23]. In this procedure, calibrated microspheres are loaded with chemotherapy and subsequently injected, along with an iodinated contrast agent, into the target hepatic artery branches. The beads occlude the blood vessel, and drug is subsequently released from the beads. The highly calibrated microspheres used in DEB-TACE result in more consistent embolization [24]. Compared to cTACE, DEB-TACE provides a far more favourable pharmacokinetic profile. The drug remains highly concentrated in the tumour bed while maintaining low concentration in the systemic circulation, significantly reducing DOX-associated side effects [25]. Correspondingly, DEB-TACE results in lower levels of liver toxicity, less severe systemic side effects, and increased tumour shrinkage relative to cTACE [23, 26, 27]. However, despite increasing tumour shrinkage, currently available evidence suggests that DEB-TACE offers no improvement over cTACE in terms of patient survival [28].

1.3 TACE DRUGS

A wide range of therapeutics have been assessed for their efficacy in TACE to treat HCC. A review of the literature was conducted by Marelli *et al.* in 2007, revealing that the most common chemotherapeutic cited was DOX, occurring in 36% of the identified publications [17]. Cisplatin and epirubicin followed DOX with 31% and 12% of publications, respectively [17]. More recent publications indicate that DOX continues to be the most popular drug for TACE targeting HCC [11]. DEB-TACE publications seem to have a similar focus on DOX, which is likely due to its use in the most widely available commercially available DEB-TACE platform: DC Beads^{TM}. There is increasing interest in the use of anti-angiogenic drugs for DEB-TACE due in large part to the finding that sorafenib is the only therapy to show a benefit to patients suffering from advanced stage

HCC; systemic sorafenib is currently the standard of care for these patients [7, 29]. Sorafenib is a logical choice for TACE considering hypoxia-induced angiogenesis that the treatment has been shown to initiate; inhibiting this process pharmacologically could drastically improve the efficacy of the embolization. However, the hydrophobicity of sorafenib has impeded its use in DEB TACE platforms, which are mostly anionic polymers. As such, DOX remains the most prevalent choice.

1.3.1 Doxorubicin

DOX is a small molecule anthracycline, derived from bacteria [30]. Its antineoplastic effects are thought to originate from several mechanisms of action: the intercalation of DNA, the inhibition of topoisomerase I and II, and the generation of free radicals [31]. Each of these mechanisms damages DNA, triggering cell death in dividing cells. The advantages of using DOX for the development of TACE platforms come from its known efficacy for treating HCC, its high water solubility, and easy detectability [32]. Aqueous solutions of DOX are red in colour, allowing the concentration of DOX in solution to be determined by UV/vis spectrophotometry at a wavelength of 488nm [33]. The hydrophilicity and cationic nature (at neutral pH) of DOX make it easy to load into a variety of microsphere compositions by immersing the beads into a DOX solution and allowing the DOX to be absorbed through ion exchange electrostatic interactions. This property has inspired the design of DEB-TACE platforms utilizing anionic polymer backbones, such as the carboxymethyl chitosan developed by the Golzarian group and that present in commercially available DC Beads, to facilitate this interaction [16, 34]. The water solubility also allows for favourable DOX release rates, as opposed to the extremely slow release observed with more hydrophobic, small molecule therapeutics such as cisplatin [35].

Despite these advantages, some questions remain regarding the stability of DOX. Kilcup *et al*. evaluated microspheres composed of polylactic-co-glycolic acid and zinc-silicate glass as DOX delivery vehicles for DEB-TACE [36]. They found that, although the loaded DOX was released and traceable using spectrophotometry, it failed to produce significant toxicity when tested on a HepG2 cell line [36]. This led the researchers to two possible conclusions: either the drug was damaged by the drug loading process, or it was

unstable in the aqueous elution media. DOX stability studies from the early 2000s seem to support the latter. Mayer, *et al*. showed that DOX in a normal saline solution at 37°C lost 13.1% of its concentration in 24 hours, and when incubated in a solution of saline and contrast agent, lost 60% of its concentration in 120 hours [37]. Chiadmi, *et al*. found that DOX in an aqueous solution lost 70% of its concentration when incubated at 40°C for 168 hours [38]. Based on these findings, it seems that the drug delivery vehicle may need to have protective properties in order to deliver a non-degraded drug at the time of elution. Speculatively, this instability may explain the lack of difference seen when comparing bland transarterial embolization to TACE in treating HCC [39].

1.4 Permanent Embolic Drug-Eluting Beads

All currently available DEB-TACE products are non-resorbable, meaning that the mass of the microspheres does not decrease over time [40]. Clinically approved products include the DC Bead™ (Biocompatibles UK), Hepasphere™ (Merit Medical, USA), Oncozene TANDEM™ (CeloNova BioSciences, USA), and Life Pearl™ (Terumo, Japan) [15]. DC Beads™ are the mostly widely used clinically, and the most prevalent in the literature [16].

Currently, the optimal DEB-TACE microsphere size is thought to be 100-300μm [9]. Examination of an explanted liver 8 hours after DEB-TACE with 100-300μm beads indicated that 42% of beads were occluding vessels within the tumour boundary [33]. Larger microspheres (300-500μm) limit the depth of penetration into the vessels being embolized [41], while smaller particles (<100μm) are associated with an increased risk of adverse effects because they are able to shunt through the tumour and injure the surrounding tissues or the lungs [42]. However, recent studies suggest that a smaller size range (70-150μm) may result in deeper, more homogeneous embolization with a limited increase in the risk of adverse effects [43-45].

1.4.1 DC Bead™ – Sulfonated Polyvinyl Alcohol

DC Beads™ are non-resorbable microspheres composed of polyvinyl alcohol-2-acrylamido-2-methylpropane sulfonic acid, an anionic polymer [19]. The negative charge on the polymer allows DOX (a cationic small molecule drug) to be loaded onto the beads

via ion exchange, as DOX displaces small cations from the bead matrix [19]. The beads are loaded with a maximum quantity 37.5mg_{DOX}/mL_{Bead} in the operating room shortly before use in the procedure (20-120 minutes, depending on the bead size) [16]. The beads are then injected into the patient along with a 50:50 saline:contrast agent mixture to provide radiopacity [16]. As with cTACE, clinicians commonly perform a repeat procedure 6-8 weeks after the initial treatment in which any patent blood vessels are identified and fortified with more drug eluting beads [16].

In vitro data indicates that DC Beads™ DOX release is characterized by an initial burst, in which half of the payload of drug is released within the first 7 days of elution, followed by a slower release thereafter [19]. The rapid release is, at least in part, due to the method of loading; DOX is unable to penetrate deeply into the polymer matrix [19]. This biphasic mechanism is supported by *in vivo* data. The concentration of DOX in human livers explanted 8 hours and 9 days after DEB-TACE were compared. Those explanted after 8 hours had significantly higher concentrations of DOX in the tissue surrounding the beads [33]. A study conducted in a porcine model showed that DOX continued to be released from the beads for at least 28 days, supporting the second, slower release phase [46].

A significant limitation of the DC Bead™ is their lack of radiopacity. The inability to image the beads after the contrast agent diffuses from the injection site compromises the clinician's ability to verify the location of the beads and the completeness of the embolization. Furthermore, it is difficult to follow-up on the strength of the embolization, and to target vessels that require additional embolization in subsequent procedures. To address these concerns, the DC Bead LUMI™ (Biocompatibles, UK) was developed. This was accomplished by coupling 2,3,5-triiodobenzaldehyde to the sulfonated polyvinyl alcohol (PVA) backbone of the original DC Bead™ [47]. This modification did not alter the DOX loading capacity but it did slightly slow the *in vitro* DOX release rate, presumably via increased hydrophobicity [47].

The permanent presence of these beads can have long-term consequences for patients. Inflammatory responses that result in the formation of a fibrous capsule around the beads can create a barrier to drug diffusion, although there is a chance this may also occur with degradable agents [48]. In addition, bead retention comes with a higher risk of

abscess formation [49]. Prolonged occlusion of the tumour's blood supply has also been shown to upregulate the expression of VEGF, a key growth factor associated with tumour growth and angiogenesis [50]. This mechanism is thought to contribute to high rates of tumour recurrence by selecting for hypoxia-resistant tumour cells [51]. Furthermore, patients are also found to benefit from multiple subsequent TACE procedures, as these help to combat recurrence and metastasis [16]. However, the administration of a second round of TACE is dependent on the patency of the blood vessels supplying the tumour [52]. Permanent embolic devices limit the availability of these arteries for subsequent treatments, reducing the maximum potential benefit patients can receive [52]. Patients would theoretically benefit most from an embolization that causes hypoxia for an optimal period of time that is long enough to cause ischemic necrosis of the tumour, but short enough not to trigger hypoxia-induced angiogenesis or result in an abscess. Permanent embolic devices are also inefficient at delivering their full payload of DOX to the tumour. An *in vivo* study demonstrated that DC Beads retained 11% of loaded DOX 90 days after injection [46]. These limitations have led to a growing interest in the field of bland resorbable embolics and resorbable drug eluting beads for application in cTACE and DEB-TACE, respectively.

1.5 Bland Resorbable Embolics

A variety of materials are being developed as bland resorbable embolic microspheres. These can be used in conjugation with delivery of unencapsulated drug, as has been the case with degradable starch microspheres, or can be used with no drug at all. Gelatin particles, commercially known as Gelfoam, are the current standard choice as an embolic agent for cTACE [15]. These particles are irregularly shaped, resulting in unpredictable depth of embolization [53]. The resorption time of Gelfoam is also unpredictable. The appeal of resorbable microspheres in cTACE is that they can be calibrated to a specific size range, and will have a more predictable resorption rate. The various materials being explored offer a range of degradation rates, though the optimal degradation rate has yet to be defined.

1.5.1 Degradable Starch Microspheres

Degradable starch microspheres are embolic agents that resorb very rapidly, on the order of 25-40 minutes [9]. These microspheres are not loaded with drug, but rather are injected intra-hepatically along with a chemotherapeutic of choice, with the goal of limiting washout of the chemotherapeutic in the brief period immediately after injection while allowing for repeat treatments [9]. Although this procedure has been deemed safe and efficacious, there is no existing evidence demonstrating that it is more efficacious than an intra-hepatic injection of chemotherapeutic alone [9, 54]. These spheres are generally thought to resorb too quickly, and fail to trap the drug in the tumour microenvironment.

1.5.2 Gelatin Microspheres

Gelatin microspheres made of the same material as Gelfoam are also being developed. They are spherical and have adjustable degradation profiles depending on the strength of the crosslinks used [55]. A biphasic degradation profile has been observed with these microspheres in the rabbit renal artery embolization model *in vivo*, with an initially high reperfusion rate 5 days after embolization followed by a drop in reperfusion rate 15 days after embolization [55]. This response was attributed to initial microsphere degradation, followed by an inflammatory reaction to the degradation products that resulted in the narrowing of the blood vessel lumen, which may limit the patency of the blood vessel, impeding access for repeat TACE procedures. This raises concerns about the biocompatibility of gelatin microspheres. This concern is potentially exacerbated by the fact that gelatin is commonly manufactured from bovine materials, creating the potential to transmit bovine spongiform encephalitis [56].

1.5.3 Additional Materials

In addition to these extensively characterized materials, a variety of other materials have been investigated as resorbable embolic microspheres. In vivo embolization of beagle renal arteries with human serum albumin microspheres was found to result in recanalization in one week [57]. Hydroxyethyl acrylate microspheres were found to exhibit a slower degradation rate in the same animal model, with recanalization occurring by 3-weeks post-embolization [57]. Chitosan, chitin, soluble PVA, and poly(lactide-co-glycolic

acid) (PLGA) have also been explored for this application [58, 59]. In a direct comparison, chitosan microspheres outperformed chitin and soluble PVA, leading to less collateral blood vessel formation, and resorbing in 24 weeks in vivo [58]. PLGA microspheres coated in type I bovine collagen were found to resorb remarkably slowly, maintaining full occlusion of a sheep uterine artery for 6 months, and finally leading to recanalization after 12 months [59]. The range of degradation rates observed in the materials studied demonstrates the uncertainty in the field regarding the optimal time of occlusion.

While the move to resorbable TACE platforms is likely to benefit patients, these resorbable bland embolic systems will do nothing to improve the pharmacokinetics of drug delivery. No matter the embolic material, cTACE will never be able to provide a slow, sustained delivery of chemotherapy, and patients will continue to suffer from adverse effects of having high systemic concentrations of drugs. For this reason, resorbable DEB-TACE platforms hold much more promise for the treatment of HCC.

1.6 Resorbable Drug Eluting Beads

Resorbable drug-eluting beads for application in DEB-TACE could ideally combine the benefits of transient embolization and that of local sustained drug release. In terms of drug delivery, the currently available non-resorbable drug-eluting beads exhibit incomplete release of their loaded drug, while resorbable beads are in theory able to release all loaded drug into the patient [60]. As mentioned above, resorbable beads have the potential to preserve hepatic artery patency, allowing for multiple subsequent procedures to be performed in accordance with ideal chemotherapy treatment schedules; oncologically, chemotherapy should be administered at 3-week intervals in order to fit with the cell cycle and prevent tumour repopulation [17]. This consideration, in combination with the advantages of resorbable embolization described above, has the potential to improve DEB-TACE efficacy and HCC patient outcomes. Resorbable DEBs hold much promise to address the shortcomings of permanent DEB-TACE platforms. A variety of materials with a variety of drugs are being explored for this application.

1.6.1 Poly(ethylene glycol) methacrylate

Microspheres composed of poly(ethylene glycol) methacrylate (PEGMA) crosslinked with PLGA-poly(ethylene glycol) (PEG) are being developed for applications in DEB-TACE [61, 62]. In vitro, these beads degrade in less than two days [63]. This is consistent with an in vivo study that demonstrated they were completely degraded 7-days after injection [61]. This material is highly cytocompatible; the hydrophilicity and small size of the degradation products limit the inflammatory reaction, and degradation is rapid enough that biological vessel occlusion does not occur [61]. Degradation products are hydrophilic and small enough to be excreted in urine [61, 64]. For angiographic detection, these microspheres must be suspended in a saline/contrast agent mixture before injection [61].

The beads have been loaded with DOX, irinotecan and the anti-angiogenic drugs suntinib and bevacizumab by soaking fully formed beads in drug solutions at pH 7 [61, 62, 65]. The hydrophilicity of the methacrylate component of the polymer makes these beads compatible with the hydrophilic drugs [61, 62]. Increasing methacrylic acid content in the polymer facilitates more efficient loading of cationic drugs (DOX, irinotecan, sunitinib), indicating that these drugs are loaded by electrostatic interactions [65]. A DOX loading efficiency of 95% was achieved with a load of $35mg_{DOX}/mL_{Beads}$; this is on the order of that achieved with DC Beads^{TM} [61]. However, DOX is released rapidly; 22% was released within the first 5 minutes of an in vitro study, and 81% by the 6-hour timepoint [61].

The pharmacological activity of released DOX has not been documented. However, the pharmacological activity of released sunitinib and bevacizumab were evaluated on a VX2 tumor cell line and human umbilical cord endothelial cells, respectively [62]. Each drug was found to have a significant effect on the cells relative to the bland degradation products and control phosphate buffered saline (PBS), indicating that the drugs the encapsulation and release process.

The main concern with this platform is the rapid rate of degradation and drug release. It is likely as well that the microspheres will degrade before substantial induction of ischemic necrosis. In addition, the extremely fast rate of drug release will likely result in very high systemic concentrations of the drug. The lack of radiopacity with this device also does nothing to improve the clinician's ability to visualize microspheres during or

after the embolization procedure. Proof of pharmacological viability of released DOX is another significant question with this platform.

1.6.2 Carboxymethyl Cellulose and Carboxymethyl Chitosan

The Golzarian research group has published several recent papers evaluating drug eluting beads composed of carboxymethyl cellulose (CMC) and carboxymethyl chitosan (CCN) for DEB-TACE applications. These microspheres must be injected with a contrast agent to be detectable by angiography [66]. Altering the crosslink density in these microspheres has been shown to greatly alter the degradation rate and drug release profile of the beads [34]. *In vitro*, the microspheres have been made that can resorb rapidly (100% mass loss in 15 days) or slowly (55% mass loss in 4 weeks) [34]. The bonds connecting the CMC to CCN are susceptible to hydrolysis, while CCN is cleaved by lysozymes; CMC chains are not degradable by mammalian enzymes [34]. Though an *in vivo* study was conducted, the *in vivo* degradation rate of these microspheres remains very unclear, and observed blood vessel damage supported concerns about biocompatibility [67].

These microspheres have been loaded with DOX by ion exchange. Here, fully formed microspheres are immersed in a solution of DOX, with DOX diffusing into the microspheres to form electrostatic interactions with the anionic carboxylated chitosan backbone [34]. The DOX is subsequently released by ion exchange, as the cations from the surrounding solution displace DOX from the polymer matrix [68]. DOX release is characterized by a large initial burst release, followed by a period of slower release as the polymer degrades [68]. While the mechanism of DOX loading and elution has been extensively characterized in several different publications, the pharmacological viability of the released drug has never been tested.

Overall, concerns with CMC/CNN as an embolics platform are centered around the biocompatibility of the degradation products, the lack of radiopacity, the poorly defined rate of in vivo degradation, and lack of evidence that the drug was not damaged through the process of loading and release.

1.6.3 Poly (D,L-Lactic Acid)

Wang *et al.* synthesized and characterized drug eluting microspheres composed of poly(D,L-lactic acid) (PDLLA) that have been loaded with cisplatin, sorafenib, or a combination of the two [35]. Though they consider these microspheres "biodegradable," this nomenclature is somewhat misleading, as they showed no appreciable weight loss after 3 months in an *in vitro* degradation study [35]. These microspheres are synthesized by an 'emulsion solvent evaporation' method in which PDLLA and the hydrophobic drug are dissolved in dichloromethane, an aqueous detergent is added, and the solution is subsequently stirred until the organic solvent evaporates [35]. This technique effectively creates pre-loaded microspheres at room temperature; the loaded drugs are exposed to inorganic solvents, but not to high temperatures which would accelerate their degradation. This technique yielded high encapsulation efficiency for sorafenib (94.2%), but a significant amount of cisplatin was lost during the synthesis process (25.7%) [35].

The *in vitro* release profiles of both drugs exhibited a burst release on the first day, followed by a slower release thereafter. Decreasing the pH from 7.4 to 6.0 did not alter cisplatin release, while sorafenib release was accelerated. This observation suggests that cisplatin is released via simple diffusion and sorafenib by ion exchange [35]. The pharmacological viability of released drug was tested on culture cells *in vitro*. Released cisplatin demonstrated no significant cytotoxicity, while released sorafenib was found to have anti-angiogenic effects. The inactivity of cisplatin highlights the need to evaluate pharmacological viability of eluted drug.

This platform is intriguing because it can be pre-loaded with non-ionic drugs including sorafenib, a drug known to be effective in treating advanced stage HCC. The finding that this drug maintains viability after loading and release is also very promising. In addition, the pre-loading of microspheres eliminates the loading step that takes place in the operating room immediately before the embolization procedure. However, the critical flaw with this material is the lack of degradability.

1.6.4 Poly(lactic-co-glycolic acid)

PLGA microspheres have been loaded with DOX and sorafenib with the intended application of DEB-TACE [69, 70]. PLGA is a hydrophobic polymer, making loading with

DOX difficult. A solid-in-oil-in-water technique involving exposing encapsulated (heat sensitive) DOX to 70°C heat for 3 hours was used, and resulted in an encapsulation efficiency of only 50.25% [69]. The synthesized microspheres were much smaller than the clinically relevant size, with a mean diameter of 26μm [69]. *In vitro*, DOX was released rapidly over the first 3 days at pH 7.4, 6.8, and 5.5, with more acidic pH significantly accelerating release [69]. Degradation was much slower than DOX release, with only a 20.2% drop in mean bead diameter in 2 weeks. DOX viability was not tested *in vitro*, and an *in vivo* study demonstrated no significant decrease in tumour size when comparing DOX-loaded and bland embolization in a rat liver cancer model [69].

PLGA microspheres have also been loaded with sorafenib, along with iron oxide to create an MRI-imagable DEB-TACE platform [70]. Sorafenib is a hydrophobic drug, and is therefore much easier to load into PLGA. This was accomplished by a double oil-in-water emulsion technique at room temperature, yielding a loading efficiency of 87.7% [70]. Synthesized microspheres had an average size of 13μm [70]. The degradation rate of these microspheres was not assessed. The *in vitro* release profile of sorafenib was biphasic, with 12% of loaded sorafenib released within 24 hours and a slower release thereafter [70]. Pharmacological activity of release sorafenib was tested *in vivo* in a rabbit VX2 tumour model, for which significantly less microvasculature development in the tissue surrounding sorafenib-loaded microspheres was observed relative to bland microspheres, suggesting that the drug was active upon release [70].

Like PDLLA, the ability to load and release active sorafenib is an exciting development for DEB-TACE. However, this platform is relatively incompatible with DOX, and the apparently very slow degradation rate may be problematic for DEB-TACE. The issue of induced angiogenesis could be countered by the sustained release of sorafenib, but other concerns about abscess formation and subsequent, limited access for repeat procedures still exists.

1.7 Polyphosphate Glass Microspheres

Polyphosphate glass microspheres (PGM) are being developed by the Filiaggi group as a radiopaque, hemostatic, and degradable drug release platform for DEB-TACE. Here, ‘degradable’ is defined as the susceptibility to hydrolytic and enzymatic cleavage of

the chemical bonds, which will theoretically result in the removal of the substance from the body [71]. Polyphosphates are linear, inorganic polymers formed by phosphate groups linked together by bridging oxygen atoms [72]. Making PGMs out of this polymer initially involves the dissolution of sodium polyphosphate (NaPP) into water, followed by the addition of divalent cations; these cations result in the precipitation of a colloid-rich viscous liquid phase, referred to as a coacervate [73]. PGMs are formed from the resulting coacervate using a low temperature water-in-oil emulsion technique.

Using barium, copper and calcium, a compositional range that yields a coacervate with the ability to form PGMs has been identified. To be successfully converted into PGMs via the water-in-oil emulsion technique that has been developed in the Filiaggi lab, the coacervate must have a low enough viscosity to be injected through a 16-gauge needle, and be sufficiently hydrophilic to be incorporated in the water-Span80 micro-emulsions. Coacervate properties are determined by the relative amounts of barium, calcium and copper cations incorporated into the polymer matrix [73]. Barium in particular contributes radiopacity while also possibly slowing the resorption of the PGMs [74]. Similar effects on degradation have been observed with alginate-based coacervates [75]. When only barium is added to the sodium polyphosphate solution, the precipitate is a flocculent: a hard solid exhibiting no flow [73]. Calcium and copper are therefore added to facilitate precipitation of a coacervate. Higher calcium levels tend to yield more viscous coacervates, while increasing the copper concentration tends to reduce the overall coacervate viscosity [73].

PGMs are readily converted to coacervate upon contact with an aqueous environment, and the degradation and resorption of coacervate has been well characterized. Momeni *et al.* found that the degree of polymerization of the polyphosphate chain has very little effect on coacervate resorption rate [74]. Coacervates tend to be stable in aqueous solutions for approximately 48 hours; during this time, it appears that chain scission is occurring but minimal products are released into solution. From 48-168 hours, the products of degradation are released from the coacervate rapidly, and degradation then slows after 1 week [74]. Barium is thought to slow this release, based on the finding that it tends to remain in the coacervate over the degradation period; pyrophosphates, orthophosphates, calcium and copper are released more quickly [74]. An unpublished *in vitro* degradation

study demonstrated that PGMs in this compositional range lose approximately 70% mass in 21 days.

PGMs have the capacity to act as drug delivery vehicles. Previously, calcium polyphosphate glass microspheres were loaded with the antibiotic minocycline [76]. This was accomplished using a low temperature technique in which the coacervate was freeze-dried and subsequently rehydrated with an aqueous drug solution before introduction into the water-in-oil emulsion. The rehydration process effectively transported the minocycline into the coacervate, achieving an encapsulation efficiency of 72.7% [76]. Minocycline is chemically similar to DOX in that it possesses an amine group, making it cationic at neutral pH, and aromatic rings that make it detectable using spectrophotometry; spectrophotometry was therefore used to determine the encapsulation efficiency of the process. Minocycline is susceptible to hydrolytic degradation in aqueous solution, which is characterized by a colour shift from yellow to brown. When encapsulated in PGMs, this colour change did not occur. This finding suggests that PGMs may offer a protective environment for encapsulated drugs. Elution studies revealed that approximately 70% of the drug was released from the coacervate after 7 days of elution in tris-buffer solution, with an initial linear portion over the first 48 hours followed by a gradually decreasing rate from 48 to 168 hours [76].

These results show great potential for PGMs to be developed as a DEB-TACE platform. The compatibility of the system with minocycline suggests that DOX loading and release will be achievable, given the similarity in molecular structure. The low temperature required for drug loading and PGM synthesis techniques should minimize DOX exposure to potentially degradative high temperatures. The capacity to store and protect drug, along with the resorbability, radiopacity, and hemostatic properties of PGMs make them a very promising potential DEB-TACE platform.

This thesis evaluates the capacity of PGMs to be used for DEB-TACE. A process was developed to synthesize DOX-loaded PGMs. The processing conditions were then optimized to yield spherical particles in the clinically relevant (100-300μm) size range. The interaction between DOX and the polymer matrix was then characterized, with emphasis on the endpoints of DOX release and polymer degradation. Finally, the pharmacological activity of released DOX was evaluated *in vitro*.

1.8 Summary and Conclusions

HCC is a prevalent and deadly form of cancer, in large part due to the late stage of diagnosis. While a number of palliative treatment options are available to patients with intermediate HCC, there is a need to advance these technologies to improve patient survival and lessen adverse effects. cTACE involves the intra-arterial injection of chemotherapy in a water-in-oil emulsion, leading to uncontrolled diffusion of the drug and harmful drug-related adverse effects. DEB-TACE offers some improvement over this technique, as the chemotherapeutic is encapsulated into drug eluting embolic beads, leading to a slower, sustained release and a more favourable side effect profile.

All current and clinically available DEB-TACE platforms are non-resorbable, which interferes with subsequent repeat chemoembolization procedures and can cause long-term occlusion, upregulating tumor angiogenesis. Additionally, most clinically available technologies lack intrinsic radiopacity; they must be suspended in contrast material before injection. This allows for detection of blood flow during the procedure, but make the beads undetectable in follow-up imaging.

PGMs have great potential to improve upon these technologies. PGMs are resorbable, allowing for restoration of hepatic artery patency for easy access for subsequent treatments. PGMs are intrinsically radiopaque, eliminating the need for contrast media and allowing for follow-up imaging post-implantation. PGMs are actively hemostatic, which has the potential to limit bead migration after injection, maintain local delivery of the eluting drug, and create an ischemic environment for the tumour. The next step in the development of PGMs as a DEB-TACE platform is to evaluate their capacity for chemotherapeutic drug loading and elution. The anionic polyphosphate backbone will likely be compatible with DOX loading, and may provide the drug with a protective environment to prevent degradation. This project will determine PGM's capacity to act as a drug delivery vehicle for pharmacologically active DOX, with the intended application of DEB-TACE.

Chapter 2: Research Objective and Hypotheses

OBJECTIVE 2.1: SYNTHESIZE AND CHARACTERIZE DOXORUBICIN-LOADED POLYPHOSPHATE GLASS MICROSPHERES

Two compositions of PGMs loaded with 1% (w/w) DOX were synthesized. Processing conditions were optimized to yield spherical particles in the clinically relevant size range (100-300μm) with high drug encapsulation efficiency. PGM morphology, size, and chemical composition were assessed.

Hypothesis 2.1.1: Doxorubicin-loaded coacervate will maintain the appropriate viscosity to form spherical, 100-300μm polyphosphate glass microspheres using the water-in-oil emulsion technique

Based on previous success by the Filiaggi group in loading calcium polyphosphate coacervate with minocycline, the addition of DOX was not expected to alter coacervate viscosity significantly enough to make it incompatible with the water-in-oil emulsion technique.

Hypothesis 2.1.2: Doxorubicin-loading will displace divalent metal cations from the coacervate, thereby altering the chemical composition of the polyphosphate glass microspheres

DOX is loaded into the majority of currently available drug eluting beads (DEBs) via ion exchange. Therefore, DOX was expected to be incorporated into the coacervate matrix by electrostatic interactions, displacing divalent cations (Ba^{2+}, Ca^{2+}, or Cu^{2+}) and thereby altering the chemical composition.

Hypothesis 2.1.3: The effects of doxorubicin loading on chemical composition and coacervate properties will vary with polyphosphate glass microsphere composition

Stemming from the hypothesis that DOX would undergo electrostatic and ion exchange interactions with the coacervate, the extent of the effects caused by DOX loading were expected to depend on the chemical composition of the coacervate. Two compositions of coacervate were evaluated.

OBJECTIVE 2.2: QUANTIFY *IN VITRO* DOXORUBICIN RELEASE AND POLYPHOSPHATE GLASS MICROSPHERE DEGRADATION

The *in vitro* degradation rate of PGMs was investigated, specifically evaluating the effects of pH, PGM chemical composition, and DOX-loading. The mechanism of DOX release was investigated *in vitro* by evaluating the effects of elution media pH and PGM chemical composition.

Hypothesis 2.2.1: Doxorubicin-loading will not alter the in vitro degradation rate of polyphosphate glass microspheres

Previous, unpublished data indicated that substantial differences in PGM chemical composition are required to alter the *in vitro* degradation rate. Therefore, it was expected that the relatively small alterations in PGM chemical composition caused by DOX loading would have minimal effect on their degradation.

Hypothesis 2.2.2: Doxorubicin release will be commensurate with PGM degradation

Previous work with calcium polyphosphate glass microspheres loaded with minocycline demonstrated a rapid release of drug over the first several days *in vitro*, followed by a slower release phase. Given the similar chemical structure of DOX and minocycline, a similar release profile was expected.

Hypothesis 2.2.3: Degradation, and therefore drug release rate, are pH-dependent

It is widely known that pH accelerates the degradation of polyphosphates; PGMs were expected to behave the same way. Stemming from the hypothesis that DOX release will be commensurate PGM resorption, it was expected that decreasing the pH of the elution media would accelerate degradation and therefore drug release.

OBJECTIVE 2.3: EVALUATE THE PHARMACOLOGICAL VIABILITY OF RELEASED DOXORUBICIN

Concerns surrounding the stability of DOX in aqueous solution exist in the literature. These concerns, along with the potential that the drug could be damaged during the loading and synthesis process, necessitated the evaluation of DOX cytotoxicity after it was released from the loaded PGMs. Additionally, the cytocompatibility of the degradation products was evaluated *in vitro*.

Hypothesis 2.3.1: Doxorubicin released from loaded polyphosphate glass microspheres will retain its pharmacological activity

Minocycline is a small molecule drug of similar structure to DOX, and is susceptible to hydrolytic degradation. The degradation is visible via a colour change from yellow to brown. When encapsulated into calcium polyphosphate glass microspheres, minocycline maintained its yellow colour over a long storage period. It was expected that DOX viability would be protected by the same mechanisms.

Hypothesis 2.3.2: Polyphosphate glass microsphere degradation products will be cytocompatible

Previous work done with *in situ* forming embolic composed of polyphosphates, Ca^{2+}, Ba^{2+}, and Sr^{2+} demonstrated cytocompatibility in a rabbit model for embolization. Based on this data, PGM degradation products were expected to be minimally cytotoxic.

Chapter 3: Process Development and Characterization

3.1 Introduction

Beads must meet a number of design criteria for application in DEB-TACE. Currently, the most commonly used size range is 100-300μm [16]. Beads must be sufficiently spherical to be injected through a microcatheter as irregularly shaped particles can lead to blockages. Given that patients tend to undergo subsequent rounds of DEB-TACE procedures at approximately 6-8 week intervals, key opinion leaders in the field have identified 4-6 weeks as the targeted time frame for bead degradation, although this is still debated [16]. In addition to these criteria, beads possessing innate radiopacity are very desirable for DEB-TACE. The currently used 50:50 contrast/saline mixture achieves a radiopacity of 2455 HU when imaged at 120kVp; this is the targeted minimum threshold for bead radiopacity [36]. From a drug release perspective, patients would benefit from a sustained release of DOX over the full 4-week period until the next round of treatment is given. Loading DOX into the surface of beads right before the procedure is performed inevitably releases DOX too rapidly; beads that can be synthesized with DOX embedded deep within the polymer matrix have the potential to yield a sustained release profile. The creation of beads that meet these design criteria has potential to greatly improve outcomes for patients suffering from intermediate stage HCC.

Prior to this thesis project, a study was conducted by others in the Filiaggi group to identify the compositional range of the NaPP - Ca^{2+} - Ba^{2+} - Cu^{2+} system that could be used to yield PGMs through a water-in-oil emulsion technique. NaPP in aqueous solution was precipitated through the addition of divalent metal cations (M^{2+}): Ca^{2+}, Ba^{2+}, and Cu^{2+}. Compositions with high Ba^{2+} content precipitated as flocculent, a solid phase exhibiting no flow. These compositions are incompatible with a water-in-oil emulsion technique requiring a coacervate, or colloid-rich liquid phase, with a low enough viscosity to be injected through an 18-gauge needle and be emulsified by mixing speeds of approximately 1000rpm. A compositional range that precipitated coacervate was identified. These coacervates were then processed into PGMs and characterized.

This prior study then evaluated radiopacity and degradation rate of the different compositions, using Design-Expert software to identify the optimal composition *(highest radiopacity and mass loss)*. From this work, two compositions of PGM were selected for

this thesis work (Table 3.1). Termed “Barry” and “Calvin” to distinguish their relatively higher levels of barium and calcium, these PGMs exhibited radiopacity values of 7806 ± 169 HFU and 6610.5 ± 197 HFU, respectively, when imaged at 120kVp, significantly more radiopaque than the 50:50 lipiodol/saline mixture used in TACE procedures. This is highly relevant for DEB-TACE applications, as it will allow for the microspheres to be imaged during and after injection into the patient.

This initial degradation study indicated that Barry seemed to degrade more rapidly than Calvin, presumably because of its high copper content, although not significantly so. Clinically, there is significant uncertainty surrounding the optimal degradation rate for resorbable DEB-TACE. Thus, the potential to synthesize DOX-loaded PGMs with a range of degradation rates is favourable. In addition to this design criterion, the differences in viscosity and chemical composition between these two compositions were beneficial to help elucidate the effects and mechanisms of drug loading and release.

Table 3.1 The theoretical compositions of Barry and Calvin

Composition	Ba^{2+}/P (%)	Ca^{2+}/P (%)	Cu^{2+}/P (%)
Barry	14	1	35
Calvin	10	13	27

Chapter 3 presents the development of optimized protocols for synthesizing DOX-loaded PGMs that are spherical and in the clinically relevant size range using both coacervate compositions. Hypotheses 2.1.1 and 2.1.3 were addressed through a process of creating a DOX loading procedure, and manipulating the emulsion parameters to best match the properties of the DOX-loaded coacervate. Differences in the optimized loading procedure and emulsion conditions between the two compositions provided insights into the PGM system, addressing Hypothesis 2.1.3. The mechanism of DOX loading was evaluated in a composition study to address Hypothesis 2.1.2.

3.2 MATERIALS AND METHODS

3.2.1 Sodium Polyphosphate Glass Synthesis

120g sodium phosphate monobasic monohydrate ($NaH_2PO_4 \cdot H_2O$; Sigma Aldrich) and 3.28g sodium carbonate (Na_2CO_3; Sigma Aldrich) were mixed to create a Na/P molar ratio of 1.07. The powders were mixed overnight. The mixture was heated in a Thermolyne Type 46200 High Temperature Furnace in a platinum-5% gold crucible from 25°C to 900°C over a 90-minute period, maintained at 900°C for 4 hours, then subsequently quenched on a copper plate. The copper plate was cleaned prior to use with a combination of sodium chloride salt and acetic acid. The NaPP glass was then manually crushed using a custom machined tool, transferred into sintered corundum aluminum oxide grinding bowls, and ground into a powder using a Planetary Micro Mill Pulverisette 7 (Laval Lab Inc.) to ease its dissolution in water during coacervate synthesis.

Degree of Polymerization (Dp)

The D_p was evaluated using liquid ^{31}P nuclear magnetic resonance (NMR). Three independent melts were analyzed. 100mg of NaPP glass was dissolved in 1mL of double deionized water (ddH_2O). 0.9mL was transferred into a liquid NMR test tube, and 0.1mL D_2O was added to the tube. The sample was analyzed by a Bruker AV 300 MHz NMR spectrometer at 101.26 MHz with an acquisition time of 0.8s, a 7.0s repetition rate and 128 scans. Spectra were reported with the d-scale. Peaks around -5ppm and -21ppm represent Q^1 (end of chain phosphorus atoms) and Q^2 (mid-chain phosphorus atoms), respectively [77]. The degree of polymerization was determined based on the area under these peaks, calculated according to Equation 3.1 [74]:

$$D_p = [2 \times (Q^1 + Q^2)] / Q^1 \qquad \text{(Eq. 3.1)}$$

3.2.2 Coacervate Synthesis

Coacervate is composed of polyphosphate chains bound and cross-linked by M^{2+}. To synthesize coacervate, NaPP was dissolved in ddH_2O at a concentration of 1g/L, mixing at 400-500rpm. 1M solutions of Ba^{2+}, Ca^{2+}, and Cu^{2+} were obtained from barium chloride dihydrate ($BaCl_2 \cdot (H_2O)_2$; Sigma Aldrich), calcium chloride dihydrate ($CaCl_2 \cdot (H_2O)_2$; Sigma Aldrich), and copper (II) chloride dihydrate ($CuCl_2 \cdot (H_2O)_2$; Alfa Aesar),

respectively. Specific quantities of the Ba^{2+}, Ca^{2+}, and Cu^{2+} solutions were sequentially added to the NaPP solution until a 0.5 M^{2+}/P molar ratio was reached; volumes depended on the composition being synthesized (Table 3.2). Ba^{2+} was always added first, followed by Ca^{2+}, and then Cu^{2+}. Ba^{2+} and Ca^{2+} solutions were added in aliquots, with volumes no larger than 4mL at a time. After each aliquot, the precipitate was given time to dissolve before the next aliquot was added. Cu^{2+} volumes were added all at once, reaching the 0.5 M^{2+}/P molar ratio, after which point the solution was mixed for 5 minutes. The coacervate subsequently precipitated out of solution and was allowed to settle on the bottom of the beaker. It was washed thrice with double deionized water to remove any excess M^{2+} adherent to its surface and then collected into an Eppendorf tube.

Table 3.2. Coacervate synthesis procedure for each composition

Composition	Mass NaPP (g)	Volume 1M Ba^{2+} (mL)	Volume 1M Ca^{2+} (mL)	Volume 1M Cu^{2+} (mL)	Coacervate Yield (mL)
Calvin	10	10	13	27	3
Barry	8	11.2	0.8	28	1

Coacervate Characterization

The chemical composition and water content of Barry and Calvin coacervates were characterized. To assess chemical composition, portions (~10mg) of each coacervate were transferred into 15mL Falcon tubes. The coacervate was then dissolved in 10mL 2% hydrochloric acid (HCl; Sigma Aldrich). Dissolved samples were subsequently analyzed with inductively coupled plasma optical emission spectrometry (ICP-OES) for Ba, Ca, Cu, and P concentrations. Standards containing 20ppm, 2.0ppm, 0.2ppm, and 0ppm of each element dissolved in 2% HCl were created. Ba, Ca, Cu and P peak emissions were measured at 233.527nm, 317.933nm, 327.393nm, and 213.617nm, respectively. A standard curve with an R^2 value greater than 0.9999 was obtained in each case. The M^{2+}/P molar ratios were calculated and compared (n=6), and averages with standard deviations were determined.

To analyze the water content of each composition, coacervate was synthesized as described above. 1mL of coacervate was transferred into a vial of known mass, weighed, frozen overnight, and freeze-dried for 8 hours (n = 12). The coacervate was weighed again after freeze-drying, and the difference in mass was calculated; this value represented the mass of water removed by freeze-drying. This mass was then divided by the initial mass of the coacervate to determine the water content of the coacervate, expressed as a mass percentage. The difference in water content between compositions was analyzed statistically using a Student's t-test. The threshold for significance was $p < 0.05$.

3.2.3 Doxorubicin Loading

Loading Protocol

The coacervate was loaded with DOX via a process in which the coacervate is dehydrated and then subsequently rehydrated with aqueous DOX solution. This process will be referred to as *reconstitution*. Following coacervate synthesis, 1mL was transferred into a vial of known mass. The mass of the coacervate was measured, then freeze-dried and reweighed (as described above), ground with a mortar and pestle, and transferred back into its vial. The resulting powder was spread across the bottom of the vial to maximize surface area. An aqueous DOX solution, equal in volume to the amount of water lost during freeze-drying, was then added dropwise to the dry coacervate powder. Care was taken to ensure the solution was distributed across the layer of powder. The vial was stored at 4°C during the reconstitution period. DOX was loaded at one of two quantities: for 1% (w/w) DOX loading, 10mg DOX was dissolved in the volume of water lost during freeze-drying; for 0.5% (w/w) DOX loading, 5mg DOX was dissolved. Note that these 1% and 0.5% designations represent theoretical DOX loads, based on the approximation that 1mL coacervate yields approximately 1g of PGMs.

Coacervate Encapsulation Efficiency

DOX that was not encapsulated into the coacervate matrix during reconstitution was quantified. 1mL Barry and Calvin coacervates were freeze-dried and reconstituted with 10mg of DOX (n = 5). At the end of the reconstitution period, coacervate was washed with 2mL ddH_2O and the wash solution collected. Wash solution was pipetted into a 96-

well plate (200µL per well, 3 wells per sample). To measure baseline absorbance, ddH_2O pipetted into wells of the 96-well plate being measured (200µL per well, 5 wells per sample). The 480nm absorbance of each sample was measured using a plate reader, and the average absorbance was calculated. The average absorbance from the water reading was treated as a baseline, and was subtracted from the sample average absorbance readings. The concentration of DOX was calculated from the absorbance values based on a DOX standard curve (Figure 3.1). DOX standards were created by dissolving 10mg of DOX in 100mL ddH_2O (0.1mg/mL), and serial diluting that solution to 0.05mg/mL, 0.01mg/mL, and 0.001mg/mL. Encapsulation efficiency was then calculated according to Equation 3.2 where $DOX_{Initial}$ is the mass of DOX originally added to the coacervate, and DOX_{wash} is the mass of DOX present in the wash solution. A Student's t-test was used to quantify differences between compositions. The threshold for significance was set at $p < 0.05$.

$$\text{Coacervate Encapsulation Efficiency} = [(DOX_{Initial} - DOX_{wash})/DOX_{Initial}] \times 100\% \quad \text{(Eq. 3.2)}$$

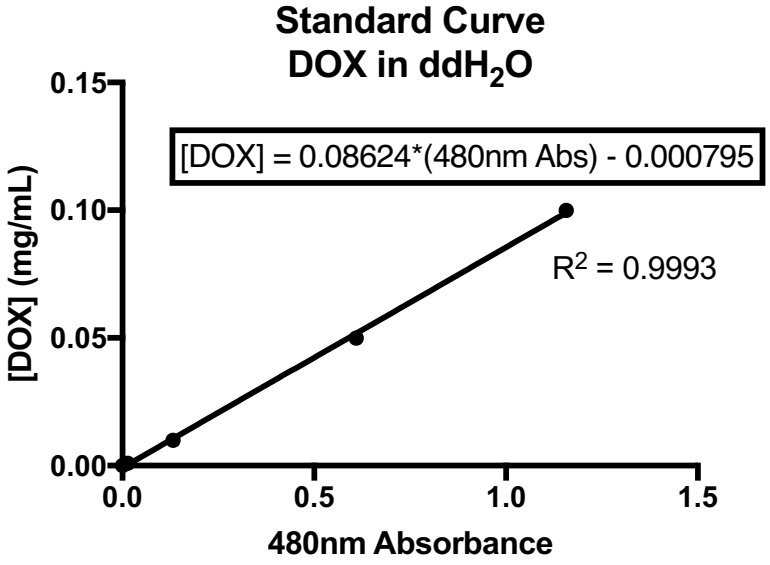

Figure 3.1 Standard Curve of DOX dissolved in ddH_2O. The line of best fit was used to calculate the concentration of DOX in wash solution.

3.2.4 Polyphosphate Glass Microsphere Synthesis

PGMs were synthesized using a water-in-oil emulsion technique (Figure 3.2). 18g Polycaprolactone (PCL; Sigma Aldrich) was dissolved in 150mL chloroform to create a

120g/L solution. While mixing the solution at an empirically determined optimal speed (500-2000rpm) with an impellor blade propelled by an overhead mixer, small volumes (0.1-1.5mL) of Span®80 (Sigma Aldrich) and ddH_2O were added to facilitate the formation of micro-emulsions. 1mL coacervate was then loaded into a 3mL syringe, and injected using a Fusion 200 Syringe-Pump (Chemyx Inc.) through approximately 12cm of polyethylene tubing connected to an 18-gauge needle at a fixed injection rate. Following injection there was a short mixing period at the empirically determined optimal mixing speed, after which the mixing speed was set to 500rpm and 300mL acetone was added to the emulsion. The solution was allowed to mix for 1 hour. Microspheres were collected via centrifugation, washed twice with chloroform to remove residual PCL, and then rinsed twice with acetone to remove residual chloroform. PGMs were stored submerged in acetone at 4°C. The following parameters were adjusted in order to optimize the size and shape of synthesized PGMs: PCL concentration, Span®80 volume, ddH_2O volume, injection rate, mixing speed from the beginning of coacervate injection until the addition of acetone, and mixing time from the end of coacervate injection until the addition of acetone.

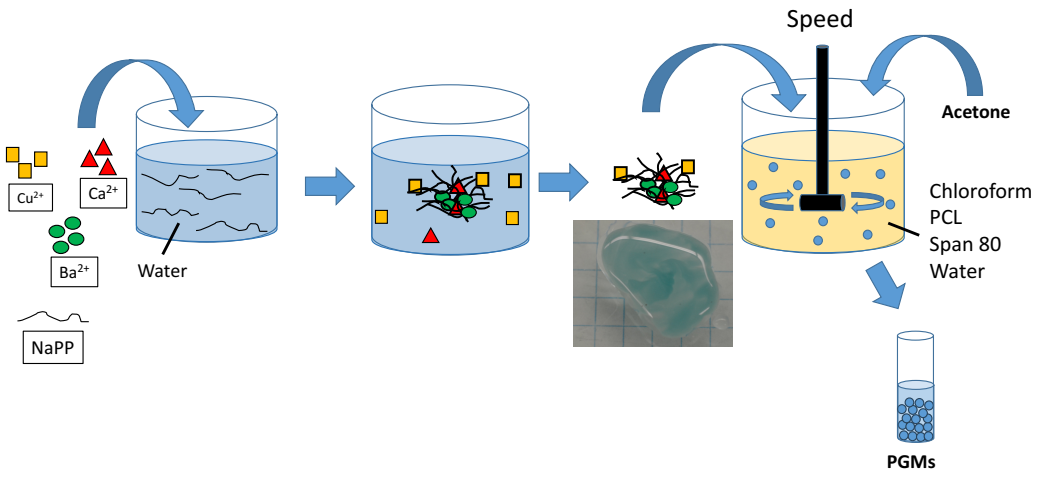

Figure 3.2 Schematic of PGM synthesis, without the introduction of drug to the system. PCL, Span80, and water are added to the chloroform first, followed by the injection of coacervate, a short mixing period, and then the addition of acetone.

PGM Encapsulation Efficiency

Barry and Calvin DOX-loaded PGMs were synthesized as described above by reconstituting 1mL of coacervate with a solution containing 10mg of DOX (n = 3). The resulting PGMs were sieved, and 100µL of the 106-300µm fraction from each sample was transferred into an Eppendorf tube of known mass, air dried and weighed. A 10cm piece of dialysis tubing was tied at one end, and the PGMs were transferred into the tube. The tube was tied at the other end, then frozen overnight prior to freeze-drying for 24 hours. This assembly was subsequently placed in 10mL of ddH_2O at 37°C for 8 weeks until the PGMs fully degraded, releasing the full load of DOX. The concentration of DOX in solution was determined by measuring the 480nm absorbance as described above. PGM encapsulation efficiency was subsequently calculated according to Equation 3.3, where '$DOX_{theoretical}$' is 1% of the mass of PGMs in the sample, and 'DOX_{actual}' is the mass of DOX released. A Student's t-test was used to quantify differences between compositions.

$$\text{PGM Encapsulation Efficiency} = (DOX_{actual} / DOX_{theoretical}) \times 100\% \qquad \text{(Eq. 3.3)}$$

Loading Capacity

Loading capacity refers to the drug content of the fully formed PGMs, and is expressed as a percent weight. Loading capacity was measured using the same samples and procedure used to determine PGM Encapsulation Efficiency, and was calculated according to Equation 3.4, where 'DOX_{actual}' is the total mass of DOX released from the PGMs, and 'PGM' is the initial mass of the PGMs. A Student's t-test was used to quantify differences between compositions.

$$\text{Loading Capacity} = [DOX_{actual}/PGM] \times 100\% \qquad \text{(Eq. 3.4)}$$

3.2.5 Size and Shape Characterization

Sieving

Each individual batch of PGMs was physically separated by size using sieves. Due to the hygroscopic nature of PGMs, they were sieved while submerged in acetone to prevent aggregation. Stainless steel sieves with size cut-offs of 300µm, 106µm, and 20µm,

along with a solid-bottom pan, were stacked and submerged in approximately 800mL acetone, in a 1L Nalgene beaker. The PGM batch being analyzed was transferred onto the 300µm sieve, the apparatus was secured to a vibrating table and placed under high vibration for 30 minutes. Size fractions were collected from atop each sieve, and the PGMs were air-dried and weighed. Percent mass yields were calculated for each size fraction.

Particle Size Analysis

Size distributions of each separate PGM batch were quantified using a Mastersizer 3000 (Malvern Panalytical). A 0.025M Sr^{2+} solution was made from strontium chloride hexahydrate ($SrCl_2 \cdot 6H_2O$; Sigma Aldrich). This solution was used as a dispersant, because this concentration of Sr^{2+} is sufficient to prevent PGM agglomeration during particle size analysis. The batch of PGMs to be analyzed was air-dried and lightly shaken to evenly disperse the PGMs of different sizes. The dispersant was stirred at 2000rpm with 10-20% sonication. A background measurement of dispersant was taken. The sample was transferred into the dispersant using a plastic spatula until 2.5-5% obscuration was achieved. For each sample, 5 measurements were taking using the 'Non-spherical particle' setting and the averages were reported. The instrument was washed thrice with ddH_2O before the next sample was tested.

Light Microscopy Imaging

Sieved PGMs were transferred onto a glass microscope slide in an evenly dispersed monolayer. The slide was placed on a glass platform and the background illuminated with a 41721 Series High Intensity Illuminator (Cole Parmer). Photographs were taken using a Nikon D3100 14.2MP digital SLR camera with a NDPL 2X microscope camera adapter lens; the lens fit into the eye-piece hole of a binocular microscope (Baush and Lomb). Images were taken under 6X magnification, with the microscope providing 3X magnification and the adapter lens a further 2X magnification.

Scanning Electron Microscopy (SEM) Imaging

1% DOX Barry and Calvin PGMs were synthesized and sieved. 106-300µm and 20-100µm size fractions from each sample were mounted on SEM stubs using silver paint.

The samples were coated with a 20nm layer of gold-palladium via gold sputtering in order to increase their conductivity. Images were taken using the Hitachi S-4700 field emission SEM operating at 3kV.

3.2.6 Chemical Composition Analysis

Barry and Calvin PGMs were synthesized as described above, with three notable variations in the coacervate precursor. 'Fresh' samples were synthesized using coacervate that did not undergo reconstitution; this coacervate was synthesized and immediately introduced into the water-in-oil emulsion to form PGMs. 'Bland Reconstituted' PGMs were synthesized from coacervate that was freeze-dried and reconstituted with ddH_2O. '1% DOX' PGMs were synthesized with coacervate that was freeze-dried and reconstituted with a solution containing 10mg DOX. 3 batches of PGMs were made for each group. The resulting PGMs were sieved and approximately 10mg of PGMs from the 106-300μm size fraction of each sample were transferred into 15mL falcon tubes and dissolved in 10mL 2% HCl. Each sample was then analyzed for Ba, Ca, Cu, and P concentrations using ICP-OES, as described in Section 3.2.2. The M^{2+}/P molar ratios were calculated and compared. For comparison, a portion (~10mg) of the coacervate precursor used for each sample group was transferred into a 15mL Falcon tube, dissolved in 10mL 2% HCl and analyzed by ICP-OES. Results were analyzed using one-way analysis of variance with Bonferroni multiple comparison's tests. The threshold for significance was set at $p < 0.05$.

3.3 Results and Discussion

3.3.1 NaPP Degree of Polymerization

The average D_p for NaPP glass was 22.7 ± 2.7 ($n = 3$); this is in accordance with prior glass production using the same procedure, indicating that the glass making process is reproducible. A representative spectrum from one of the melts is shown in Figure 3.3. It should be noted that the use of liquid NMR for this measurement creates the potential for hydrolytic degradation of the polyphosphate chains between when the sample is prepared and when the measurement is taken. To minimize this degradation, samples were prepared on the day of analysis, no more than 3 hours in advance.

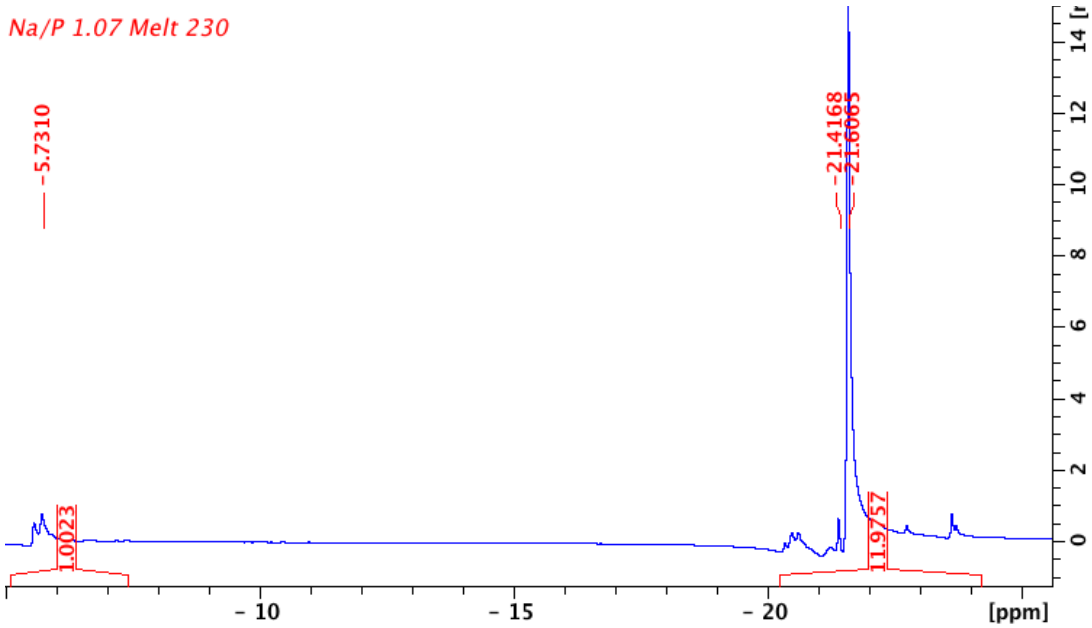

Figure 3.3 The ^{31}P-NMR spectrum from NaPP Melt #230.

3.3.2 DOX Loading

Coacervate Encapsulation Efficiency

DOX was efficiently encapsulated into the coacervate matrix using the loading procedure that was developed. Barry and Calvin both achieved coacervate encapsulation efficiencies of 99.9 ± 0.005% and 99.6 ± 0.6%, respectively (n = 5). This indicates that DOX has a high affinity for the coacervate matrix. Interestingly, when lyophilized DOX was manually mixed with wet coacervate in preliminary trials, the DOX was not easily incorporated into the polymer. It is therefore likely that the mechanism of encapsulation is mediated by water transport. As water molecules reintegrate with the polymer matrix, the space they create in the polymer matrix allows DOX to enter and bind to the coacervate.

An interesting question remains as to which part of the DOX molecule plays a more significant role in this binding. The molecular structure of DOX consists of aromatic rings and an amine group, making the molecule amphipathic. Pharmacological studies of DOX have shown that DOX disrupts cellular membrane stability by inserting its aromatic rings into the hydrophobic region of the cell lipid bilayer [78]. In the coacervate matrix, regions with higher concentrations of Ba-P bonds are more hydrophobic than regions with more Cu-P bonds, as Ba-P bonds are stronger [73]. It is possible that the DOX aromatic rings

have a high affinity to these Ba-P regions, but that the large DOX molecule relies on the space created by water infiltrating the material to reach these areas.

PGM Encapsulation Efficiency and Loading Capacity

The average PGM encapsulation efficiencies were 64.9 ± 4.3% and 73.4 ± 6.9% for Barry and Calvin PGMs, respectively. There was no significant difference between these values ($p = 0.15$). The average loading capacities were 0.67 ± 0.02% and 0.75 ± 0.05%, for Barry and Calvin PGMs, respectively, with no significant difference noted ($p = 0.065$). While these values are much lower than the theoretical DOX load in these samples, they may not be indicative of a significant loss of drug. The theoretical DOX load of 1% (w/w) is based on the approximation that 1mL of coacervate yields 1g of PGMs. This is very much an approximation; the volume of coacervate is measured relatively imprecisely with a 2mL Eppendorf tube, and the exact yield of PGMs varies depending on the amount of coacervate remaining in the polyethylene tube after injection into the emulsion. Coacervate encapsulation efficiency likely gives a more accurate measurement of DOX encapsulation into the material.

Nevertheless, these low PGM encapsulation efficiencies calculated indicate that less DOX is present in the PGMs than expected. During PGM synthesis, the addition of acetone may remove DOX from the coacervate matrix along with water. However, this is very unlikely given that DOX is not soluble in acetone or chloroform and there is no visible change in the colour of the emulsion dispersant relative to that used in bland PGM synthesis; the loss of 3mg of DOX into the dispersant would create a noticeable colour change. It is more likely that the coacervate with higher DOX content tends be emulsified more easily, forming PGMs in the smaller size fraction. DOX may intercalate the polyphosphate chains, facilitating molecular slippage. This theory is supported by the observation that bland reconstituted Barry coacervate had a higher viscosity than Barry coacervate loaded with DOX. This effect may be occurring at a smaller scale, within DOX-loaded coacervate. Regions of the coacervate with a higher DOX content would be more easily emulsified, resulting in smaller beads. Disproportionally high DOX-load in smaller PGMs would account for the low DOX load in these larger PGMs. Further investigation

into the PGM encapsulation efficiency of each PGM size fraction will be necessary to address this theory.

3.3.3 PGM Synthesis Optimization

Coacervate Characterization

Barry and Calvin differ in terms of chemical composition and water content. Barry has higher Cu^{2+} and Ba^{2+} content (23.4 ± 0.2% and 19.8 ± 0.7% respectively), while Calvin has higher Ca^{2+} (14.7 ± 0.4%) (Table 3.3). Relative to Ca^{2+} and Cu^{2+}, Ba^{2+} is the strongest crosslinker of polyphosphate chains. The difference in crosslinking strength is apparent when comparing theoretical and experimental compositions; more Ba^{2+} and less Cu^{2+} are incorporated into the coacervate than predicted (Table 3.3). Due to its higher Ba^{2+} content, Barry is the more viscous composition and is also more hydrophobic, containing 35.7 ± 1.6% (w/w) water, while Calvin is less viscous and contains approximately 40.3 ± 1.4% (w/w) water (Figure 3.4). These differences were found to have a significant impact on the emulsion parameters required to convert the coacervate into PGMs.

Table 3.3. Theoretical and Experimentally determined coacervate compositions, expressed as M^{2+}/P molar ratio (n = 6).

Composition	Theoretical/Experimental	Cu/P (%)	Ba/P (%)	Ca/P (%)
Barry	Theoretical	35	14	1
	Experimental	23.4 ± 0.2	19.8 ± 0.7	1.3 ± 0.03
Calvin	Theoretical	27	10	13
	Experimental	18.6 ± 0.3	13.6 ± 0.1	14.7 ± 0.4

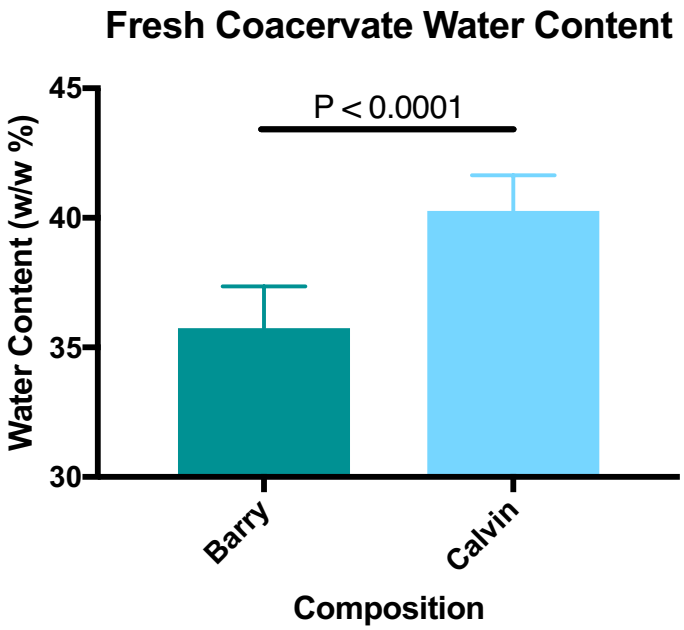

Figure 3.4 Compositional water content, expressed as a mass percentage (n = 12). Barry has a significantly lower water content than Calvin ($p < 0.0001$).

DOX-Loaded PGM Synthesis

Each composition required an independent set of emulsion parameters to form spherical beads with high yields in the 100-300µm size fraction (Table 3.4). Barry required a higher volume of water in the emulsion to increase the likelihood that pieces of coacervate became incorporated into the hydrophilic micro-emulsions. Barry also required higher mixing speeds to effectively break up the coacervate as it was injected into the emulsion.

Loading coacervate with DOX through the process of reconstitution increased the coacervate viscosity of both compositions. Mixing speeds and water volumes were increased, and injection rates decreased, to account for these differences. The effect of reconstitution on PGM synthesis seemed to be more significant with Barry than for Calvin. Due to its hydrophobicity, Barry required a longer reconstitution time. After 24 hours of reconstitution, the viscosity of the coacervate was qualitatively observed to be very high, making it difficult to inject through a 16-gauge needle. Once injected into the emulsion, the 24-hour reconstituted Barry coacervate tended to adhere to itself, the impellor blade, and the beaker wall rather than be emulsified. To allow the water to more fully reintegrate into the coacervate matrix, the reconstitution time was increased to 48 hours. This decreased the coacervate viscosity enough for it to be emulsified, although a very slow

injection rate was required to prevent the coacervate from adhering to itself in the emulsion. The processing parameters as described in Table 3.4 below were deemed optimal based on characterizations of PGM size and shape from each independent batch.

While the DOX-loading procedure ultimately increased the viscosity of coacervate, DOX actually seemed to mitigate this increase somewhat; bland reconstituted coacervate was qualitatively more viscous and difficult to emulsify than DOX-loaded coacervate. This effect was more prominent with Barry than Calvin. Polyphosphate coacervate is known to have two levels of water within its matrix: one level is considered structural, and is presumably bound directly to the polyphosphate chain via hydrogen bonds, while the other is not directly bound to the polymer backbone (Appendix A) [79]. When the loosely bound water reintegrates with the coacervate, making room for DOX to enter the polymer matrix and bind the polyphosphate chains, a positive feedback effect may occur. DOX in the coacervate matrix may increase the osmotic gradient, effectively pulling more water into the coacervate. This may be increasing the amount of structural water that is reconstituted, thereby decreasing coacervate viscosity. Alternatively, the presence of DOX may slightly disrupt M^{2+}-P bonds, facilitating molecular slippage within the coacervate. These hypotheses seem to coincide with the finding PGMs in the 106-300μm fraction contain less DOX than expected; regions of the coacervate with higher DOX content could be less viscous, and more easily emulsified. Further investigation into the relative DOX load of each PGM size fraction is warranted to test this hypothesis.

Table 3.4. Optimized water-in-oil emulsion parameters for each coacervate composition and DOX load.

Parameter	Fresh Barry	Fresh Calvin	1% DOX Barry	1% DOX Calvin
Mixing Speed	750rpm	500rpm	1000rpm	800rpm
[Polycaprolactone]	120g/L	120g/L	120g/L	120g/L
Span80 Volume	1.5mL	1.5mL	1.5mL	1.5mL
Water Volume	0.25mL	0.1mL	0.6mL	0.2mL
Injection rate	0.2mL/min	0.2mL/min	0.025mL/min	0.15mL/min
Reconstitution Time	N/A	N/A	48 hours	24 hours

Moving forward, it may be beneficial to optimize the length of time the coacervate is freeze-dried to only remove the loosely bound water. A more concentrated solution of DOX could then be used to load the coacervate with drug. In theory, the loosely bound water should be sufficient to facilitate the integration of DOX with the polymer matrix. Limiting removal of structural water may help to prevent the changes in viscosity that the current reconstitution method produces.

3.3.4 Size and Shape Characterization

Bead Size Distribution

Particle size characterization by mechanical separation provided the percent mass yields in the size fractions of >300µm, 106-300µm, 20-106µm, and < 20µm size fractions (Table 3.5). Synthesizing 1% DOX Barry PGMs with the parameters outlined in Table 3.5 yielded the majority of particles (71.5 ± 7.5%) in the 106-300µm size fraction. The parameters for 1% DOX Calvin yielded fewer particles in this size range (34.5 ± 14.2%). These yields are consistent with particle size analysis distributions (Figure 3.4). The peak volume density of 1% DOX Barry samples was consistently at approximately 200µm. However, the peak volume density of 1% DOX Calvin samples was more variable and tended to be at, or slightly below, 200µm.

Table 3.5 Average percent mass yields ± standard deviation in each size fraction, as determined by sieving (n = 4)

Size (µm)	1% DOX Barry	1% DOX Calvin
> 300	5.5 ± 2.8	1.8 ± 1.4
106-300	71.5 ± 7.5	34.5 ± 14.2
20-106	16.3 ± 8.5	51.9 ± 11.7
< 20	6.8 ± 2.7	11.8 ± 3.9

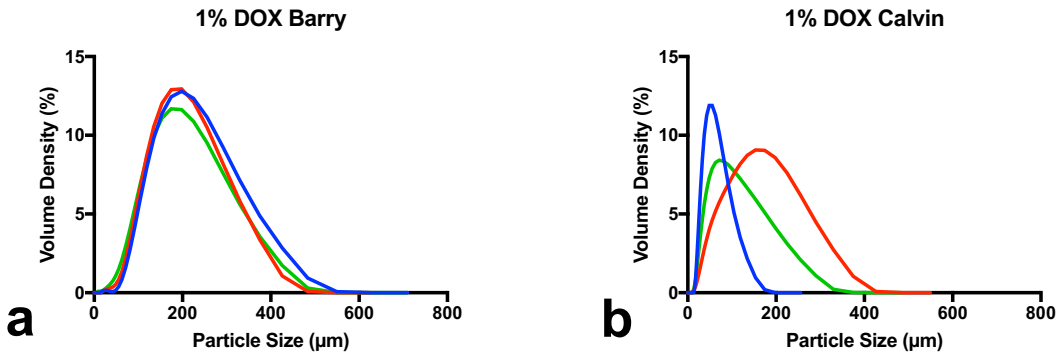

Figure 3.5 Size distributions of independent batches (each batch corresponds to a different colour) of 1% DOX Barry (a) and 1% DOX Calvin (b) (n = 3).

The variability in Calvin particle size is likely due to variability during the injection of the coacervate. With the current equipment used to synthesize PGMs, the location of the needle tip in the beaker is inexact. During the injection phase of each batch of PGMs, the polyethylene tubing is taped to the lip of the beaker. The goal is to position the needle approximately 2cm from the side of the beaker so that the coacervate will be injected as a stream that is pulled towards the impellor blade. If the needle is too close to the impellor blade, the stream of coacervate cannot form; the coacervate is pulled from the needle in large chunks. The differences that result from this inconsistency are more pronounced with Calvin because it is injected at a higher rate than Barry.

To address this variability, a glass or metal sleeve connected to the lip of the beaker through which the polyethylene tube could be fed is a possibility (Figure 3.6). Having this solid structure in place to control the exact placement of the needle would greatly reduce the variability in the size yields of each batch.

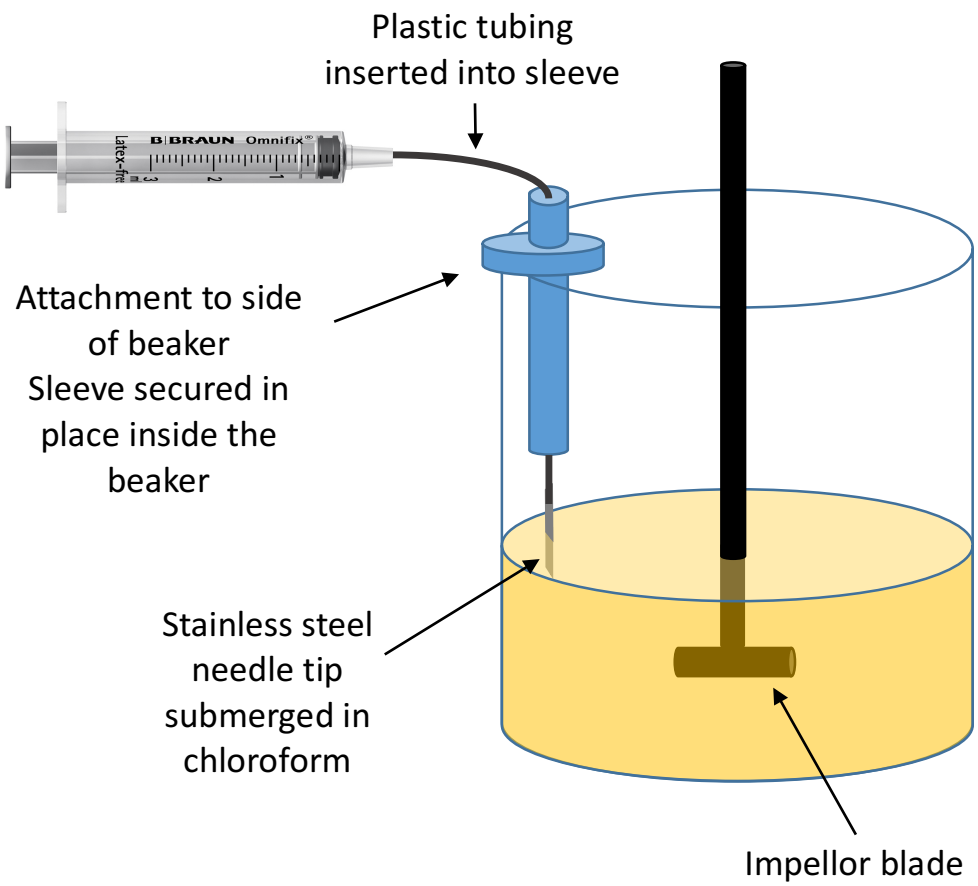

Figure 3.6 Schematic of the needle-stabilizing apparatus.

Bead Shape

Initial characterization of PGM shape was conducted using light microscopy (Figure 3.7). These images provided a low-resolution, low-magnification means of characterizing PGM shape. These images allowed for the identification of defective PGMs in the 106-300µm fraction, and were used in the optimizing PGM synthesis parameters.

Size (µm)	1% DOX Barry	1% DOX Calvin
106-300	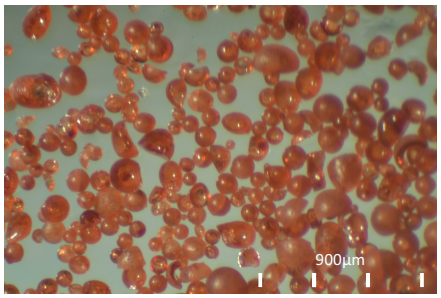	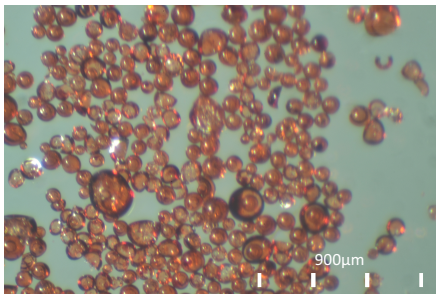
20-106	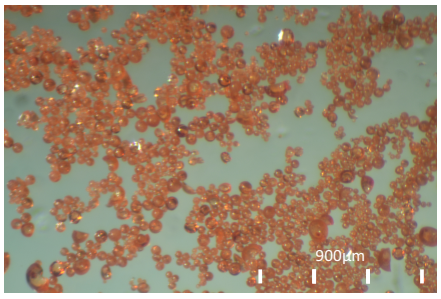	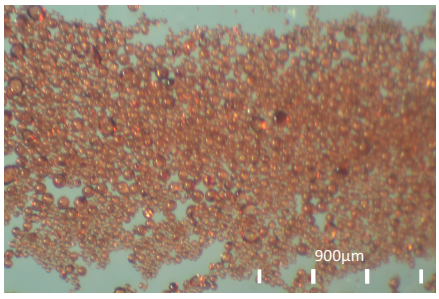

Figure 3.7 Light microscope images of DOX-loaded PGMs. These images are representative of the overall bead quality of the size fraction. Scale bars on the images were created manually using a photograph of a 300µm sieve taken under the same magnification.

Samples synthesized using the optimized processing conditions were further characterized with SEM (Figures 3.8-3.11). These high-resolution, high-magnification images reveal features of the PGMs in greater detail. The SEM images taken at lower magnifications were representative of the overall bead quality of the sample on the SEM stub. Additional, higher magnification SEM images were taken of defective beads to inform about the exact nature of these defects. It is clear that larger PGMs are less stable, showing greater susceptibility to fracturing. The smooth internal surfaces of the cracked PGMs suggest that the PGM structure failed via brittle fracture. These fractures must have occurred after the coacervate was dehydrated into a glass with the addition of acetone to the emulsion. Fractures were less common in the 20-106µm size fraction for both compositions, suggesting that these smaller spheres are structurally more stable. As the PGMs approach 300µm in size, fracturing seems to become more likely. Between the two compositions, fracturing was more common in Barry PGMs. This coincides with the size distributions in Figure 3.5. The emulsion parameters used for 1% DOX Barry shift the

distribution peak towards larger bead sizes, which in turn increases the likelihood of some beads fracturing. This may prove to be a significant processing challenge if larger embolic beads are desired. Interestingly, the optimal size range for DEB-TACE seems to be trending downwards; several papers have found that decreasing the microsphere size from 100-300μm to 75-150μm increased the depth of embolization without significantly increasing the adverse effects [43-45]. This particle size range would be much more suitable for this material and method of synthesis.

The SEM images further show that the PGMs are hollow. This could potentially be beneficial, as there is some concern in the literature about the density of microspheres; lower density makes microspheres easier to suspend in contrast agent, which increases their deliverability through conventional delivery systems [47]. Although there are delivery systems designed specifically for higher density beads. Figure 3.11 shows invaginations in spheres that have not cracked. It may be that the spheres are hollow because the coacervate effectively wraps around the water-Span80 microbubbles in the emulsion, and that with the addition of acetone, the water in microbubble escapes from the core of the coacervate via this invagination. The invagination likely weakens the structural strength of the sphere, and leads to cracking when the sphere is too large. It is possible that adjusting the speed at which acetone is added to the emulsion may limit these invaginations from forming, and ultimately limit cracking.

Barry PGMs in both size ranges seem to have pitted surfaces, while Calvin PGMs do not. These pits do not penetrate deeply into the spheres, meaning that they probably do not contribute to the microspheres cracking. These pits may be present because a larger volume of water is used for Barry (0.6mL) than for Calvin (0.2mL). The increased water may lead to microbubbles forming on the surface of emulsified coacervate, leaving behind these pores after the addition of acetone. Alternatively, these apparent pits may actually be the result of phase separation between regions of highly concentrated barium and the rest of the polymer matrix. Highly concentrated barium would appear as dark spots when imaged with SEM. These regions may rise to the surface of the beads as a result of hydrophobic interactions; the surface is closer to the chloroform/PCL emulsion, relative to the supposedly hydrophilic centre of the emulsified coacervate. Energy-dispersive X-ray spectroscopy could be used to investigate the elemental content of these dark regions.

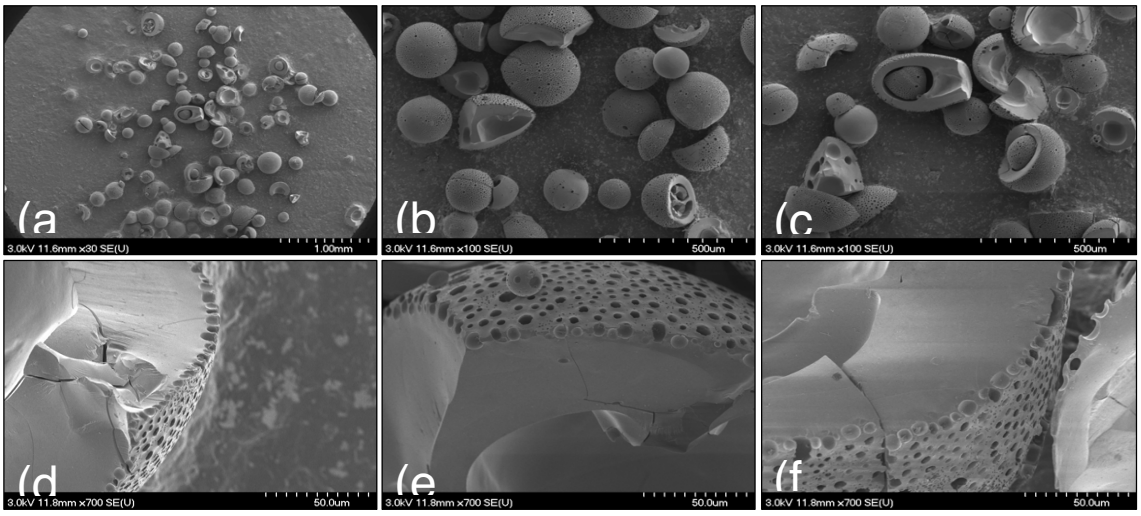

Figure 3.8 SEM images of the 106-300µm size fraction of a single batch of 1% DOX Barry PGMs. (a) is representative of the overall bead quality of the sample. (b-f) are higher magnification images of defective beads.

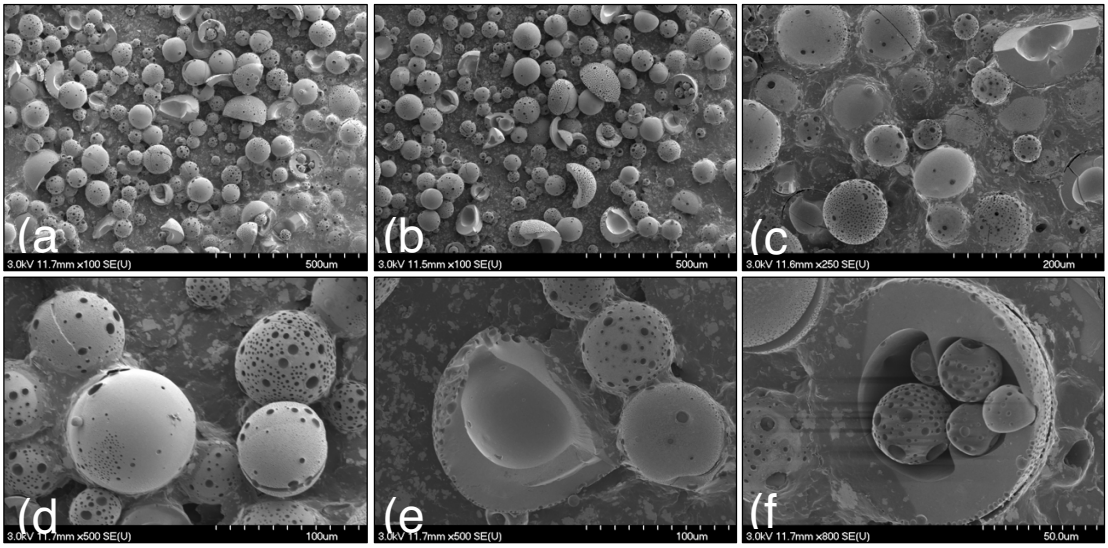

Figure 3.9 SEM images of the 20-106µm fraction of a single batch of 1% DOX Barry PGMs. (a-b) are representative of the overall bead quality of the sample. (c-f) are higher resolution images of lower quality beads.

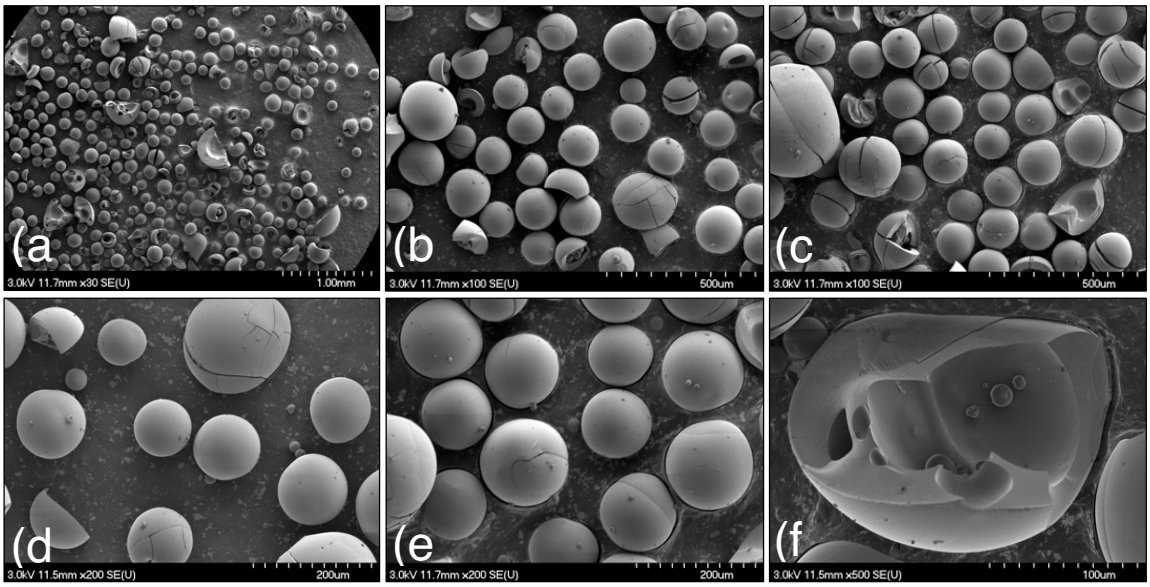

Figure 3.10 SEM images of the 106-300µm size fraction of a single batch of 1% DOX Calvin PGMs. (a) is representative of the overall bead quality of the sample.

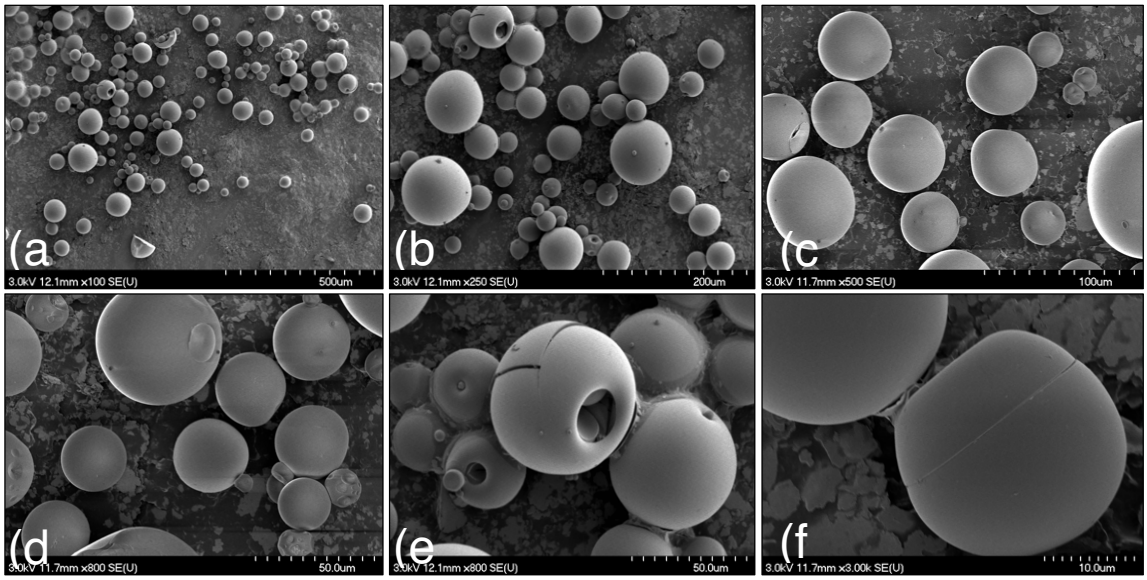

Figure 3.11 SEM images of the 20-106µm size fraction of a single batch of 1% DOX Calvin PGMs. (a-b) are representative of the overall bead quality. (c-f) are higher resolution images of lower quality beads.

3.3.5 PGM Chemical Composition

The DOX-loading procedure had minimal effect on PGM chemical composition. No significant differences in M^{2+}/P ratios were present between fresh, bland reconstituted, and DOX-loaded Barry PGMs (Figure 3.12a). This indicates that the reconstitution process

does not result in the loss of any divalent cations from the coacervate and that DOX does not displace these cations, disproving Hypothesis 2.1.2.

Some small, but statistically significant differences were present between groups of Calvin PGMs (Figure 3.12b). There was a significant decrease in the Cu^{2+}/P ratio between Fresh and Bland Reconstituted PGMs ($p = 0.0024$), and the same decrease was present between Fresh and DOX-loaded PGMs ($p = 0.0036$). There was no significant difference between DOX-loaded PGMs and Bland Reconstituted PGMs, indicating that this difference resulted from the reconstitution process and is not the result of DOX displacing Cu^{2+} from the coacervate matrix.

DOX-loaded Calvin PGMs also showed a significant increase in Ba^{2+}/P, relative to Fresh PGMs ($p = 0.0222$). Figure 3.13b shows that the Ba^{2+}/P ratio did not change significantly as Calvin coacervate was loaded with DOX and then converted into PGMs. Figure 3.13f shows that, in these Fresh Calvin samples, there was a significant decrease in Ba^{2+}/P as the coacervate was converted to PGMs. This decrease is responsible for the differences seen in Figure 3.12b. It is possible that, during the conversion from coacervate to PGMs, Calvin coacervate loses some Ba^{2+} after the addition of acetone to the emulsion. The addition of DOX to the coacervate matrix may prevent this loss from occurring through the association of its hydrophobic aromatic rings with the hydrophobic Ba-P regions of the coacervate. However, the loss of Ba^{2+} during water removal does seem unlikely, given that Ba^{2+} is noted as a strong crosslinking cation in these polyphosphate chains, and that this loss is not observed with Barry PGMs, despite them having higher Ba^{2+} content.

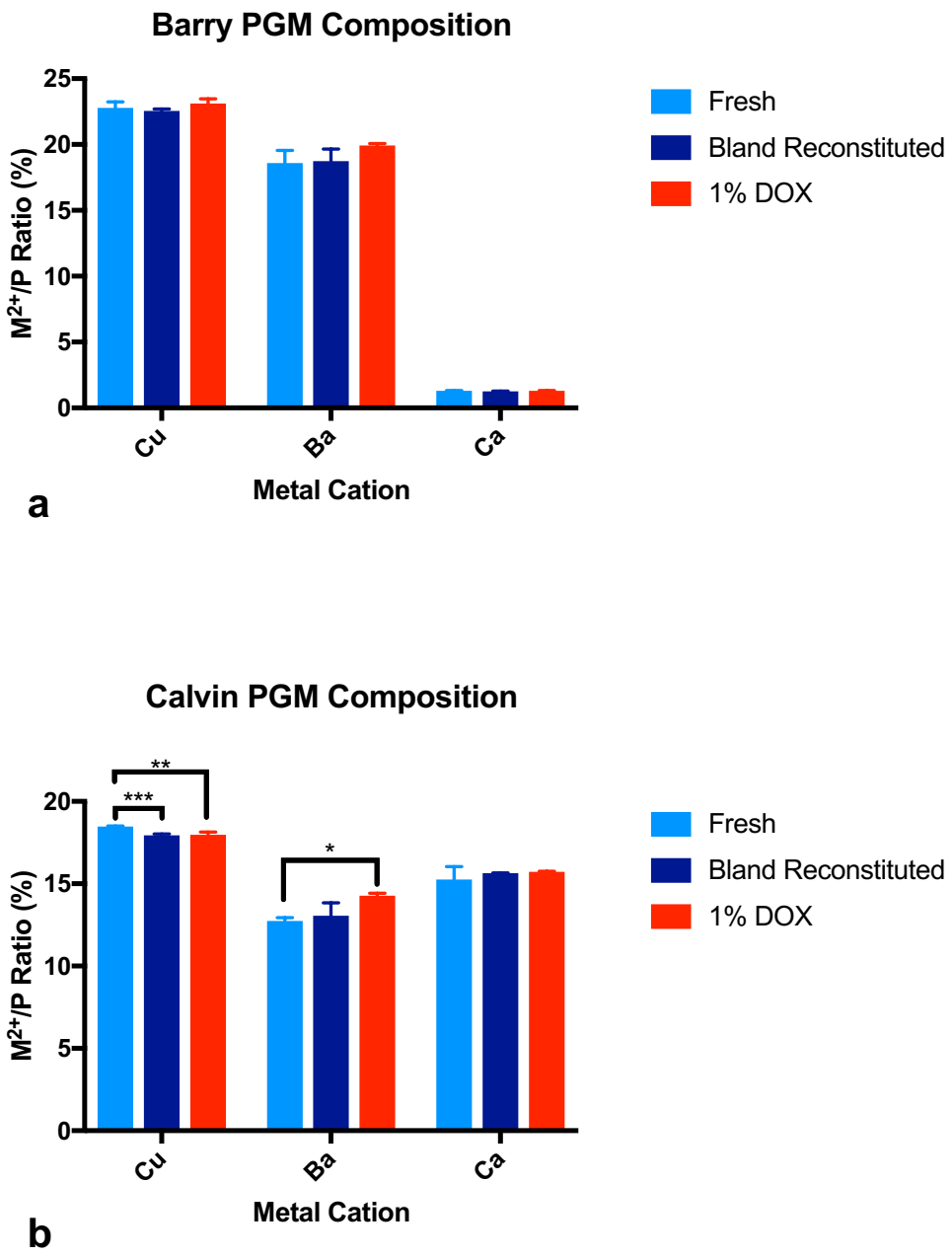

Figure 3.12 Composition of fresh, bland reconstituted, and 1% DOX-loaded Barry (a), and Calvin (b) PGMs, expressed at M^{2+}/P molar ratio. Three batches of each group (3 batches of Fresh Barry, 3 batches of Bland Reconstituted Barry, etc.) were analyzed Average values are presented, and the error bars represent the standard deviation. The data was analyzed using one way ANOVAs with Bonferroni multiple comparison analysis. *$p < 0.05$; **$p < 0.01$; ***$p < 0.005$.

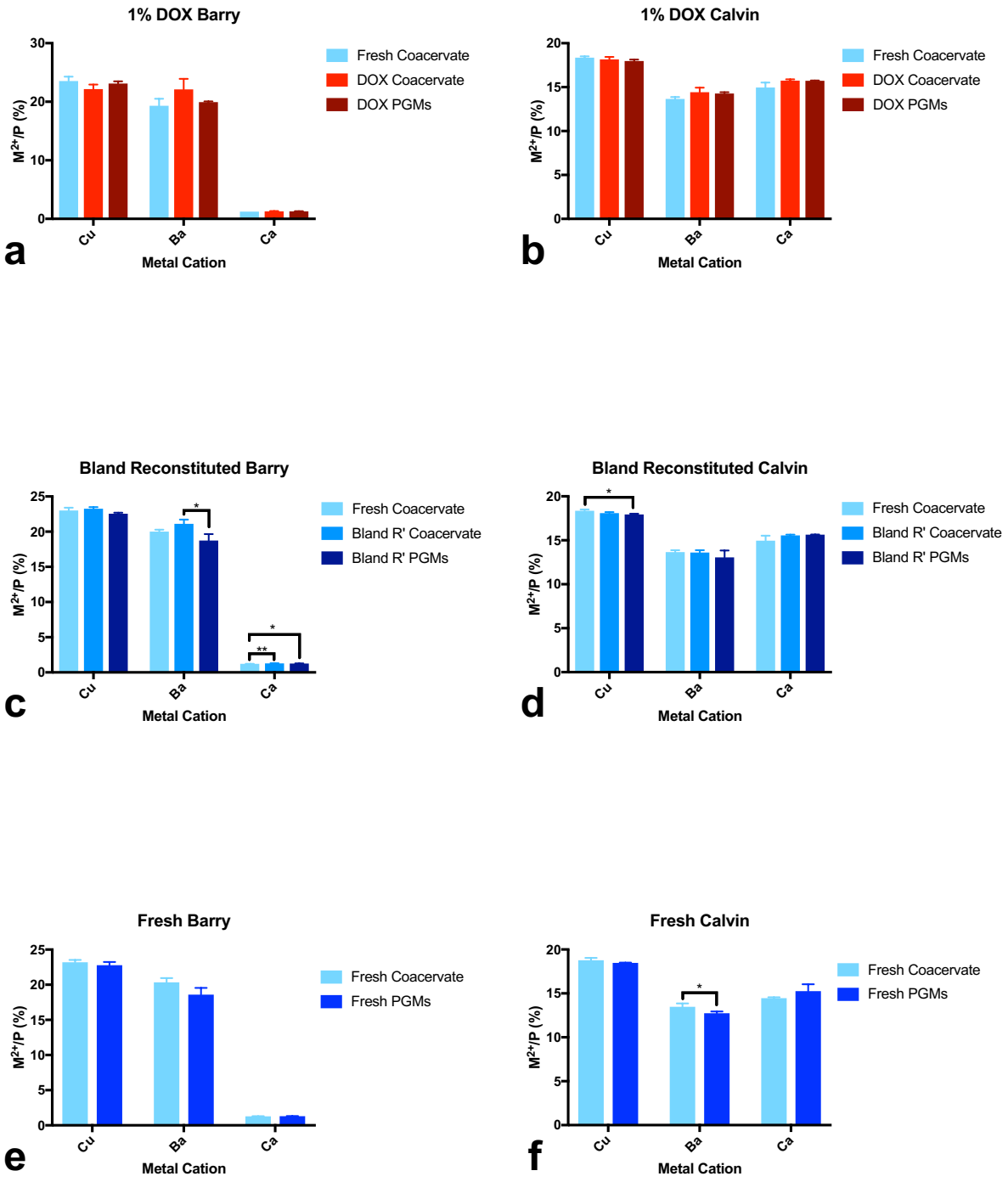

Figure 3.13 Changes in PGM and coacervate composition tracked through the reconstitution, DOX-loading, and PGM synthesis process. Composition is expressed as the M^{2+}/P molar ratio. Each graph represents the average values from three batches of PGMs. Average values are presented, and the error bars represent the standard deviation. Data was analyzed using one way ANOVAs with Bonferroni multiple comparison analysis. *$p < 0.05$; **$p < 0.01$.

The mechanism of DOX-loading remains unclear. DOX is not loaded through the displacement of Ba^{2+}, Ca^{2+}, or Cu^{2+}, leaving several other possible mechanisms. It may be that Na^{+} ions are being displaced from the coacervate as DOX is loaded. It is worth noting that the majority of DEB-TACE microspheres are loaded with DOX through electrostatic interactions with the anionic polymer backbone; DOX is subsequently released through ion exchange, as Na^{+} from the buffered saline in the elution media enters the polymer and displaces DOX [19, 68]. This indicates that, in most cases, Na^{+} has a higher affinity for the negatively charged polymer than DOX. This fact, in addition to the substantial size difference between Na^{+} (22.98g/mol) and DOX (543g/mol), seems to indicate that DOX is not loaded via ion exchange with Na^{+}. This leaves the possibility that DOX is occupying niches in the coacervate matrix that were otherwise occupied by water. It is also possible that the more hydrophobic aromatic region of the DOX molecule is responsible for its loading. This region may associate with the more hydrophobic regions within the coacervate, such as niches with high concentrations of Ba-P crosslinks. The reconstitution process may facilitate the aggregation of Ba-P regions, which may have a higher affinity for DOX. Proposed DOX interaction is described in figure 3.14.

The pH within the polymer matrix may play a role in determining which DOX-loading mechanism dominates. If some of the polyphosphate chains are degrading within the polymer matrix, the environment will become more acidic, tending to protonate DOX. Protonated DOX is more likely to bind with the polyphosphate chains electrostatically, occupying hydrophilic niches. If this is not the case, hydrophobic interactions with Ba-P regions may be more likely. The DOX elution data in chapter IV will allow for further comment on this topic.

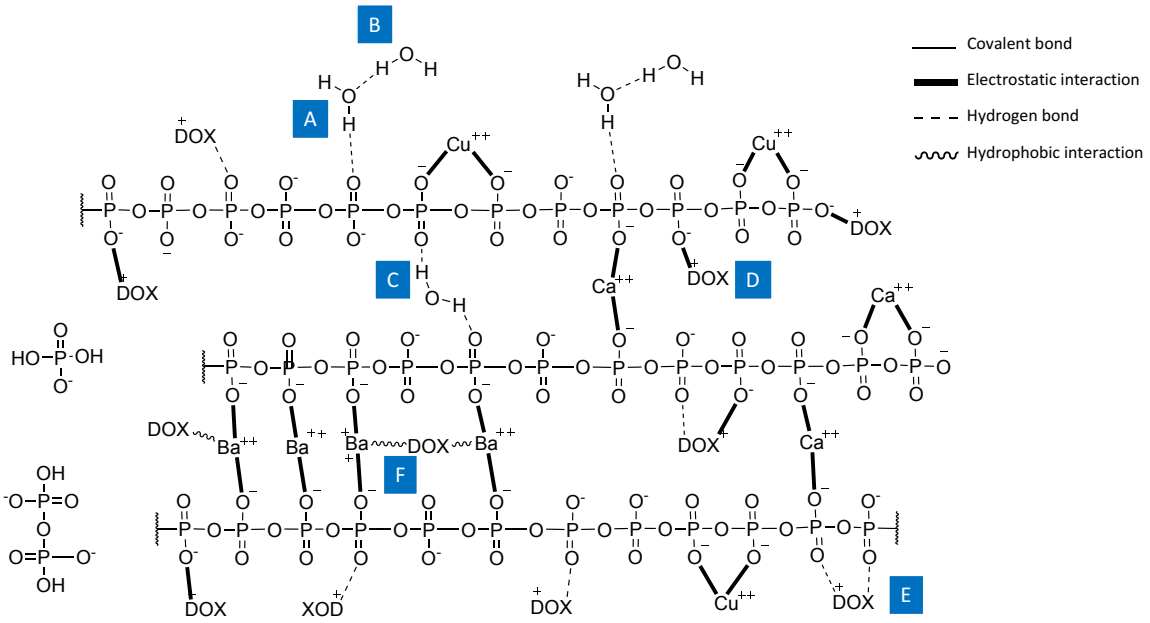

Figure 3.14 Schematic of proposed DOX binding to the PGM polymer matrix. The matrix is composed of polyphosphate chains crosslinked by divalent cations, non-bridging (A) and bridging (C) structural water, loosely bound water (B), and DOX bound to the polyphosphate chains via electrostatic interactions (D), hydrogen bonds (E), and hydrophobic interactions.

3.4 Concluding Remarks

This experimental package provided insights into the NaPP–Ba^{2+}–Ca^{2+}–Cu^{2+} system and the interplay between the polymeric glass matrix and DOX. The development and optimization of the DOX-loading procedure demonstrated that DOX can be loaded into this NaPP–Ba^{2+}–Ca^{2+}–Cu^{2+} system. The process of reconstitution increased the viscosity of the coacervate, and this effect was somewhat mitigated by the presence of DOX in solution. The mechanism of DOX loading was explored and demonstrated that DOX is not loaded through the displacement of divalent cations in the coacervate matrix. These findings will be beneficial as this drug delivery platform continues to be developed. A plethora of drugs are similar in structure to DOX; these will likely be equally as compatible with this compositional range of coacervate and PGMs.

The process of troubleshooting the emulsion parameters to yield reasonably spherical beads within a targeted size range led to a deeper understanding of the impact of each emulsion parameter. With the addition of the 'injection sleeve' (Figure 3.6), and some adjustments to further optimize the sphericity of the beads, reproducibly high quality

particles will be attainable. Given the movement towards smaller bead sizes, efforts should perhaps be focussed on optimizing yields in the 75-150μm fraction; coincidentally, the synthesis methods developed here seem to be more compatible with this size range. Loading higher quantities of drug as well as different drugs into the coacervate may lead to further changes in coacervate viscosity. This experimental work will help to provide a framework for the kinds of adjustments that may be required to compensate for these potential viscosity changes as this drug delivery platform continues to be developed.

This chapter has demonstrated that DOX-loaded PGMs can be synthesized using the water-in-oil emulsion technique, verifying Hypothesis 2.1.1. Hypothesis 2.1.2 was disproven, indicating that DOX does not displace M^{2+} from the coacervate matrix. This chapter also demonstrated that differences exist between DOX-loaded compositions, especially regarding the effect on coacervate viscosity, verifying Hypothesis 2.1.3. The following chapters will evaluate the interplay between PGM degradation and DOX release as well as the pharmacological activity of DOX that has gone through the process of being encapsulated into, and released from, PGMs.

Chapter 4: *In Vitro* Degradation and Drug Elution

4.1 Introduction

Following the successful synthesis of DOX-loaded Barry and Calvin PGMs, a study was conducted to evaluate PGM degradation and DOX elution, addressing Objective 2.2. An *in vitro* degradation system was created to approximately simulate the tumour microenvironment. PGMs degrade by rapidly absorbing water, converting back to coacervate. When injected into a blood vessel in a DEB-TACE procedure, the enclosed space will force PGMs into contact with one another, and the aqueous environment of blood will instigate the change from PGM to coacervate. This conversion to coacervate will likely affect the degradation and drug release properties of the material, and so it was important to capture this in the *in vitro* model system. To this end, dialysis tubing was used to force the PGMs into an enclosed space, effectively creating a bolus of coacervate. This system was subsequently used to evaluate the interplay between PGM degradation and DOX release by looking at the effects of PGM composition, DOX-loading, and the pH of the elution media on the rate of DOX release, PGM mass loss and ion release.

Chapter 4 presents the results from these degradation/drug elution studies. By using DOX-loaded, Bland Reconstituted, and Fresh PGMs, these studies were able to evaluate the effect of the DOX-loading process on degradation, addressing Hypothesis 2.2.1. Collecting DOX elution and degradation data simultaneously allowed for the quantification of differences between DOX, Cu^{2+}, Ba^{2+}, Ca^{2+}, and P release rates, addressing Hypothesis 2.2.2. Finally, the use of solutions buffered at pH 7.4 and 6.5 revealed the effect of pH on the system and addressed Hypothesis 2.2.3.

4.2 Materials and Methods

4.2.1 Elution / Degradation Study Preparation

PGM Sample Preparation

In vitro elution/degradation studies were conducted to quantify the rate of PGM degradation and DOX release from DOX-loaded PGMs. Barry and Calvin PGMs were synthesized and sieved as described above (Sections 3.2.2-3.2.5). Dialysis tubing (Sigma Aldrich) was cut into 10cm pieces, weighed and tied at one end. Using a Pasteur pipette,

approximately 100µL of 20-300µm of PGMs (submerged in acetone) were transferred into each piece of dialysis tubing. This size fraction was chosen to efficiently use synthesized PGMs; a previous project with minocycline-loaded PGMs found that PGM size did not affect degradation rate. The tubing was tied at the other end and placed in the freezer overnight. Samples were then freeze-dried for 24 hours to remove any water or acetone, weighed, and placed in 10mL buffered saline solution at 37°C.

Elution Media Preparation

Buffered solutions were prepared at pH 6.5 and pH 7.4. To make a solution of 0.1M ACES buffered saline (ABS) at pH 6.5, 18.22g of N-(2-acetamido)-2-aminoethanesulfonic acid (ACES; Alfa Aesar) and 9g of sodium chloride salt (NaCl; Fisher Scientific) were dissolved in 1L ddH_2O. The solution was heated to 37°C, and the pH of the solution was then raised to 6.5 by dropwise addition of 1M NaOH (Sigma Aldrich). 0.1M solution of ACES was made via the same method, without the addition of NaCl. To make a solution of 0.1M tris-buffered saline (TBS) at pH 7.4, 3.32g of Trizma base (Sigma Aldrich), 11.44g of Trizma hydrochloride (Sigma Aldrich), and 9g of sodium chloride were dissolved in 1L ddH_2O. The solution was heated to 37°C, and the pH was adjusted to 7.4 via dropwise addition of 1M HCl (Sigma Aldrich).

4.2.2 Elution / Degradation Study Procedure

10mL of elution media (ACES, ABS or TBS) was transferred into 15mL Falcon tubes. One freeze-dried PGM sample in dialysis tubing was transferred into each Falcon tube, and each tube subsequently capped and inverted once to ensure the PGMs were submerged. All samples were stored at 37°C on an oscillating table under light vibration (150rpm). At specific time points, PGM samples were transferred into 10mL of fresh elution media. Old media was then analyzed to determine the concentrations of DOX, Ba, Ca, Cu, and P. pH readings were taken at each time point to ensure the buffering capacity of the media was not overwhelmed. At specific time points samples were sacrificed. Coacervate that remained in the dialysis tubing, hereafter referred to as 'remnant coacervate,' was freeze-dried, weighed, and dissolved in 25mL 2% HCl for analysis (described in section 4.2.3).

pH–Mediated Effects

To evaluate the effects of elution media pH 1% DOX, 0.5% DOX, and Bland Reconstituted Calvin PGMs were synthesized. Samples were degraded in 10mL TBS (pH 7.4) or 10mL ACES (pH 6.5) at 37°C for 28 days (n = 7). The elution media was replenished and analyzed at 1 hour, 4 hours, 8 hours, 12 hours, 24 hours, 36 hours, 2 days, 3 days, 7 days, 14 days, 21 days, and 28 days.

PGM Composition–Mediated Effects

The effects of PGM Composition on PGM degradation and DOX release were evaluated. 6 groups of PGMs were synthesized: 1% DOX Calvin, Bland Reconstituted Calvin, Fresh Calvin, 1% DOX Barry, Bland Reconstituted Barry, and Fresh Barry. All samples were degraded in ABS (pH 6.5) at 37°C. pH 6.5 was selected so that DOX would be released from the PGMs, allowing the release profiles from each composition to be compared. Elution media was replenished at 4 hours, 1 day, 3 days, 7 days, 14 days, 21 days, 28 days, and 42 days. The pH of the elution media was measured at each time point using an Accumet AB 15/15+ bench-top pH meter (Fischer Scientific). 4 samples from each group were sacrificed at 7 days, 14 days, 21 days, 28 days, and 42 days.

Elution Media Osmolarity

To assess the potential impact of NaCl in the elution media on degradation and DOX release, the results from the pH study and the composition study were compared. In both studies, 1% DOX and Bland Reconstituted Calvin PGMs were degraded at pH 6.5 over 28 day periods. In the pH study, the elution media was 0.1M ACES, while the composition study used media containing 0.1M ACES and 0.9% NaCl. One limitation of this comparison is difference in extraction frequency; the pH study used more frequent time points early on. Despite this difference, the results were compared to determine the effect of NaCl on PGM degradation and DOX release.

4.2.3 Sample Analysis

DOX Concentration

DOX concentration was quantified by measuring the absorbance at 480nm using a Biotek Synergy HT microplate reader (Fisher Scientific). Standard DOX solutions were prepared at concentrations of 0 mg/mL 0.1 mg/mL, 0.05 mg/mL, 0.01 mg/mL, and 0.001 mg/mL in ACES, ABS, TBS, and ddH_2O. A 10mL aliquot of each standard was taken, and 200µL of 12M HCl was added to decrease the pH of the solution below 2. Elution media samples needed to be acidified to dissociate DOX-Cu^{2+} complexes (see below), and so it was important for the standard solutions to be at the same pH as the samples being measured. The solutions were mixed, and 200µL of each sample was pipetted, in triplicate, into wells of a 96-well plate. The 480nm absorbance was then measured with a plate reader. The average absorbance measurement from blank media (0 mg/mL) was treated as a baseline and was subtracted from all other absorbance values. A standard curve was created for DOX dissolved in each elution media; linear regression was preformed and the equation of the line of best fit was used to calculate the concentration of DOX in each elution media sample, based on its measured 480nm absorbance.

To quantify the DOX concentration in elution study samples, 200µL 12M HCl was added to each sample to decrease the pH of the solution below 2, thereby dissociating DOX-Cu^{2+} complexes [80]. DOX-Cu^{2+} complexing shifts the peak absorbance of DOX to 577nm, and so the complexes needed to be dissociated to reliably quantify DOX. The total mass of DOX in each PGM sample (eluted + remnant) was calculated, and DOX release values were expressed as a percentage of this total. Cumulative release percentages were plotted over the period of the elution study, and were analyzed using linear regression.

PGM Mass Loss

The concentrations of Ba, Cu, Ca, and P in each elution sample, and in dissolved remnant coacervates, were measured and used as a surrogate measurement for PGM mass loss. The dialysis tubing underwent highly variable mass loss over the period of the degradation/elution studies, and so freeze-drying the remnant coacervates was not a viable means of measuring mass loss. The method described below is limiting in that relies on assumptions to calculate the loss of oxygen in the polyphosphate chain. To calculate the

mass loss associated with oxygen, polyphosphate chains were assumed to have a D_p of 22, based on the findings in section 3.3.1. This means that each polyphosphate chain contains 22 P atoms and 67 O atoms, yielding a O:P molar ratio of 3.04545. Each mole of detected P was multiplied by this factor, and then divided by the molar mass of $PO_{3.04545}$ (79.6979g/mol) to determine the mass loss associated with the polyphosphate chain.

The concentrations of Ba, Cu, Ca, and P from each sample of elution media were quantified using ICP-OES. After acidification to dissociate DOX-Cu^{2+} complexes so that DOX concentration could be quantified, samples were diluted at a 1:10 ratio in 2% HCl. Diluted samples were analyzed with ICP-OES as described in Section 3.2.6. To determine the release profile of each element, the mass of each element in each sample was calculated, summed, and the cumulative release profiles of each element were expressed as a percentage of the total amount of that element in the sample. The surrogate mass of each PGM sample was calculated by summing the mass of all elements (including assumptions made to account for oxygen) at all time points. Mass loss was then expressed as a percentage of the total surrogate mass. Differences between PGM mass loss and ion release at each time point were tested statistically using two-way ANOVAs with Bonferroni multiple comparisons post-hoc testing. To account for the large number of statistical tests performed, the Bonferroni correction factor was applied to the resulting p-values. The threshold for significant was set at $p < 0.05$.

Compositional Ion Release Profiles

Release profiles of Ba, Cu, Ca, and P from each PGM sample were also determined. The total mass of each individual element (eluted + remnant coacervate) was calculated. At each time point the cumulative mass of eluted element was expressed as a percentage of the total element mass for that PGM sample. Differences in cumulative element release from different PGM groups at specific time points were quantified using two-way analysis of variance with Bonferroni multiple comparisons post-hoc testing, with the Bonferroni correction factor.

4.3 Results and Discussion

4.3.1 pH–Mediated Effects

DOX Release

The release of DOX is highly dependent on the pH of the elution media (Figure 4.1). At pH 7.4, only 0.67 ± 0.98% of the total DOX load was released from 1% DOX PGMs, and virtually no DOX was released from 0.5% DOX PGMs. At pH 6.5, DOX was clearly released from PGMs, with 1% DOX PGMs and 0.5% DOX PGMs releasing an average of 37.9 ± 6.5%, and 41.9 ± 9.3% of their respective total DOX loads by the end of the 28-day period. Surprisingly, these release profiles were highly linear; regression analysis revealed R^2 values of 0.9989 and 0.9986 for 1% DOX PGMs and 0.5% DOX PGMs, respectively. The means that DOX is released by zeroth-order kinetics: a special case of non-Fickian transport [81].

At both pH 7.4 and 6.5, DOX retained a high affinity for the coacervate throughout the 28-day elution period. The sample that released the most DOX still retained approximately 50% of its payload. This high affinity is likely mediated by electrostatic interactions. The pKa corresponding to the amine group on the DOX molecule is 8.46 [82]. The pKa_1 of the phosphates in the polyphosphate chain is between 1 and 2 depending on the D_p [83]. Therefore, at pH 7.4 and 6.5, DOX tends to be positively charged, and the phosphates tend to be negatively charged. Decreasing the pH from 7.4 to 6.5 allowed some DOX to be released from the coacervate. The pKa_2 of the terminal phosphates in polyphosphate chains, corresponding to the terminal hydroxyl group, range from 6.5-8.2, again depending on the D_p [83]; the pKa_2 of orthophosphates (D_p = 1) is 7.20, while pyrophosphates (D_p = 2) have a pKa_2 of 6.7 [83]. Decreasing the pH of the elution media from 7.4 to 6.5 will tend to protonate these groups, shifting the charge of these terminal hydroxyl groups from -1 to neutral. This change makes the polyphosphates less negatively charged, presumably decreasing their affinity for DOX.

The pKa of DOX may play a role in this release mechanism. pKa represents the isoelectric point of a molecular species and is defined as the pH at which 50% of a molecular species possess a net charge. The Henderson-Hasselbalch Equation (Equation 4.1) describes pKa, where pH is the pH of the environment, [HA] is the concentration of acid and $[A^-]$ is the concentration of conjugate base. When the pH of the environment is 1

pH unit below the pKa, 10% of the molecular species will be neutral. Decreasing the pH 2 units below the pKa results in only 1% of the molecular species exhibiting 0 net charge. In the case of DOX, approximately 10% of molecules will be neutral at pH 7.4, and only approximately 1% will be neutral at pH 6.5. This may contribute to the release mechanism. At pH 7.4, some of the neutral DOX molecules may remain bound to the Ba-P hydrophobic regions of the coacervate. Decreasing the pH to 6.5 will result in more DOX molecules becoming cationic, forcing DOX into interactions with the polyphosphate chains. Increasing interactions with the polyphosphate chains may help to facilitate the release mechanism involving the pKa_2 of the terminal phosphates, as described above.

$$pH = pKa + \log([A^-]/[HA]) \qquad \text{(Eq. 4.1)}$$

Interestingly, this release profile corresponds with a study that characterized coacervate degradation [74]. This study found that, as coacervates in this compositional range degraded, the polyphosphate chains underwent scission down to ortho and pyrophosphates. The ortho and pyrophosphates were then released from the coacervate matrix. Within the coacervate, the chain scission continued over a 27-day period. As the prevalence of ortho and pyrophosphates in the degrading coacervate increases, the pH shift from 7.4 to 6.5 will have a more exaggerated effect on coacervate net charge. As more chains are cleaved, more terminal phosphates are present. This means that a coacervate degrading in pH 6.5 elution media will have a considerably less negative net charge than coacervate degrading in elution media at pH 7.4; this difference could account for the change in DOX affinity.

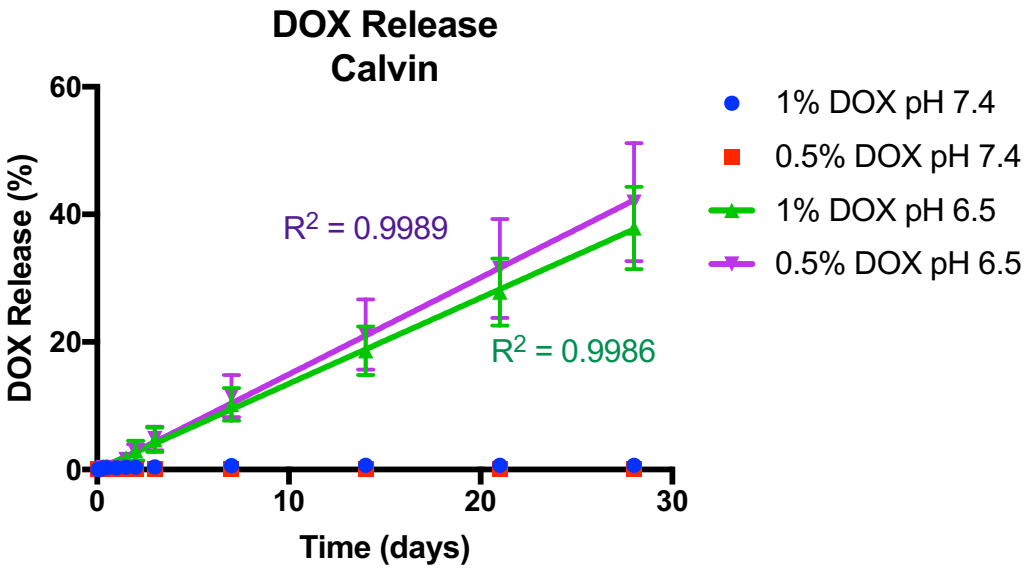

Figure 4.1 Cumulative DOX release from 1% DOX and 0.5% DOX Calvin PGMs, degrading at pH 7.4 and 6.5. R^2 values were calculated using linear regression.

PGM Mass Loss

PGM Degradation was not commensurate with DOX release. All groups tested exhibited a rapid release of ions during the first 7 days of degradation, followed by a slower release of ions for the remaining 21 days (Figure 4.2). This profile was observed for both pH conditions. DOX release did not match this profile at either pH, disproving the hypothesis that DOX release is commensurate with PGM degradation (Hypothesis 2.2.2).

Interestingly, DOX load did not alter PGM degradation rate. At every time point tested, no significant differences were found between 1% DOX, 0.5% DOX and Bland Reconstituted PGMs maintained under the same pH conditions. This suggests that the association of DOX to the polymer matrix is not structural; relative to the cross-linking strength of Ba^{2+}, Ca^{2+}, Cu^{2+}, and the overall integrity of the polyphosphate chains, the association of DOX with the polymer has a negligible effect on degradation.

At both pH values, PGM degradation plateaued at approximately 75% mass loss (Figure 4.2). While this plateau was conserved across all groups tested, comparing the mass loss at earlier time points revealed that decreasing the pH of the elution media did significantly accelerate degradation. At 4-hour, 1-day, 3-day, and 7-day time points, the PGMs maintained at pH 6.5 had degraded significantly more than their counterparts at pH 7.4 ($p < 0.002$). This is in accordance with an extensive body of literature surrounding

polyphosphate degradation; hydrolytic degradation is known to be accelerated by reducing the pH of the environment [84]. After 14 days of degradation this effect is no longer present; the remnant coacervates in all groups released very few ions during the last week of degradation. At 28 days, there was no significant difference in mass loss between DOX-loaded PGMs degrading at pH 6.5 and 7.4.

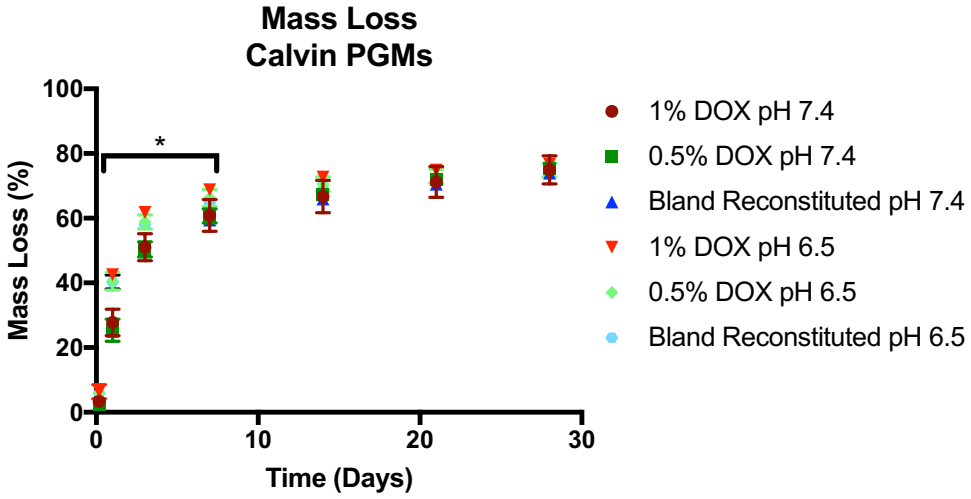

Figure 4.2 Cumulative 28-day mass loss of Calvin PGMs. 3 groups of PGMs (1% DOX loaded, 0.5% DOX loaded, and Bland Reconstituted) were used at each pH. 10mL pH 7.4 (TBS) and pH 6.5 (ACES) were used as elution media. Average values are plotted, with the error bars representing standard deviation (n = 7).

Compositional Ion Release

ICP analysis revealed the release profiles of each element: P, Ba, Cu, and Ca (Figure 4.3). All elements exhibited an initial burst release during the first 7 days of elution, followed by a slow release for the remaining elution period. After 28 days 70-80% of Cu^{2+} was released, approximately 45% of Ca^{2+}, and just 25% of Ba^{2+} was released. The release of ions from the coacervate is inversely proportional to their affinity for the polymer matrix, and these affinities correspond with coacervate properties [74]. Ba^{2+} forms very strong crosslinks with the polyphosphate chains; it is not easily released from degrading coacervate and increases coacervate viscosity [74]. Cu^{2+} is more loosely associated with the polyphosphates; it is easily rapidly released from degrading coacervate and tends to reduce viscosity. The effects of Ca^{2+} fall in between those of Ba^{2+} and Cu^{2+}.

Decreasing the pH of the elution media accelerated the burst release of each ion, corresponding to the differences in mass loss described above (Figure 4.2). The largest difference was seen with Cu^{2+} release. Significantly more Cu^{2+} was released from samples at pH 6.5 over the first 14 days ($p < 0.0002$). Differences in P release were less notable, and were only statistically significant at 4 hours, 1 day and 3 days ($p < 0.0001$). Ca^{2+} was also released more rapidly from samples at pH 6.5, achieving significant differences at 1 day, 3 day, and 7 day time points ($p < 0.0028$). Similarly, Ba^{2+} release was slightly accelerated in pH 6.5, with significant differences existing at 1-day, and 3-day time points ($p < 0.004$). DOX loading did not significantly alter the release of any of the elements at any of the time points tested, aside from Ba^{2+} at 3 days, 7 days, and 14 days. At these time points 1% DOX Calvin at pH 6.5 had released more Ba^{2+} than any other PGM group tested. However, given the high variability in these samples and the lack of differences at earlier or later time points, this was likely a Type I error (a statistically significant difference where no real difference exists).

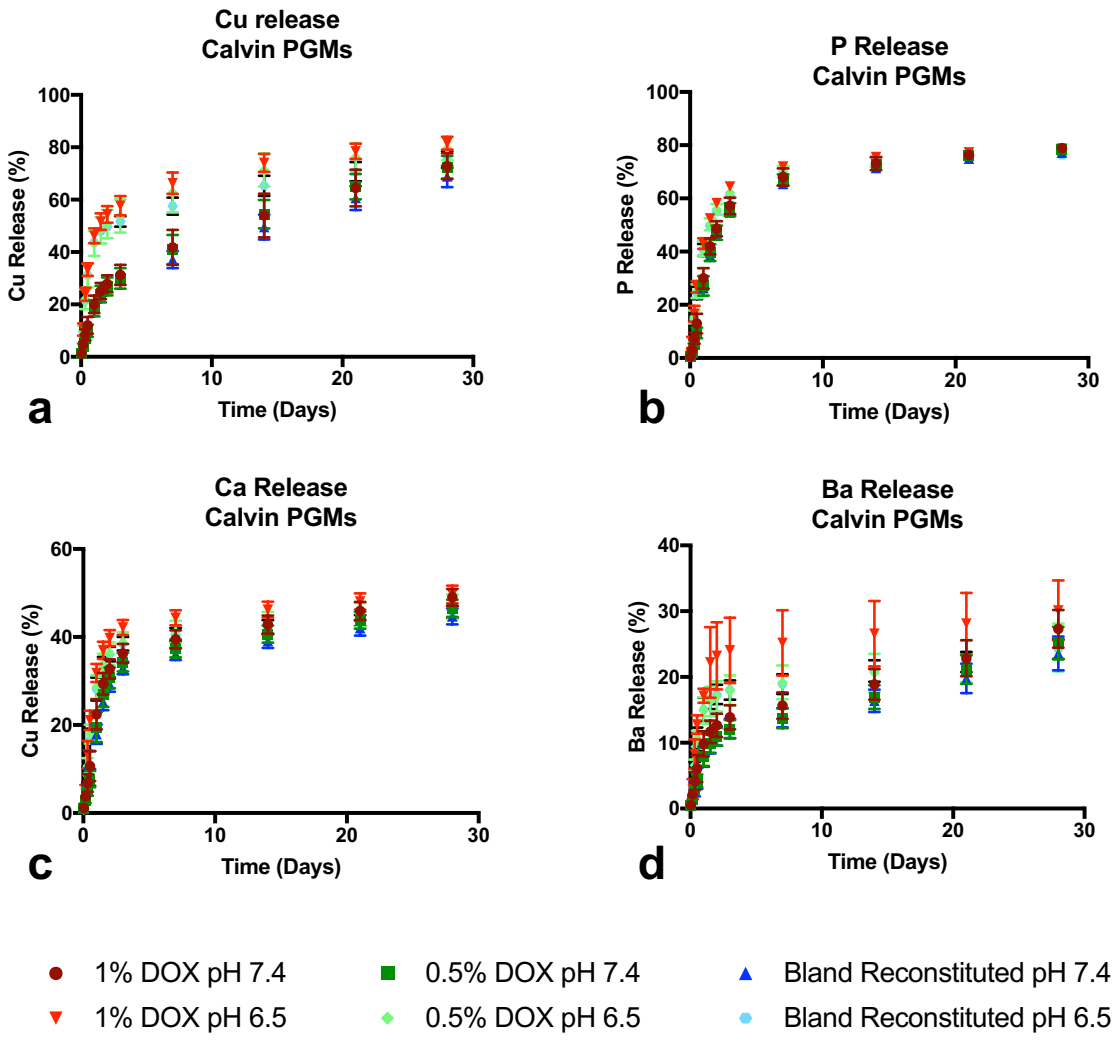

Figure 4.3 Cumulative Cu (a), P (b), Ca (c), and Ba (d) release from 1% DOX, 0.5% DOX and Bland Reconstituted Calvin PGMs degrading at pH 7.4 (TBS) and pH 6.5 (ACES). The average cumulative release of each ion over the 28-day elution period is shown, with error bars representing the standard deviation (n = 7).

In Vivo Correlations

pH 7.4 and 6.5 are very conservative estimates of the acidity that the material will be exposed to *in vivo*. Before any treatment, the tumour microenvironment is already slightly acidic within the range of pH 6.5-6.8, meaning that the buffering capacity of the extracellular fluid is already slightly overwhelmed [85, 86]. The purpose of embolization is to induce ischemic necrosis within the tumour; ischemic necrosis is known to cause a decrease in pH [87]. In addition, there will likely be some degree of foreign body response resulting from the introduction of PGMs into the blood vessel. Macrophages will attempt

to degrade the invading material through the release of H^+ and reactive oxygen species, contributing to the acidity of the environment [88]. Further driving down the pH of the microenvironment will be the degrading polyphosphate chains; the release of pyrophosphates and orthophosphates into the tumour microenvironment will also decrease the pH. The severity of the cumulative drop in pH will depend on the amount of circulation within the local environment. Presumably there will be washout of H^+ and degradation products on the proximal side of embolization. The distal side (closer to the tumour) will likely have minimal circulation, potentially exaggerating the drop in pH.

The ultimate effect of this drop in pH remains an interesting question. Intuitively, this acidity seems to compromise the biocompatibility of PGMs. However, taking into account the local delivery of the material, its proximity to the malignant tissue, and the fact that the goal of the treatment is to trigger tumour necrosis, all of these factors may end up enhancing the efficacy of the treatment, and ultimately benefit the patient. Alternatively, the acidity may exacerbate post-embolization syndrome in treated patients (a common side effect of TACE) [89]. This is an important consideration as PGM development moves into animal models. A method to assess post-procedural pain should be included in these studies, as well as histological measurements of cell damage and inflammatory markers. Subcutaneous implantation could also be used to assess the extent of damage caused by the material alone. In a past study, *in situ* forming calcium polyphosphate coacervate was implanted subcutaneously into a rabbit, and the results indicated only a minor increase in inflammatory markers after 14 days post-implantation relative to control materials [72]. This indicates that the relative contribution of PGM degradation products will likely be minimal, relative to the inflammatory and necrotic responses the procedure is meant to trigger.

In this study, DOX was released linearly, but only approximately 40% of loaded DOX was released over the 28-day period (Figure 4.1). In the highly acidic *in vivo* environment, significantly more DOX will likely be released from the degrading coacervate. Based on this study and the proposed mechanism of DOX release, as the pH of the environment decreases, more DOX will be liberated from the coacervate matrix. The polyphosphate degradation products are released rapidly over the first 3 days of degradation; during this time the inflammatory response and ischemic necrosis will also be

occurring. This drop in pH will presumably release a significant amount of DOX from the coacervate in the first 3 days. It is therefore possible that the *in vivo* release profile will be characterized by an initial burst, followed by a slower, sustained release thereafter rather than the linear profile observed *in vitro*. The question of how long a therapeutic dose of DOX will be administered to the cancerous tissue is difficult to answer based on this study. This therapeutic window depends on a number of factors: the size of the tumour, the depth of embolization, the circulation of extracellular fluid in the tumour microenvironment, the distance DOX is able to diffuse from the material, the impact of blood coagulation on the diffusion of DOX, and the pH mediated effects discussed above. These factors cannot be addressed with this study; *in vivo* testing, followed by extensive histological analysis will have to be used to answer some of these questions.

4.3.2 PGM Composition–Mediated Effects

DOX Release

DOX release rates from 1% DOX Calvin and 1% DOX Barry PGMs were compared over a 42-day period (Figure 4.4). Linear regression was performed on the curves, and a t-test comparing the slopes quantifiably determined that DOX is released more rapidly from Barry than Calvin PGMs ($p < 0.0001$). This suggests that hydrophobic-hydrophilic interactions play a role in DOX release. As described in Section 3.3.3, Barry coacervate is significantly more hydrophobic than Calvin. The higher Ba^{2+} content in Barry coacervates likely occupies more of the binding sites for mid-chain phosphate groups, reducing available space for water molecules in the coacervate matrix and leaving DOX to be more loosely associated with the hydroxyl groups on terminal phosphates. The more hydrophobic environment had a lower affinity for the hydrophilic cationic DOX molecule, and therefore expelled DOX from the coacervate at a faster rate than DOX encapsulated in Calvin. As described above, at pH 6.5 the vast majority of DOX molecules will be cationic, dissociating most of the hydrophobic-hydrophobic interactions between DOX and the Ba-P regions of the coacervate.

Extending the elution period from 28 to 42 days revealed what appears to be a plateau in the release profile. The release profiles were fitted to both linear and sigmoidal curves, with linear regression analysis achieving larger R^2 values compared to nonlinear

(sigmoidal) regression. However, it is very likely that if the elution period was extended for another week, the sigmoidal model would have been a better fit, as DOX release is slower between 28 and 42 days (Figure 4.4). By this time ion release from the coacervate is very minimal (Figure 4.4). It is possible that, at this point, all of the DOX associated with the terminal hydroxyl groups has been released, with the unreleased DOX remaining tightly bound to the coacervate matrix via electrostatic interactions with mid-chain phosphate groups.

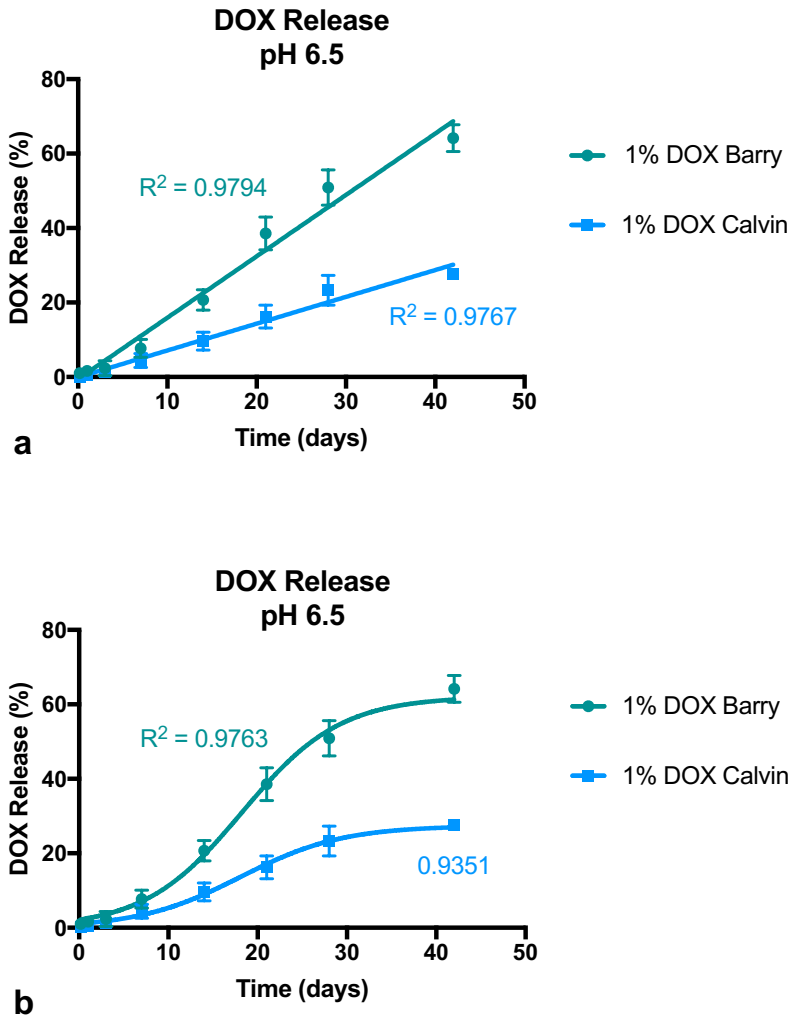

Figure 4.4 Cumulative DOX release from 1% DOX Barry (teal) and 1% DOX Calvin (pale blue) over a 42-day period, degrading in ABS at pH 6.5. Average values are plotted at each time point, and error bars represent standard deviation ($n \geq 3$). Curves were fitted via linear regression (a) and a variable-slope sigmoidal model (b).

PGM Mass Loss as a Function of Composition

This study was designed to evaluate differences in degradation rate between Barry and Calvin PGMs, and to determine the effect of DOX and the DOX loading process on PGM degradation rate. All PGM groups were observed to degrade via the same mechanism: an initial burst ion release during the first 7 days of degradation, followed by a slow release thereafter (Figure 4.5). No significant differences existed between samples sacrificed at 7 days or 14 days. Fresh Calvin PGMs sacrificed at 21, 28, and 42 days degraded significantly faster than all other PGM groups ($p < 0.05$). This was the only significant difference. This finding is in contrast to the original preliminary study characterizing PGM degradation (described in section 3.1), which indicated that Barry tended to degrade more quickly than Calvin over 21 days at pH 7.4. While the differences observed between Barry and Calvin PGMs prior to invoking a drug loading protocol is interesting, the fact that it is apparently mitigated by the reconstitution process makes it less important. Having the ability to synthesize PGMs with a range of degradation rates would be more commercially useful if these differences are retained after DOX-loading.

The difference in Calvin PGM degradation with and without reconstitution raises some interesting questions about the changes this process causes. It is possible that by removing the water and adding it back to the coacervate, the hydrophobic effect results in more tightly bound hydrophobic regions in the coacervate (presumably these areas would contain higher concentrations of Ba-P). The reconstituting water is likely unable to effectively penetrate into these regions of coacervate; this is supported by the reconstitution-caused increase in viscosity described in Section 3.3.3. After the conversion to PGMs and rehydration into coacervate during the degradation study, these tight bonds may be conserved. This would make it more difficult for water to penetrate into the material, relative to Fresh Calvin PGMs. This may account for the observed differences in degradation rate. This theory is supported by Figure 4.6, which indicates that Fresh Calvin released significantly more Ba and Ca than all other PGM groups. Notably, this did not occur for Barry PGMs. It is possible that this difference is not present with the Barry composition because of its high initial hydrophobicity. The fresh coacervate may contain such tightly bound hydrophobic regions that the process of reconstitution (for 48 hours)

ultimately does not increase the prevalence of the hydrophobic effect and therefore does not affect degradation.

The question of whether or not reconstitution degrades the polyphosphate chains remains unanswered. However, it seems unlikely that the chains underwent significant cleavage. If they had, reconstituted samples would likely have exhibited larger burst release of P in the degradation study. Additionally, in a previous study (unpublished data) in which calcium polyphosphate coacervate was loaded with minocycline by a similar reconstitution procedure, the chain length was not altered.

1% DOX Barry and 1% DOX Calvin PGMs degraded at the same rate, indicating that the difference in DOX release rate depicted in Figure 4.4 is not mediated by PGM degradation, providing further support for the hydrophobic-hydrophilic release mechanism proposed above.

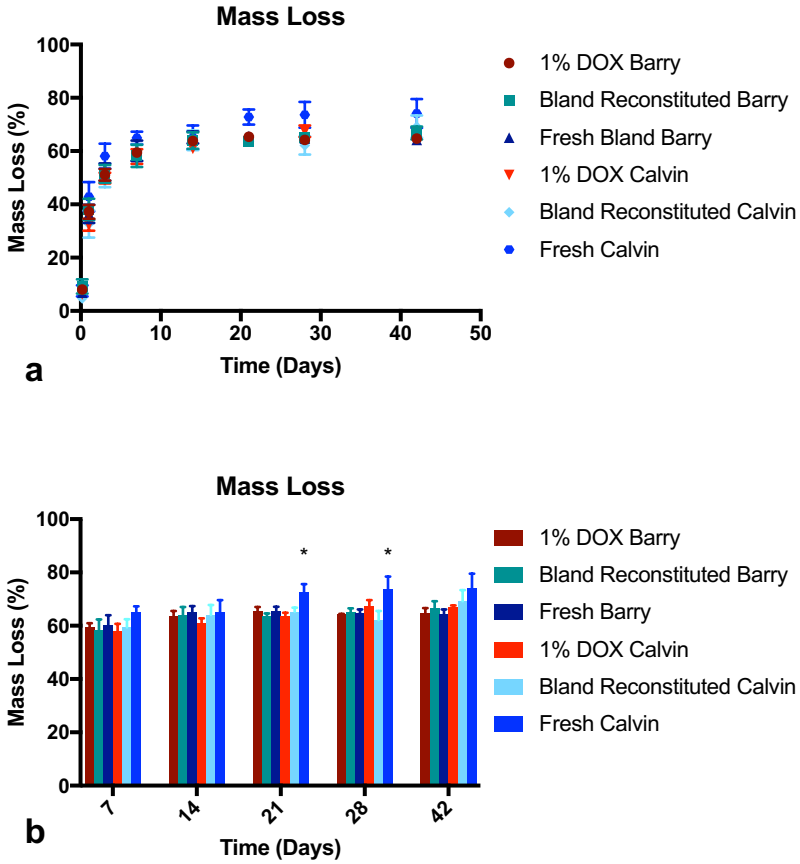

Figure 4.5. The cumulative degradation of PGM samples. (a) presents the cumulative mass loss over the full 42-day degradation period, while (b) presents a higher resolution mass loss data from samples sacrificed at 7 days, 14 days, 21 days, 28 days and 42 days ($n \geq 3$). * $p < 0.05$ analyzed via two-way ANOVA with Bonferroni multiple comparisons.

Compositional Ion Release

Barry and Calvin PGMs follow the same patterns of compositional ion release. Cu and P are released to the greatest extent, followed by Ca, and then Ba. The percent release of each element is displayed in Figure 4.6. In general, the percentage of total Cu, P, Ba, and Ca that was released from each PGM group was statistically equivalent. Fresh Calvin PGMs released a greater portion of their Ba and Ca content than every other PGM group; these were the only significant differences. With both compositions, degradation significantly decreased the Cu/P molar ratio ($p < 0.001$), and increased the Ba/P ($p < 0.001$) and Ca/P ($p < 0.001$) molar ratios (Figure 4.7). This further supports the theory that, in terms of crosslinking strength, Ba > Ca > Cu.

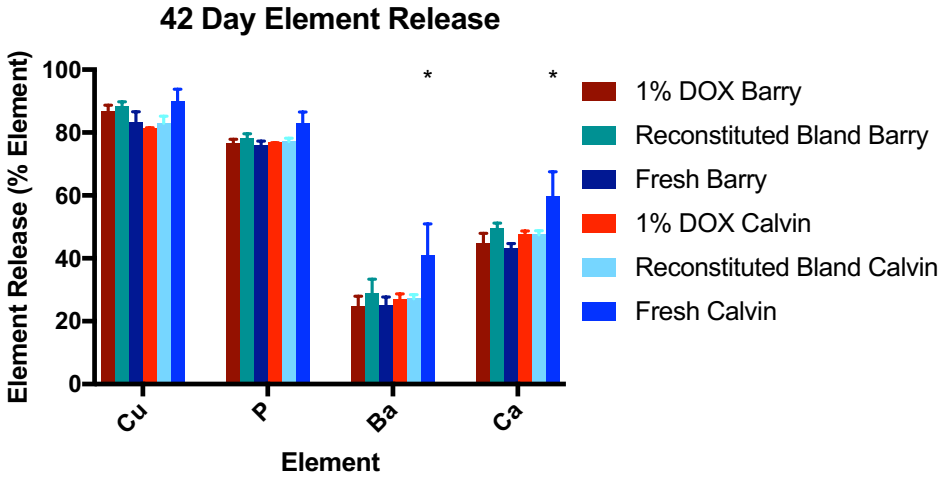

Figure 4.6 Cumulative element release, expressed as a percentage of the total element load, from each PGM group over a 42-day degradation period at pH 6.5. Average values were reported, with error bars representing standard deviation ($n \geq 3$). * $p < 0.05$ analyzed via two-way ANOVA with Bonferroni multiple comparisons.

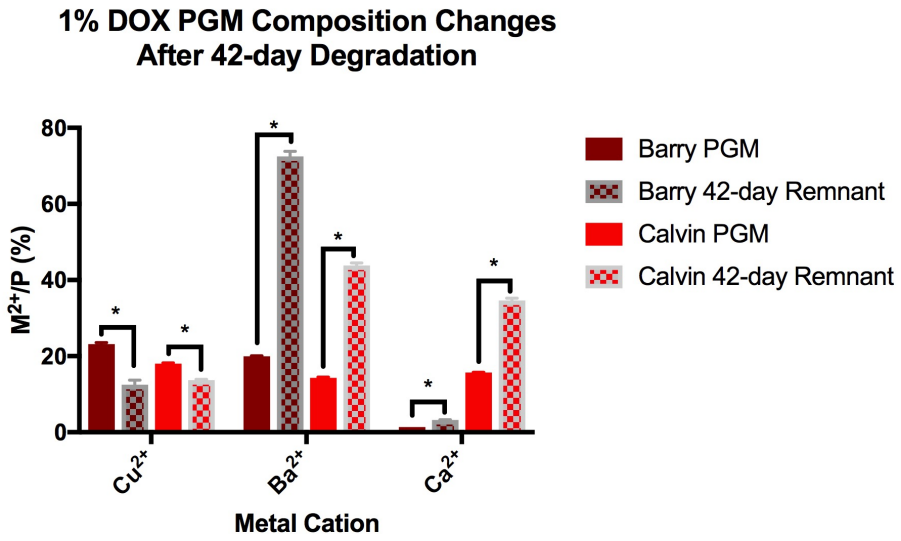

Figure 4.7 Composition, expressed as M^{2+}/P mol %, of 1% DOX loaded PGMs (solid red), and the corresponding coacervate remnant (checkered red) at the end of the 42-day degradation period. Average values were plotted, with error bars representing standard deviation (n = 3).* $p \leq 0.001$, analyzed via one-way ANOVA with Bonferroni multiple comparisons.

It is possible that ion release contributed to the acceleration of DOX release from Barry relative to Calvin. DOX loaded Barry and Calvin PGMs released the same percentage of their respective Cu^{2+} loads (Figure 4.6). Barry contains a higher initial Cu^{2+} load than Calvin, meaning that a greater mass of Cu^{2+} was released from Barry than Calvin. Given that DOX is known to form complexes with Cu^{2+}, it is possible that the greater efflux of Cu^{2+} from the Barry coacervate matrix may have contributed to the larger release of DOX [80]. However, it should be noted that the release profiles of DOX and Cu^{2+} are quite dissimilar; if Cu^{2+} complexing did play a role in DOX release it would be relatively minor compared to the proposed pKa and hydrophilic-hydrophobic mechanisms described above.

4.3.3 Elution Media Osmolarity

DOX Release

By comparing DOX elution data from the above pH and composition studies, an interesting NaCl-mediated difference in DOX release was observed (Figure 4.8) Recall that in the study of pH-mediated effects, NaCl was omitted from the elution media buffered at pH 6.5. In a subsequent study of composition-mediated effects, the elution media was buffered at pH 6.5 and contained 0.9% NaCl. 1% DOX Calvin PGMs degrading at pH 6.5

released DOX significantly faster when no NaCl was present in the elution media relative to an environment containing 0.9% wt NaCl. This is a particularly interesting finding because it indicates that DOX is not released via ion exchange with Na^+. The majority of DEB-TACE materials in development release DOX via ion exchange with Na^+; the most extreme example of this mechanism is seen with DC Beads™. These microspheres do not release DOX in ddH_2O; they require ions in solution to displace DOX from the polymer [19]. This is clearly not the case with PGMs. In fact, NaCl in the elution media appears to slow DOX release, suggesting that the rate of DOX release is partially controlled by the osmotic gradient between the coacervate matrix and the elution media. Increasing the osmotic gradient between the coacervate and the elution media may have led to relatively more water penetrating the polymer matrix. This is an interesting finding because it coincides with the classical theory behind non-Fickian Case II transport [90]. In this mechanistic explanation of zero-order drug release, it is theorized that as water penetrates the matrix of a glassy polymer, the polymer matrix undergoes relaxation leading to the liberation of encapsulated drug (Figure 4.9) [91]. In the case of PGMs, this mechanism does not encompass the full mechanism of drug release because it does not account for the observed pH effects. However, it is possible that decreasing the osmolarity of the elution media increased the penetration of water into the material, and that the increased water content allowed more DOX to be released.

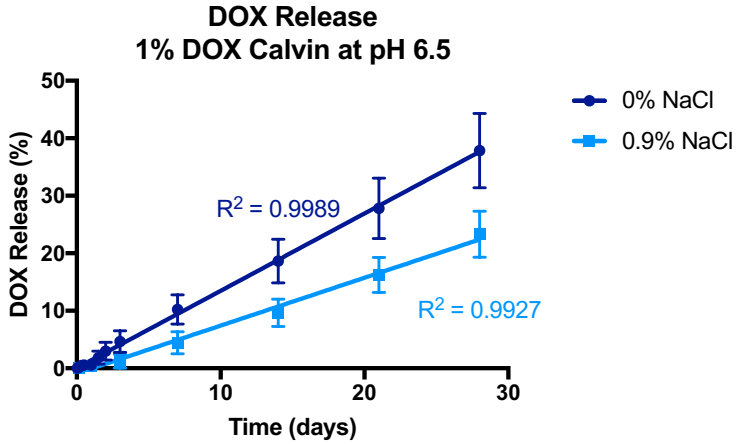

Figure 4.8 Cumulative DOX release from 1% DOX Calvin PGMs, degrading at pH 6.5 with 0.9% NaCl (pale blue) and without NaCl (dark blue). in the elution media. Average values were plotted at each time point, and error bars represent standard deviation ($n \geq 3$). R^2 values were calculated using linear regression.

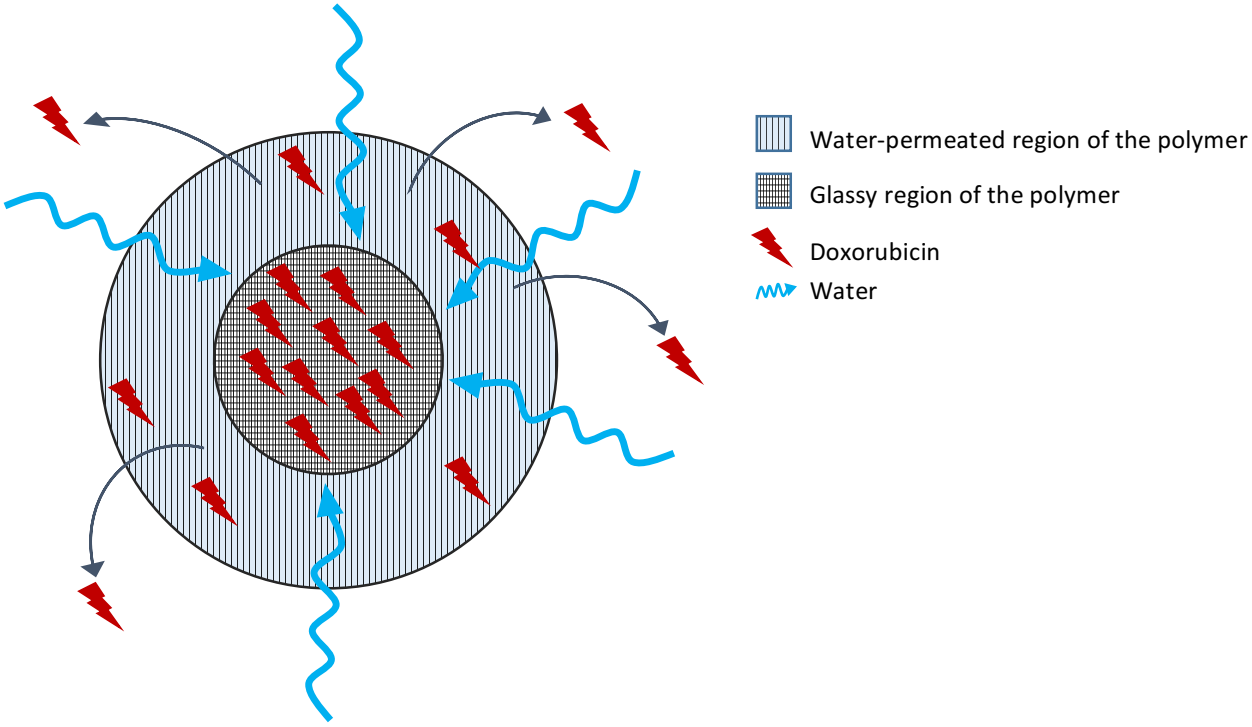

Figure 4.9 Schematic of Case II non-Fickian transport. Water penetrates the polymer as a front converging on the centre. The water acts as a plasticizer, decreasing the glass transition temperature of the polymer and facilitating relaxation.

PGM Mass Loss

While DOX-release was greatly influenced by the presence of NaCl in the elution media, PGM degradation was not (Figure 4.10). The only time point at which there was a significant difference in mass loss between 1% DOX Calvin PGMs degrading at pH 6.5 with and without NaCl occurred at 3 days ($p < 0.05$); at all other time points these PGMs degraded equivalently. This finding further refutes the hypothesis that DOX release is commensurate with PGM degradation. In this case, PGMs were degrading at the same rate yet releasing DOX at drastically different rates, emphasizing the apparent independence of these two processes.

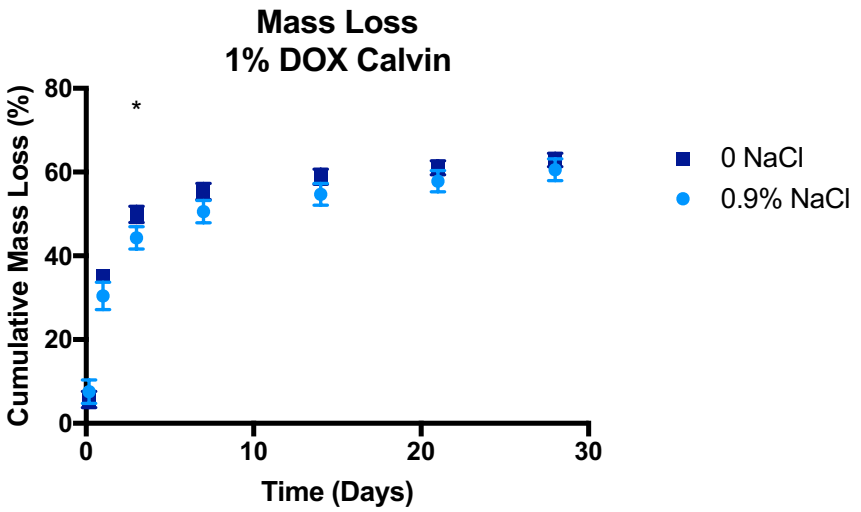

Figure 4.10 Cumulative 28-day degradation of 1% DOX Calvin PGMs at pH 6.5 with 0% NaCl (dark blue) and 0.9% NaCl (pale blue) in the elution media. Average values at each time point are shown, with error bars representing standard deviation ($n \geq 3$). * $p < 0.05$.

Compositional Ion Release

Comparing the release rates of Cu, P, Ba, and Ca from these samples of Calvin PGMs revealed very minimal differences (Figure 4.11). Cu and Ba cumulative release values were similar at all of the time points tested. P release was observed to be higher at 1-day and 3-days in the absence of NaCl, although the magnitude of the difference was small enough to be overcome by the 7-day time point. Ca release was greater in the absence of NaCl only at the 3 and 7-day time points. Overall, ion release from the coacervate matrix appeared to be minimally effected by NaCl, indicating that Na^+ plays no role in displacing these ions from the coacervate. Importantly, this finding eliminates the possibility that the diffusion of the degradation products through the dialysis tubing is controlled by the osmotic gradient of the elution media. This means that the differences observed in DOX release in Figure 4.7 are likely not caused by NaCl altering the ability of DOX to diffuse through the dialysis tubing.

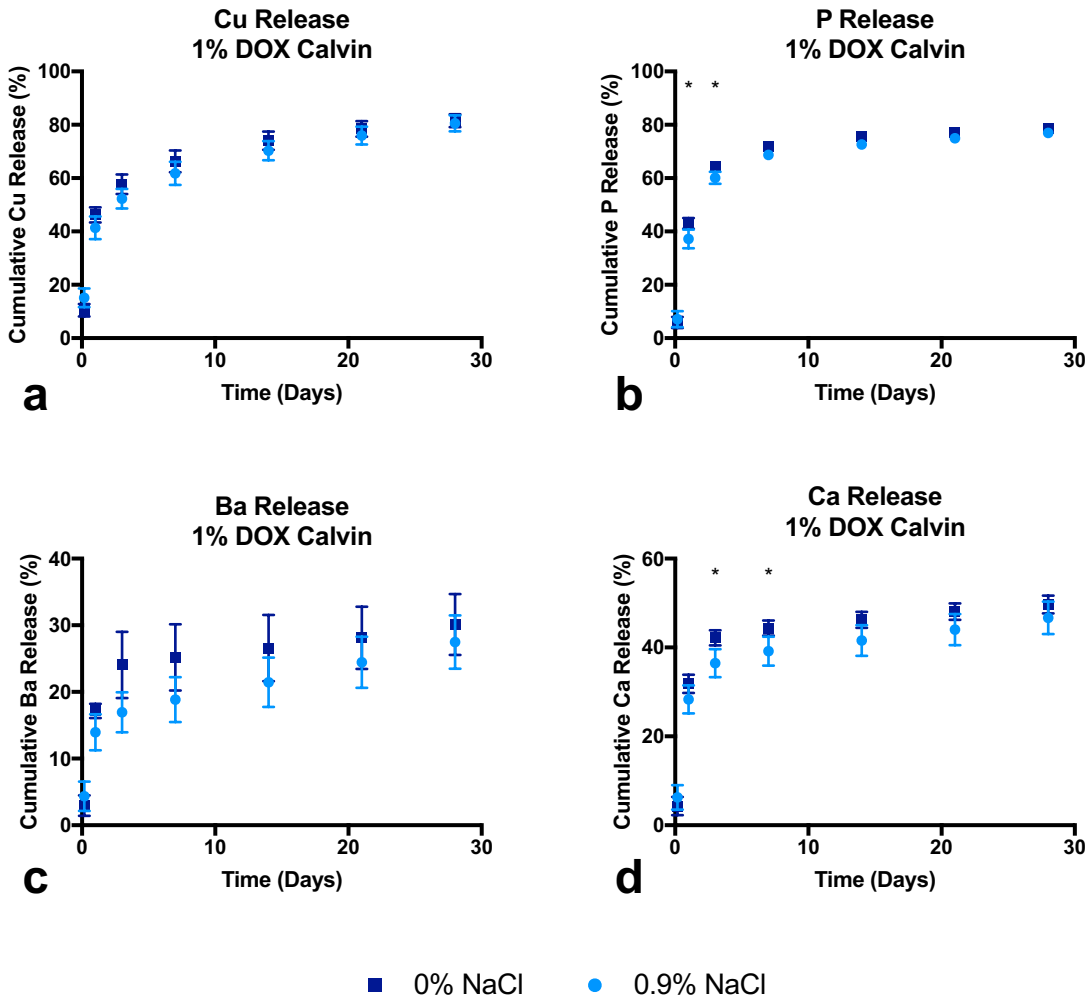

Figure 4.11 Cumulative release of each Cu (a), P (b), Ba (c), and Ca (d) from Calvin PGMs degrading at pH 6.5 with 0% NaCl (dark blue) and 0.9% wt NaCl (pale blue) in the elution media. Average values were plotted, with error bars representing standard deviation ($n \geq 3$). * $p < 0.05$ analyzed via multiple t-tests.

4.4 Concluding Remarks

This chapter evaluated the mechanisms underlying DOX release and PGM degradation. DOX release is highly dependent on the acidity of the elution media, requiring a pH below 7.4 before measurable quantities of DOX are detected in the elution media. DOX release is also accelerated by increasing the hydrophobicity of the coacervate polymer matrix and increasing the osmotic gradient in the elution media. At pH 6.5, DOX release is highly linear over a 28-day period, but approaching 42 days the release seems to plateau.

PGM degradation is not commensurate with DOX release. Instead, it is characterized by an initial burst of ion release during the first 7 days of degradation, followed by a very slow degradation thereafter. Decreasing the pH of the elution media from 7.4 to 6.5 moderately accelerated the initial burst phase, but did not alter the degradation of PGMs after 7 days. Elution media osmolarity, DOX loading, and PGM composition had minimal effect on PGM degradation; Barry and Calvin PGMs with and without DOX, and in elution media with or without NaCl, degraded at approximately the same rate.

Chapter 5: Degradation Product Biocompatibility and DOX Pharmacological Viability

5.1 Introduction

As described in chapter 1, a considerable gap in the literature exists when it comes to testing the efficacy of DOX after it has been loaded into and eluted from microspheres. Degradable microspheres composed of PEGMA, CMC/CCN, and PLGA have all been loaded with DOX for application in DEB-TACE, but the efficacy of released DOX was not reported [34, 61, 69]. For the PGM synthesis process under investigation here, it is important therefore to assess whether DOX retains its chemotherapeutic potential. There is some limited evidence suggesting that DOX may be susceptible to hydrolytic degradation, an important consideration given that DOX is exposed to an aqueous environment throughout the reconstitution process [37, 38]. In addition, there is potential exposure as well to an acidic pH in the coacervate matrix and elution media, and to organic solvents during PGM synthesis. Furthermore, DOX is known to form complexes with divalent cations, and these interactions may alter its efficacy. It was therefore crucial to ensure that the DOX loading and elution did not hinder the pharmacological viability of the drug.

In addition to verifying DOX activity, it was important to evaluate the cytotoxicity of the PGM degradation products. *In vitro* characterization of cytocompatibility is a typical first-step in implantable biomaterials development; it provides information about the kinds of risks that may be associated with the material as its development moves forward, and may be beneficial in explaining results seen in future *in vivo* studies. The degradation products of PGMs include pyrophosphates, orthophosphates, as well as the divalent cations required for initial coacervation (Ba^{2+}, Ca^{2+}, and Cu^{2+}). Notable cytocompatibility concerns exist surrounding the acidity of polyphosphate degradation, Ba^{2+}, and Cu^{2+}. Additionally, the potential presence of trace amounts of residual acetone and chloroform from PGM synthesis should be considered.

After investigating the mechanisms underlying DOX release and PGM degradation, the following study was conducted to test the cytocompatibility of PGM degradation products, and to verify the cytotoxicity of loaded and released DOX against an established cancer cell line.

5.2 Materials and Methods

5.2.1 Cell Viability

Cell Culture

Whole cell culture media was prepared by adding 50mL fetal bovine serum and 5mL of anti-bacterial/anti-fungal solution to 500mL of RPMI 1640 1X with L-glutamine (Sigma Aldrich). HepG2 cells (received from Dalhousie University Medicine, Saint John New Brunswick) were cultured in this media in 100mm petri dishes at 37°C and 5.0% CO_2. Cells were passaged upon reaching confluency; a 1:10 passage required 7 days to reach confluency. Assays were run on cells between passage 20-30.

Cell Treatment and MTT Assay

HepG2 cells were plated at 30,000 cells/well in 150µL of whole media in a 96 well plate and left overnight in the incubator to achieve 80% confluency. The following day, sterile treatment solutions of aqueous DOX (Sigma Aldrich), DOX elution media, bland elution media, PBS (VWR), or dimethyl sulfoxide (DMSO; Sigma Aldrich) were prepared. PBS was used as the negative control (100% cell viability), and DMSO was used as the positive control (highly cytotoxic). The media was suctioned out of each well, and 135µL of fresh whole media was added. 15µL of treatment solution was then added to each well to effectively create a 1:10 dilution (Figure 5.1). The cells were returned to the incubator for a treatment period of 24 hours.

	1	2	3	4	5	6	7	8	9	10	11	12
A												
B		DOX	DOX	Bland	Bland	PBS	PBS	DMSO	DMSO			
C		DOX	DOX	Bland	Bland	PBS	PBS	DMSO	DMSO			
D		DOX	DOX	Bland	Bland	PBS	PBS	DMSO	DMSO			
E		DOX	DOX	Bland	Bland	PBS	PBS	DMSO	DMSO			
F		DOX	DOX	Bland	Bland	PBS	PBS	DMSO	DMSO			
G		DOX	DOX	Bland	Bland	PBS	PBS	DMSO	DMSO			
H												

Figure 5.1 96-well plate layout for the MTT cell viability assays. 1:10 dilutions of DOX elution media (DOX), Bland elution media (Bland), PBS, and DMSO were administered (n = 12).

A standard MTT Assay was used to evaluate the cytotoxicity of each treatment solution, as per manufacturer's instructions [92]. A 5mg/mL solution of 3-(4,5-dimethylthiazol-2-yl)-2,5-diphenyltetrazolium bromide (MTT; Sigma Aldrich) dissolved in 0.1M PBS was created and sterilized via passage through a 0.20µm filter. 16.7µL of MTT was added to each well, and the plate was placed back in the incubator for 4 hours. This incubation allowed living cells to reduce MTT (a yellow dye) into formazan (a purple dye) intracellularly. After incubation, the media was removed from each well and 100µL DMSO was added to dissolve the intracellular formazan crystals. The plate was wrapped in aluminum foil to prevent photolytic degradation, and lightly agitated for 5 minutes at room temperature. Absorbance readings were then taken at 570nm, the peak absorbance of formazan. 'Cell viability' was calculated according to Equation 5.1, in which A_T is the average absorbance of the treatment group (aqueous DOX, DMSO, DOX elution media, or bland elution media) and A_C is the average absorbance of the negative control treatment (water or PBS). The cell viability of each treatment group was compared statistically via one-way ANOVA with Bonferroni multiple comparisons testing. The threshold for significance was set at $p < 0.05$.

$$\text{Cell Viability} = (A_T / A_C) \times 100\% \qquad \text{(Eq. 5.1)}$$

5.2.2 DOX LC_{50}

A 1000µM solution of DOX was prepared in sterile ddH_2O. This solution was serial diluted to 100µM, 50µM, 10µM, 1µM, and 0.1µM. An MTT assay was then performed as described above. Cells were treated with a 1:10 dilution of a standard DOX solution. DOX solutions were prepared immediately before treating the cells in order to minimize any potential degradation of the drug in solution. The negative control treatment (100% cell viability) was ddH_2O. Cell viability was plotted on a logarithmic scale and the LC_{50} (concentration that results in a 50% reduction in cell viability) was calculated using GraphPad Prism 7 software.

5.2.3 Degradation Product Cytocompatibility and DOX Activity

Elution Media Treatment Preparation

As there is no way of isolating DOX from the products of PGM degradation, DOX activity was assessed by allowing DOX loaded PGMs and Bland PGMs to degrade for 24 hours, and comparing the cytotoxicity of each elution media. In theory, with the same concentrations of Cu, Ba, P, and Ca, the elution media containing active DOX should be significantly more cytotoxic. 1% DOX PGMs and Bland Reconstituted PGMs were synthesized as described in section 3.2. Approximately 100µL of PGMs were transferred into dialysis tubing, freeze-dried, and placed in elution media as described in section 4.2.1. For this study, the elution media was 0.1M PBS at pH 7.4. Samples wrapped in aluminum foil were allowed to degrade in 10mL of media for 24 hours; this time period was enough for the acidic degradation products to overwhelm the buffering capacity of the media, decreasing the pH to approximately 3.2, thus facilitating DOX release.

Elution Media Analysis

The concentration of DOX in each elution sample was quantified by measuring the 480nm absorbance of the sample, as described in section 4.2.3. The concentrations of P, Ca, Cu, and Ba were measured with ICP-OES as described in section 4.2.3. After taking aliquots of the elution media for DOX and ion concentration measurements, the pH of each sample was quantified using an Accumet AB 15/15+ bench-top pH meter (Fisher

Scientific). Elution media was sterilized via filtration through a 0.20µm filter in preparation for cell treatment.

5.2.4 pH-Adjusted Degradation Product Cytocompatibility and DOX Activity

Elution media treatment samples were prepared and analyzed as described in section 5.2.3. After taking aliquots of each sample for analysis with absorbance and ICP-OES, all samples (DOX and Bland) underwent a pH adjustment to 7.2-7.4 via dropwise addition of 1M NaOH. Elution media was then sterilized via filtration through a 0.20µm filter in preparation for cell treatment.

5.3 RESULTS

5.3.1 DOX LC_{50}

The LC_{50} of DOX was 30.17µM, an order of magnitude larger than reported DOX LC_{50} [93]. The DOX used in this project was a secondary reference standard. Using this quality of DOX accounts for the reduced activity relative to the literature, and potentially compromises the ability to assess the impact of PGM processing on the drug, particularly higher grade DOX. Future studies need to be conducted with pharmacopeia grade DOX to fully determine if it retains its activity upon release.

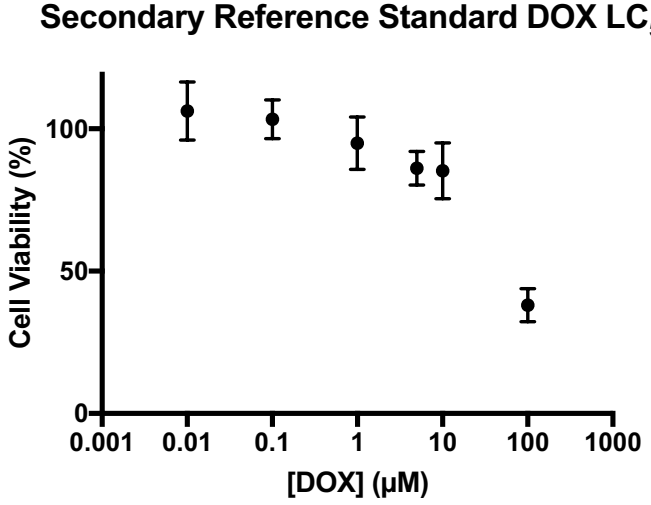

Figure 5.2 Cytotoxicity of freshly prepared aqueous DOX, treating HepG2 cells. Error bars represent standard deviations (n = 12).

5.3.2 Degradation Product Cytocompatibility and DOX Activity

The elution media from both 1% DOX and Bland Reconstituted Barry PGMs without pH-adjustment were significantly cytotoxic (Figure 5.3). Treating HepG2 cells with DOX elution media, bland elution media and DMSO yielded cell viabilities of 8.0 ± 1%, 14.6 ± 2.6%, and 2.9 ± 0.2%, respectively (n = 12). Significant differences existed between each of the three treatment groups ($p < 0.0001$). The concentration of DOX in the DOX treatment group was 1.3μM. The concentration of degradation products in each elution media treatment are shown in Table 5.1. DOX elution media contained slightly higher concentrations of each degradation product; the differences did not exceed 6.9ppm. Even with the presence of similar degradation product concentrations, DOX treatment was found to be significantly more cytotoxic than the bland counterpart, with a reduction in cell viability (6.6%) corresponding to the 5.1 (± 9.2)% reduction in cell viability observed with as-prepared 1μM DOX in the LC_{50} experiment (Figure 5.2). This indicates that DOX may have retained its activity after being loaded into and released from PGMs.

Of particular note is the incredibly low cell viability measurements in this experiment. Both elution media treatments killed the vast majority of cells in the assay. It is likely that the greatest contributor to this cytotoxicity was the pH of the elution media. Before the 1:10 dilution in the 96-well plate, the pH of DOX and bland elution media was approximately 3.2. Exposing the cells to such harsh pH conditions undoubtedly caused significant cytotoxicity. Whether or not the drop in pH associated with polyphosphate degradation will be clinically relevant with this application remains an interesting question, as was discussed at length in section 4.3.1.

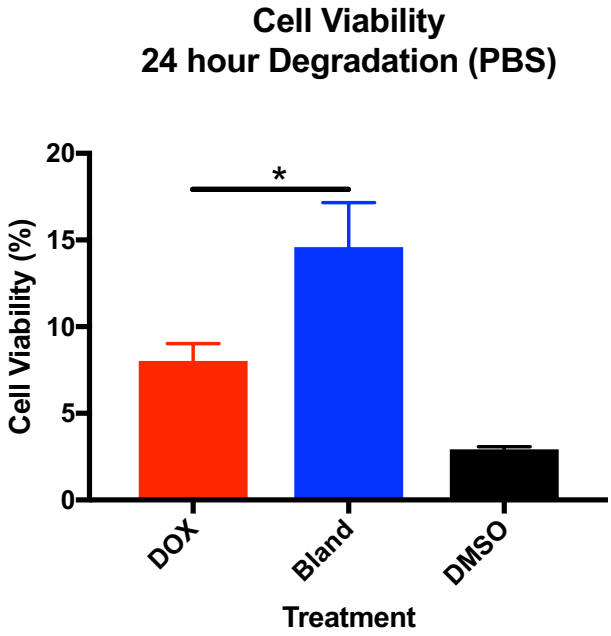

Figure 5.3 Cell viability of HepG2 cells treated with elution media from 1% DOX Barry PGMs (red), Bland Reconstituted Barry PGMs (blue), and DMSO for a 24-hour period. Average values were reported, with error bars representing the standard deviation (n = 12). * $p < 0.0001$ analyzed via one-way ANOVA with Bonferroni multiple comparisons.

Table 5.1 The concentrations of each degradation products in each elution media treatment, corresponding to the cytotoxicity data in Figure 5.1

Degradation Product Concentration (ppm)				
Treatment	**[Cu]**	**[P]**	**[Ba]**	**[Ca]**
DOX	42.5	110.5	31.7	1.4
Bland	37.9	103.6	31.0	1.2

5.3.3 pH-Adjusted Degradation Product Cytocompatibility and DOX Activity

To control for pH-mediated toxicity and to gain insight into the cytotoxicity of the other degradation components and potential residuals from PGM synthesis, an additional cell viability study was conducted in which the pH of the elution media was neutralized before treating the cells. As depicted in Figure 5.4, treating HepG2 cells for 24 hours with pH-adjusted DOX elution media, pH-adjusted bland elution media, and DMSO resulted in viability measurements of 51.3 ± 5.4%, 58.1 ± 5.0%, and 5.8 ± 0.1%, respectively (n = 12). Statistically significant differences were found between each treatment group ($p < 0.005$). DOX elution media contained 2.1μM of DOX, and (slightly) lower concentrations of Cu, P, Ba, and Ca than the bland elution media (Table 5.2). The fact that DOX treatment was

significantly more cytotoxic than the bland treatment despite having lower concentrations of Cu, P, Ba, and Cu, indicates that DOX retained at least some of its activity after loading and release from the PGMs. As with the more acidic conditions, the 6.8% difference in cell viability between Bland and DOX treatments corresponded approximately to reductions seen in the LC_{50} experiment; 1µM DOX decreased cell viability by 5.1%, and 5µM DOX decreased cell viability by 13.8%.

Degradation product concentrations were comparable to those in Table 5.1, aside from the higher concentrations of Ca present in the pH-adjusted experiment. Despite comparable concentrations of degradation products, the pH-adjusted elution media was far less cytotoxic than in elution media that did not undergo pH adjustment, indicating that a significant portion of the PGM degradation cytotoxicity is mediated by the acidity of the degrading polyphosphate chains.

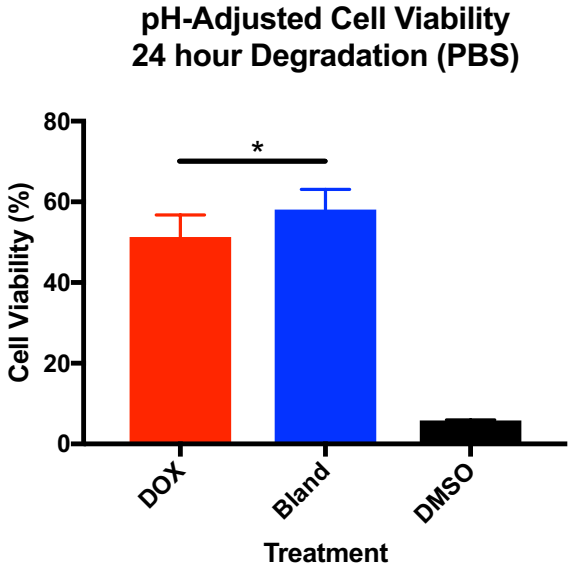

Figure 5.4 Cell viability of HepG2 cells treated with pH-adjusted elution media from 1% DOX Calvin PGM (red), elution media from Bland Reconstituted Calvin PGMs (blue), and DMSO for a 24-hour period. Average values were reported, with the error bars representing the standard deviation (n = 12). * $p < 0.005$ analyzed via one-way ANOVA with Bonferroni multiple comparisons.

Table 5.2 The concentrations of degradation products in each elution media treatment, corresponding to the cytotoxicity data in Figure 5.2.

Degradation Product Concentration (ppm)				
Treatment	**[Cu]**	**[P]**	**[Ba]**	**[Ca]**
DOX	38.6	111.1	26.7	19.3
Bland	45.2	125.45	29.1	20.1

5.4 Discussion

5.4.1 Eluted DOX Activity

The results of the cell viability assays seem to indicate that DOX does retain some cytotoxicity after being loaded into, and subsequently released from, PGMs. With and without adjusting the pH of the elution media, DOX elution media was significantly more cytotoxic than bland elution media despite having similar concentrations of degradation products. However, these results are not conclusive. A number of concerns exist surrounding the quality of the DOX used, and the potential for it to undergo degradation at various steps through the process of loading and release.

DOX Quality

The DOX used in this project was "Pharmaceutical Secondary Reference Standard." Bains et al. treated HepG2 cells with DOX for a period of 24 hours, and evaluated cell viability using the MTT assay [93]. Under these conditions, the average LC_{50} was 3.4μM [93]. The LC_{50} determined experimentally with the DOX used in these studies was 30.17μM (Figure 5.2). This indicates that the efficacy of the drug is suboptimal, even before being loaded into PGMs. Pharmacopeia Reference Standard drug will have to be tested moving forward.

DOX – Degradation Product Interactions

Interactions between DOX and PGM degradation products may also impact its pharmacological activity. These interactions have been shown to alter the efficacy of DOX against some cell lines. Monti et al. demonstrated that Cu^{2+}-DOX complexing limited the ability of DOX to enter rat cardiomyocytes *in vitro*, but did not have any effect on cytotoxicity against cancerous cell lines (HeLa and B16 melanoma) [94]. If this Cu^{2+}-DOX complexing affects the uptake of DOX into malignant hepatocytes, it could hinder its pharmacological activity. Notably, this complexing is known to dissociate in acidic environments, and so is less likely to occur in close proximity to degrading PGMs [80]. Additionally, interactions with the polyphosphate degradation products may alter the activity of DOX. Degrading polyphosphate chains decreased the pH of the elution media to approximately 3.2, meaning that essentially all of the DOX was positively charged. It is

possible that electrostatic interactions with the degraded, negatively charged polyphosphates may alter its uptake into the cells, or potentially preventing it from binding to its target sites (DNA and topoisomerase I/II).

Photolytic Degradation

In addition to interactions with PGMs degradation products, the pharmacological activity of DOX can be compromised by photolytic degradation. Wood et al. demonstrated that aqueous DOX degrades when exposed to ambient light, with 70% DOX degradation noted within a 7-day period [95]. When stored in the dark, only 10% of the drug was lost in the same period [95]. Some exposure to light is inevitable in the PGM synthesis process, especially during the water-in-oil emulsion, potentially subjecting the DOX to degradative conditions. Wrapping the degrading PGM samples in aluminum foil was meant to limit, at least, any exposure to light during the elution period.

Hydrolytic Degradation

DOX is also reported to be vulnerable to hydrolytic degradation. In saline at 37°C, DOX was shown to lose 13.1% of its concentration in 24 hours [37]. Another study found that concentration of DOX dissolved in PBS (pH 7.4) decreased by 24% in 24 hours at 37°C [96]. There were several periods during this experimental work where DOX was maintained in an aqueous environment, including the reconstitution period required for drug loading. Additionally, in the procedure described in section 5.2.1, PGMs were allowed to degrade for 24 hours before eluted DOX was tested on cells. The goal of this study was to determine if DOX was damaged during reconstitution or PGM synthesis. To limit any degradation that may occur during the elution period, it was important to test DOX as early as possible. This was made difficult by the slow release of DOX. To accelerate release, the buffering capacity of the elution media was allowed to be overwhelmed by the acidic degradation products, dropping the pH to approximately 3.2. Even with the drop in pH, a period of 24 hours was required to achieve a concentration of DOX that would be pharmacologically relevant after a 1:10 dilution. It is entirely possible that this 24-hour period of exposure to an aqueous environment may have hindered the pharmacological viability of DOX. In the future, potential DOX degradation during reconstitution could be

quantified by dissolving DOX-loaded coacervate with ethylenediaminetetraacetic acid (EDTA) prior to PGM production, and then treating cells with this DOX solution. Additionally, to minimize the elution period, a greater mass of PGMs could be used to achieve pharmacologically relevant quantities of DOX in a shorter period of time.

pH–Mediated Effects

The pH of the elution media may have impacted the chemical stability of DOX. Interestingly, the drop in the pH of the elution media may have been protective against degradation. Studies investigating the effect of pH on DOX degradation found that DOX reaches maximum stability at pH 4 [96, 97]. In an aqueous buffered solution at pH 4, less than 10% degradation occurred over a 40-hour period at 37°C [96]. Below pH 4, DOX is susceptible to acid-catalyzed hydrolysis and the rate of degradation is proportional to the acidity of the solution [98]. One study found that aqueous DOX stored at pH 2 and 37°C lost 26% in 24 hours [99]. The pH of the elution media was 3.2 at the end of the 24-hour degradation period. This means that as the PGMs degraded, decreasing the pH from 7.4 to 4, DOX was exposed to an increasingly protective environment; continued PGM degradation may have then led to the acid-catalyzed hydrolysis of DOX. Future DOX viability studies should consider utilizing solutions buffered at pH 4. This would allow DOX to be released rapidly from the PGMs while providing the DOX with a protective environment.

5.4.2 Cytocompatibility of Degradation Products

The pH of the elution media contributed significantly to the cytotoxicity observed in Figure 5.3. The elution media reached pH 3.2, resulting in significant reductions in cell viability. When the pH was adjusted to 7.2-7.4, the elution media still caused significant reductions in cell viability. This is likely due to high concentrations of Cu, Ba, and Ca in both elution media. Ca^{2+} is the most cytocompatible of the degradation products, showing negligible cytotoxicity at concentrations as high as 5600ppm when treating the MCF-7 breast cancer cell line [100]. Therefore, Ca^{2+} likely had minimal impact on the cytotoxicity of the elution media. In contrast, Cu^{2+} has well documented cytotoxicity, and its mechanisms of action have been characterized [101]. Cu^{2+} accumulates in intracellular

lysosomes, increasing production and release of reactive oxygen species, which then damage the mitochondria and trigger cell death [101]. The LC_{50} of a 24-hour treatment of $CuCl_2$ on HepG2 cells was found to be 80ppm, using the MTS viability assay [102]. When treating HL60 cells (an acute myeloid leukemia cell line) for 18 hours with $CuCl_2$, the trypan blue viability assay demonstrated an LC_{50} of 45ppm. The concentration of Cu^{2+} in the elution media treatments was within this range (Table 5.1 and 5.2), indicating that the Cu^{2+} released from the cells contributed to the reductions in cell viability seen in Figures 5.3 and 5.4.

Some literature indicates that $BaCl_2$ is less cytotoxic than $CuCl_2$ *in vitro* [103]. Ba^{2+} toxicity is primarily mediated through stimulation of muscle cells; its cytotoxicity depends on the type of cell it is being tested on [104]. When treating human urothelial cells, $BaCl_2$ is highly toxic, causing a significant drop in viability (according to an MTT assay) at a concentration of 1ppm [104]. At the same time, treating HepG2 cells with $BaCl_2$ showed no cytotoxicity using concentrations up to 68.7ppm, according to the In-Cell Western viability test [105]. The toxicity of Ba^{2+} is also highly dependent on its counter-ion. While $BaCl_2$ is considered to be cytotoxic, $BaSO_4$ is very generally considered to be cytocompatible [106]. $BaSO_4$ is commonly used to diagnose patients suffering from diverticular colon in a procedure known as a barium enema [107]. The cytocompatibility of $BaSO_4$ compared to $BaCl_2$ is caused by differences in solubility; $BaCl_2$ is highly soluble in water, while $BaSO_4$ is not. This raises an interesting question as to the state of released Ba. Ba is a very strong crosslinker of polyphosphates, making it very likely that Ba will be released in association with orthophosphates and pyrophosphates. This interaction may mitigate Ba^{2+} cytotoxicity. It is possible that these interactions may alter the cytotoxicity of released Cu^{2+} and Ca^{2+} as well.

5.4.3 Cytocompatibility of Residuals

In addition to possible concerns surrounding released Ba^{2+}, Ca^{2+}, and Cu^{2+}, there is the risk of residual chloroform and acetone from PGM synthesis. Risk can be described by Equation 5.1, where "Hazard" represents the danger associated with a substance, and "Exposure" represents the likelihood that the substance will come into contact with cells.

The risk associated with residual chloroform and acetone depends both on the toxicity of the chemical, and the likelihood that it will be present in the elution media.

$$\text{Risk} = \text{Hazard} \times \text{Exposure} \qquad \text{(Eq 5.1)}$$

Chloroform is highly toxic, representing a considerable hazard in the PGM synthesis process. However, the probability of chloroform ending up in the elution media is very low. After PGMs are synthesized they are washed twice in acetone, to remove residual chloroform. Then PGMs are sieved in a beaker containing 800mL of acetone; any residual chloroform will very likely be dissolved in the acetone. Although chloroform is a significant hazard, the probability of exposing cells to it is low enough to effectively mitigate the risk.

Acetone has been shown to have an *in vitro* LC_{50} is on the order of 39000ppm (~5% v/v), making it much less hazardous than chloroform [108]. The difference in risk is substantially less drastic, because the chances of trace acetone reaching the elution media are much higher for acetone than chloroform. PGMs are washed, sieved and stored in acetone, and are subsequently transferred into dialysis tubing in acetone for these studies. The freeze-drying of the dialysis tube samples should, in theory, remove the acetone from the sample. Acetone is highly volatile, and therefore should easily evaporate under the low pressure (0.45mBar) of the freeze-dryer. Under the current experimental set up, the elution media undergoes a 1:10 dilution when treating cells, meaning that the original elution media would have to consist of 50% (v/v) acetone to achieve the LC_{50} in the cell treatment. Therefore, it can be stated with certainty that the presence of acetone is not a significant contributor to the cytotoxicity seem in Figures 5.3 and 5.4. Moving forward, the presence of trace acetone and chloroform should be assessed using thermogravimetric–gas chromatography–mass spectrometer analysis.

5.4.4 In Vivo Correlations

pH–Mediated Effects

The results of this cytotoxicity study highlighted several important considerations as the development of PGMs moves toward the clinic. The acidity of the degradation

products and the potential cytotoxicity of released compositional ions will be need to be considered. The buffering capacity of 0.1M PBS at pH 7.4 and 37°C is 53.3mEq/L·pH, as per the Van Slyke equation (Equation 5.2), where β is the buffering capacity, C is the concentration of the buffer, and Ka is the acid dissociation constant of the buffer at that pH and 37°C. This means that the addition of 53.3mmol of H^+ to a 1L solution of 0.1M PBS will reduce the pH of solution by one unit. In the studies presented in this document, 10mL of 0.1M PBS was used, meaning that the buffering capacity of the system was 0.533mEq/pH. The buffering capacity of blood is 38.5mEq/ L·pH [109]. A conservative estimate of the diameter of intermediate stage HCC nodule is 3cm, as per the BCLC staging system [8]. This means that the volume of a tumour being treated with TACE is approximately 14.4mL, yielding a buffering capacity of approximately 0.554mEq/pH. This is a very imprecise approximation, but it does indicate that the buffering capacity of this *in vitro* system is somewhat similar to the *in vivo* environment. The finding that the acidic degradation products were sufficient to overwhelm the buffering capacity of the *in vitro* system emphasizes that this factor should be considered as PGM development moves forward. The *in vivo* implications of this acidity remain to be determined. The acidity could ultimately improve the efficacy of the treatment, as was discussed in some detail in section 4.3.1.

$$\beta = 2.303 \times C \times (Ka \times [H_3O^+]) / (Ka + [H_3O^+])^2 \qquad \text{(Eq. 5.2)}$$

Increasingly sophisticated animal studies may be needed to address this concern. Subcutaneous implantation, followed by histological analysis for inflammatory markers, will be important to verify the general biocompatibility of PGMs, as was done with *in situ*-forming calcium polyphosphate coacervate [72]. More interesting would be a study using the swine hepatic artery embolization model. This would place PGMs in the environment of an embolization, capturing interactions with blood and the clearance/build-up of degradation products. Analyzing this environment for pH and histological markers of inflammation would be a very informative study, building on the results of this *in vitro* cytotoxicity work.

Copper

In addition to concerns around acidity, the potential *in vivo* effects of Cu^{2+} are an important consideration. The liver is largely responsible for regulating Cu in the body [110]. The majority of Cu is cleared from the body through biliary clearance, and is rarely excreted through urine [111]. This means that, in theory, the delivery of a large dose of Cu directly to the liver may not result in increased systemic concentrations. In most cases, patients only receive TACE if their liver is maintaining sufficient normal function, meaning that these patients will likely have the capacity to clear Cu^{2+} released from PGMs. If the liver is able to clear Cu effectively, it should not pose a problem for the patient. If it is not cleared effectively, its cytotoxicity may result in the death of healthy liver cells, it may kill malignant cells in the liver, or it may promote malignancy in the tumour. The role of Cu in promoting cancer has been studied quite extensively in the literature. Increased serum Cu levels have been correlated with a number of cancers, as well as chemotherapeutic resistance [111]. Copper salts have been shown to stimulate endothelial cell proliferation and migration *in vitro* [112]. These, among other findings, have led to the development of copper chelators as anti-angiogenic drugs to treat cancer [113]. It is possible that the release of Cu^{2+} in PGMs may compromise their efficacy as a cancer treatment if the delivery of Cu^{2+} does in fact stimulate angiogenesis.

Barium

The potential effects of Ba *in vivo* are also important to consider. Ba toxicity is largely mediated through the dysregulation of K^{+}, specifically targeting a subclass of ion channel that is important in the function of muscles, the pancreas, and the kidney [114]. Ba is excreted mainly in feces, with a small percentage cleared in urine [115]. Ba is also known to form deposits in bone and teeth [115]. The toxicity of Ba depends on its counter-ion, and the pH of the solution [114]. It is possible that Ba released from PGMs will remain in complexes with the pyrophosphates and orthophosphates, effectively chelating Ba and preventing it from exerting its cytotoxic effects. It is also possible that the acidic microenvironment will dissociate these complexes, increasing Ba-mediated toxicity. The local delivery of Ba to the liver may help to mitigate its toxicity, especially if the liver is healthy enough to clear it through bile. As PGMs degrade, the Ba/P molar ratio increases.

Ultimately, this may lead to the formation of Ba-P flocculent in the blood vessel, which could migrate from the embolization sight and lead to an off-target embolization, weeks after the original TACE procedure. It is also possible that remnant flocculent will be phagocytosed and solubilized by macrophages. Long-term animal studies should be designed to investigate the ultimate fate of the degraded coacervate.

5.4 Concluding Remarks

This chapter evaluated cytocompatibility of PGM degradation products, and the pharmacological viability of released DOX. The elution media from DOX loaded PGMs was significantly more cytotoxic than that of bland PGMs, indicating that DOX retained at least some of its pharmacological viability through the process PGM synthesis and degradation. This is a promising result, especially considering the poor quality of drug used and its exposure to the aqueous, acidic environment needed to facilitate its rapid release. As PGMs continue to be developed for application in DEB-TACE, a higher quality of DOX will be necessary to quantify the extent of degradation (if any) caused by the PGM synthesis process.

The results of the cytotoxicity studies indicate that the degradation products of PGMs under the conditions studied are significantly cytotoxic, having reduced the cell viability by more than 30% [116]. The cytotoxicity is partially mediated by the pH of polyphosphate degradation, and partially by the compositional ions released from the PGMs. Ca is ubiquitous in the human body and is highly cytocompatible, meaning that it likely contributed minimally to the cytotoxicity observed. The degradation product-mediated cytotoxicity was largely attributed to Ba and Cu, as they are known cytotoxins. As PGM development continues to progress, animal models will be necessary to evaluate the ultimate physiological relevance of these concerns, especially within the context of DEB-TACE. The findings of this chapter will help in the design of future *in vivo* experiments, and will help in the interpretation of the results of these studies.

Chapter 6: Conclusion

6.1 Final Comments

This thesis contributed to the development and understanding of DOX-loaded PGMs for the intended application of DEB-TACE to treat HCC. A procedure to introduce DOX to the NaPP–Ca^{2+}–Ba^{2+}–Cu^{2+} system was developed. This process resulted in significant changes in coacervate viscosity that had to be compensated for in the emulsion conditions. This provided an opportunity to gain insight into the impact of each emulsion parameter on the shape and size of the microspheres. These new insights allowed the emulsion parameters to be optimized for each composition, yielding reasonably spherical particles in the clinically relevant size range. More importantly, these insights will provide a framework for the kinds of adjustments that will need to be made in the future when higher quantities of drug are loaded into coacervate, different drugs are introduced, and the production undergoes scale-up.

The degradation and drug release properties of PGMs were then studied *in vitro*. Surprisingly and excitingly, DOX release is linear and highly dependent on the pH of the elution environment. The ability to release drug at a constant rate over an extended period of time has potential to greatly improve the efficacy of DEB-TACE and certainly justified the continued pursuit of this project.

Finally, an investigation into the cytocompatibility of degradation products was able to identify several areas of potential concern as the development of PGMs continues. DOX seems to retain at least some of its pharmacological viability, but further studies are needed to quantify any molecular or structural changes that may be occurring in this therapeutic agent. The cytotoxicity of the degradation products was mediated by a combination of acidity related to the degrading polyphosphates, and released M^{2+}, with the possibility of contributions from residual chloroform and acetone. The physiological relevance of this cytotoxicity requires further study with animal models of embolization, but they are important considerations and will contribute to the design and interpretation of these future studies.

6.2 Hypotheses Revisited

6.2.1 Process Development and Characterization

Hypothesis 2.1.1: Doxorubicin-loaded coacervate will maintain the appropriate viscosity to form spherical, 100-300μm polyphosphate glass microspheres using the water-in-oil emulsion technique

DOX-loaded coacervate was successfully synthesized formed into PGMs using the water-in-oil emulsion technique. The reconstitution process did increase the viscosity of the coacervate, but this viscosity remained low enough to be emulsified under the appropriate conditions.

Hypothesis 2.1.2: Doxorubicin-loading will displace divalent metal cations from the coacervate, thereby altering the chemical composition of the polyphosphate glass microspheres

DOX-loading did not alter the chemical composition of the PGMs. Instead of displacing divalent cations from the coacervate, DOX was thought to be loaded by occupying niches in the coacervate that were otherwise occupied by water.

Hypothesis 2.1.3: The effects of doxorubicin loading on chemical composition and coacervate properties will vary with polyphosphate glass microsphere composition

The process of loading DOX through reconstitution increased the viscosity of both compositions. The effects were more exaggerated with Barry, presumably because of its higher initial viscosity, and lower water content.

6.2.2 Degradation and DOX Release

Hypothesis 2.2.1: Doxorubicin-loading will not alter the in vitro degradation rate of polyphosphate glass microspheres

DOX did not alter the degradation of either composition of PGM. Reconstitution did selectively decrease the degradation of higher Ca-containing (Calvin) PGMs.

Hypothesis 2.2.2: Doxorubicin release will be commensurate with PGM degradation

DOX release was not commensurate with PGM degradation. At pH 7.4 and pH 6.5, both compositions of PGMs exhibited an initial rapid phase of degradation over the first 7 days, followed by a slow compositional ion release thereafter. Contrarily, DOX release was

dependent on the pH of the elution media, exhibiting highly linear release at pH 6.5 and negligible release at pH 7.4 from both compositions.

Hypothesis 2.2.3: Degradation, and therefore drug release rate, are pH-dependent

Decreasing the pH of the elution media accelerated only the initial phase of PGM degradation. In contrast, DOX release is highly dependent on the pH of the elution media.

6.2.3 Cytocompatibility and Pharmacological Activity

Hypothesis 2.3.1: Doxorubicin released from loaded polyphosphate glass microspheres will retain its pharmacological activity

Released DOX appeared to retain at least some of its pharmacological activity despite a low overall drug quality (lower as-reconstituted activity) and potentially damaging elution conditions.

Hypothesis 2.3.2: Polyphosphate glass microsphere degradation products will be cytocompatible

PGM degradation products were cytotoxic under the conditions studied (24-hour elution with no media change). This cytotoxicity was attributed to a combination of the acidity of polyphosphate degradation and the release of compositional ions from the PGMs.

6.3 LIMITATIONS OF THE CURRENT WORK

6.3.1 Process Development and Characterization

There is a lot of uncertainty surrounding the ideal characteristics of resorbable microspheres for use in DEB-TACE to treat HCC. The optimal degradation time remains poorly defined in the literature. This uncertainty confounds the design criteria outlined in this project; the 4 week targeted degradation time arose from key opinion leaders in the field, but was not supported substantially by the literature. Additionally, the uncertainly surrounding the optimal size range of the microspheres limited this work, as it focused primarily on the 100-300μm size fraction. Clinically, bead sizes are trending downward for treating HCC with DEB-TACE, and so designating the 75-150μm size fraction as the targeted size output may be beneficial as the project moves forward.

The emulsion conditions were optimized through a process of trial and error. Key variables were identified and optimized one at a time. This method did not allow for interactions between the variables to be elucidated. Moving forward, the Design of Experiments software could be used to further optimize the emulsion conditions, with specific focus on water volume, mixing speed, and injection rate. This would allow for interactions between these variables to be clarified.

In terms of the characterization of the beads, the use of SEM was limited in that it is impossible to determine with certainty if the dark spots on the 1% DOX Barry microspheres were pits in the bead surface, or regions of highly concentrated barium that would indicate phase separation. Investigation with energy-dispersive X-ray spectroscopy may help to resolve this limitation. Additionally, the quantification of PGM loading capacity and encapsulation efficiency was limited by the selective use of the 100-300μm fraction, and the imprecise measurement of coacervate volume and resulting PGM mass.

6.3.2 Degradation and DOX Release

The *in vitro* degradation experiments were limited in their ability to accurately simulate the *in vivo* environment. The diameter of the dialysis tubing is approximately 0.6cm, while the blood vessels the beads will be injected into may be as small as 100μm in diameter. *In vivo*, the material will have a much larger surface area to volume ratio than was present in these studies. This will likely accelerate the degradation and DOX release. Biological factors that will have a substantial impact on the degradation of the material will also be present *in vivo*. Lysozymes, phosphatases, phagocytic cells, the local drop in pH associated with the degradation of the material, and the pH of the inflammatory reaction will all likely accelerate the degradation of the material, while clotting factors and fibrotic inflammation may ultimately slow the degradation. None of these factors were captured in this project, and the results presented are therefore limited.

6.3.3 Cytocompatibility and Pharmacological Activity

Elution media was prepared using 100mg of material in 10mL of media, yielding a mass to volume ratio of 10mg/mL, and this media then underwent a 1:10 dilution in the 96-well plate. ISO 10993-5 recommends up to 100mg/mL with no media dilution [116].

This means that the mass to volume ratio used in this study was relatively low. The evaluation of the pharmacological viability of the released DOX was limited by the cytotoxicity of the degradation products, the potential of residuals from PGM synthesis, potential interactions between each of these components, and the low grade of DOX used as was discussed at some length.

The cells used in these assays may be cause for some concern. Standard practice is to use cells with relatively low passage number (5-10). In this study, the HepG2 cells were at relatively high passage numbers (20-30) when the assays were conducted. This high passage number may have resulted in epigenetic or genetic changes in the cell line, potentially altering their susceptibility to the eluted drug and degradation products. Additionally, the subtype of HepG2 cells is unknown. HepG2 cell lines can vary according to the CYP450 enzymes they express. These enzymes may alter the metabolic activity of the cells, and therefore change their susceptibility to cytotoxins.

6.4 Recommendations for Future Work

6.4.1 Process Development and Characterization

DOX Loading

The process of loading DOX through reconstitution has some room for improvement. Making spherical, 100-300μm PGMs is difficult due to the large increase in coacervate viscosity that occurs in the current procedure. The increase in viscosity may be due to removal of structural water in the coacervate that is not replaced through reconstitution. It is possible that by freeze-drying the coacervate just long enough to remove only the loosely bound water, DOX could be added through reconstitution with minimal change in viscosity. Minimizing the change in coacervate viscosity caused by DOX loading would ease PGM synthesis. Additionally, loading higher quantities of DOX will be important moving forward. To achieve levels currently used in DC Beads, 37.5mg should be loaded into 1mL coacervate. The emulsion conditions will need to be optimized to coacervate loaded with this quantity of DOX.

PGM Stability/Deliverability

PGM stability in saline and Sr^{2+}-doped solutions has been quantified for bland PGMs, but never for DOX-loaded PGMs. Some concerns exist surrounding the deliverability of PGMs, as they tend to agglomerate together while being suspended in saline before injection through a microcatheter. This aggregation was mitigated when suspended in a 50:50 mixture of contrast and saline. The stability of DOX-loaded PGMs needs to be assessed under similar conditions to ensure that they will not agglomerate in the syringe or catheter during injection. Additionally, irregularly shaped particles will impede the deliverability of the microspheres, meaning that the emulsion conditions will have to be further optimized to maximize the sphericity of PGMs. Optimizing the reconstitution process will help increase sphericity, as will further optimization of the emulsion parameters. Focusing on the 75-150μm size fraction would also greatly ease the production of spherical beads.

6.4.2 Degradation and DOX Release

In Vitro Degradation Study

In order to verify the proposed mechanism of DOX release, and to further characterize the effect of pH on PGM degradation, another *in vitro* degradation study in buffered saline at pH 5.5 should be conducted. The inflammatory response has been shown to decrease pH to values as low as 5.5; this might more accurately simulate the environment the material will be exposed to *in vivo* [88].

6.4.3 Cytocompatibility and Pharmacological Activity

In Vitro DOX Pharmacological Activity

A study needs to be conducted to further verify the activity of released DOX. Pharmacopeia Reference Standard quality DOX needs to be used. An *in vitro* cell viability should be conducted as described in section 5.2. In order to shorten the time that released DOX is exposed to the aqueous, acidic elution environment, a larger PGM sample could be used. This would allow for pharmacologically relevant quantities of DOX to be released more rapidly. If the elution period could be limited to 4 hours, the potential for acidic degradation would ideally be negligible. In this study, a control group treated with aqueous

DOX equal in concentration to the DOX in the elution media should be included. If DOX was not cytotoxic under these conditions, further investigation would be warranted to determine where in the PGM synthesis process the degradation occurred.

In Vivo Study

An animal model for embolization should be used to evaluate the *in vivo* performance of PGMs. Although expensive, the swine hepatic embolization is a very good simulation of a human TACE procedure given that swine vasculature is relatively very similar to that of a human. This study would allow for quantification of PGM deliverability, *in vivo* radiopacity, biocompatibility, ability to form robust embolizations, *in vivo* degradation, and potentially drug release rates and pharmacokinetics.

References

[1] J. Ferlay, I. Soerjomataram, R. Dikshit, S. Eser, C. Mathers, M. Rebelo, D.M. Parkin, D. Forman, F. Bray, Cancer incidence and mortality worldwide: sources, methods and major patterns in GLOBOCAN 2012, Int J Cancer 136(5) (2015) E359-86.

[2] M.C. Wong, J.Y. Jiang, W.B. Goggins, M. Liang, Y. Fang, F.D. Fung, C. Leung, H.H. Wang, G.L. Wong, V.W. Wong, H.L. Chan, International incidence and mortality trends of liver cancer: a global profile, Sci Rep 7 (2017) 45846.

[3] M.M. Center, A. Jemal, International trends in liver cancer incidence rates, Cancer Epidemiol Biomarkers Prev 20(11) (2011) 2362-8.

[4] J.F. Perz, G.L. Armstrong, L.A. Farrington, Y.J. Hutin, B.P. Bell, The contributions of hepatitis B virus and hepatitis C virus infections to cirrhosis and primary liver cancer worldwide, J Hepatol 45(4) (2006) 529-38.

[5] W. Blonski, D.S. Kotlyar, K.A. Forde, Non-viral causes of hepatocellular carcinoma, World J Gastroenterol 16(29) (2010) 3603-15.

[6] H.T. Sorensen, S. Friis, J.H. Olsen, A.M. Thulstrup, L. Mellemkjaer, M. Linet, D. Trichopoulos, H. Vilstrup, J. Olsen, Risk of liver and other types of cancer in patients with cirrhosis: a nationwide cohort study in Denmark, Hepatology 28(4) (1998) 921-5.

[7] J. Bruix, M. Sherman, D. American Association for the Study of Liver, Management of hepatocellular carcinoma: an update, Hepatology 53(3) (2011) 1020-2.

[8] J.M. Llovet, C. Bru, J. Bruix, Prognosis of hepatocellular carcinoma: the BCLC staging classification, Semin Liver Dis 19(3) (1999) 329-38.

[9] R. Iezzi, M. Pompili, A. Posa, G. Coppola, A. Gasbarrini, L. Bonomo, Combined locoregional treatment of patients with hepatocellular carcinoma: State of the art, World J Gastroenterol 22(6) (2016) 1935-42.

[10] S.F. Altekruse, K.A. McGlynn, M.E. Reichman, Hepatocellular carcinoma incidence, mortality, and survival trends in the United States from 1975 to 2005, J Clin Oncol 27(9) (2009) 1485-91.

[11] R. Lencioni, P. Petruzzi, L. Crocetti, Chemoembolization of hepatocellular carcinoma, Semin Intervent Radiol 30(1) (2013) 3-11.

[12] A. Schlachterman, W.W. Craft, Jr., E. Hilgenfeldt, A. Mitra, R. Cabrera, Current and future treatments for hepatocellular carcinoma, World J Gastroenterol 21(28) (2015) 8478-91.

[13] O. Matsui, Imaging of multistep human hepatocarcinogenesis by CT during intra-arterial contrast injection, Intervirology 47(3-5) (2004) 271-6.

[14] K. Takayasu, Y. Shima, Y. Muramatsu, N. Moriyama, T. Yamada, M. Makuuchi, H. Hasegawa, S. Hirohashi, Hepatocellular carcinoma: treatment with intraarterial iodized oil with and without chemotherapeutic agents, Radiology 163(2) (1987) 345-51.

[15] T. de Baere, Y. Arai, R. Lencioni, J.F. Geschwind, W. Rilling, R. Salem, O. Matsui, M.C. Soulen, Treatment of Liver Tumors with Lipiodol TACE: Technical Recommendations from Experts Opinion, Cardiovasc Intervent Radiol 39(3) (2016) 334-43.

[16] R. Lencioni, T. de Baere, M. Burrel, J.G. Caridi, J. Lammer, K. Malagari, R.C. Martin, E. O'Grady, M.I. Real, T.J. Vogl, A. Watkinson, J.F. Geschwind, Transcatheter treatment of hepatocellular carcinoma with Doxorubicin-loaded DC Bead (DEBDOX): technical recommendations, Cardiovasc Intervent Radiol 35(5) (2012) 980-5.

[17] L. Marelli, R. Stigliano, C. Triantos, M. Senzolo, E. Cholongitas, N. Davies, J. Tibballs, T. Meyer, D.W. Patch, A.K. Burroughs, Transarterial therapy for hepatocellular carcinoma: which technique is more effective? A systematic review of cohort and randomized studies, Cardiovasc Intervent Radiol 30(1) (2007) 6-25.

[18] Q.V. Nguyen, J.S. Lym, C.T. Huynh, B.S. Kim, H.J. Jae, Y.I. Kim, D.S. Lee, A novel sulfamethazine-based pH-sensitive copolymer for injectable radiopaque embolic hydrogels with potential application in hepatocellular carcinoma therapy, Polym Chem-Uk 7(37) (2016) 5805-5818.

[19] A.L. Lewis, M.V. Gonzalez, A.W. Lloyd, B. Hall, Y. Tang, S.L. Willis, S.W. Leppard, L.C. Wolfenden, R.R. Palmer, P.W. Stratford, DC bead: in vitro characterization of a drug-delivery device for transarterial chemoembolization, J Vasc Interv Radiol 17(2 Pt 1) (2006) 335-42.

[20] P.J. Johnson, C. Kalayci, N. Dobbs, N. Raby, E.M. Metivier, L. Summers, P. Harper, R. Williams, Pharmacokinetics and toxicity of intraarterial adriamycin for hepatocellular carcinoma: effect of coadministration of lipiodol, J Hepatol 13(1) (1991) 120-7.

[21] W.M. Melia, P.J. Johnson, R. Williams, Induction of remission in hepatocellular carcinoma. A comparison of VP 16 with adriamycin, Cancer 51(2) (1983) 206-10.

[22] T. Clark, S. Maximin, J. Meier, S. Pokharel, P. Bhargava, Hepatocellular Carcinoma: Review of Epidemiology, Screening, Imaging Diagnosis, Response Assessment, and Treatment, Curr Probl Diagn Radiol 44(6) (2015) 479-86.

[23] J. Lammer, K. Malagari, T. Vogl, F. Pilleul, A. Denys, A. Watkinson, M. Pitton, G. Sergent, T. Pfammatter, S. Terraz, Y. Benhamou, Y. Avajon, T. Gruenberger, M. Pomoni, H. Langenberger, M. Schuchmann, J. Dumortier, C. Mueller, P. Chevallier, R. Lencioni, P.V. Investigators, Prospective randomized study of doxorubicin-eluting-bead embolization in the treatment of hepatocellular carcinoma: results of the PRECISION V study, Cardiovasc Intervent Radiol 33(1) (2010) 41-52.

[24] J.L. Raoul, B. Sangro, A. Forner, V. Mazzaferro, F. Piscaglia, L. Bolondi, R. Lencioni, Evolving strategies for the management of intermediate-stage hepatocellular carcinoma: available evidence and expert opinion on the use of transarterial chemoembolization, Cancer Treat Rev 37(3) (2011) 212-20.

[25] M. Varela, M.I. Real, M. Burrel, A. Forner, M. Sala, M. Brunet, C. Ayuso, L. Castells, X. Montana, J.M. Llovet, J. Bruix, Chemoembolization of hepatocellular carcinoma with drug eluting beads: efficacy and doxorubicin pharmacokinetics, J Hepatol 46(3) (2007) 474-81.

[26] T.J. Vogl, J. Lammer, R. Lencioni, K. Malagari, A. Watkinson, F. Pilleul, A. Denys, C. Lee, Liver, gastrointestinal, and cardiac toxicity in intermediate hepatocellular carcinoma treated with PRECISION TACE with drug-eluting beads: results from the PRECISION V randomized trial, AJR Am J Roentgenol 197(4) (2011) W562-70.

[27] M.J. Song, H.J. Chun, D.S. Song, H.Y. Kim, S.H. Yoo, C.H. Park, S.H. Bae, J.Y. Choi, U.I. Chang, J.M. Yang, H.G. Lee, S.K. Yoon, Comparative study between doxorubicin-eluting beads and conventional transarterial chemoembolization for treatment of hepatocellular carcinoma, J Hepatol 57(6) (2012) 1244-50.

[28] Z.B. Xie, X.B. Wang, Y.C. Peng, S.L. Zhu, L. Ma, B.D. Xiang, W.F. Gong, J. Chen, X.M. You, J.H. Jiang, L.Q. Li, J.H. Zhong, Systematic review comparing the safety and efficacy of conventional and drug-eluting bead transarterial chemoembolization for inoperable hepatocellular carcinoma, Hepatol Res 45(2) (2015) 190-200.

[29] J.M. Llovet, S. Ricci, V. Mazzaferro, P. Hilgard, E. Gane, J.F. Blanc, A.C. de Oliveira, A. Santoro, J.L. Raoul, A. Forner, M. Schwartz, C. Porta, S. Zeuzem, L. Bolondi, T.F. Greten, P.R. Galle, J.F. Seitz, I. Borbath, D. Haussinger, T. Giannaris, M. Shan, M. Moscovici, D. Voliotis, J. Bruix, S.I.S. Group, Sorafenib in advanced hepatocellular carcinoma, N Engl J Med 359(4) (2008) 378-90.

[30] I.R. Dubbelboer, E. Lilienberg, E. Ahnfelt, E. Sjogren, N. Axen, H. Lennernas, Treatment of intermediate stage hepatocellular carcinoma: a review of intrahepatic doxorubicin drug-delivery systems, Ther Deliv 5(4) (2014) 447-66.

[31] O. Tacar, P. Sriamornsak, C.R. Dass, Doxorubicin: an update on anticancer molecular action, toxicity and novel drug delivery systems, J Pharm Pharmacol 65(2) (2013) 157-70.

[32] C.L. Olweny, T. Toya, E. Katongole-Mbidde, J. Mugerwa, S.K. Kyalwazi, H. Cohen, Treatment of hepatocellular carcinoma with adriamycin. Preliminary communication, Cancer 36(4) (1975) 1250-7.

[33] J. Namur, S.J. Citron, M.T. Sellers, M.H. Dupuis, M. Wassef, M. Manfait, A. Laurent, Embolization of hepatocellular carcinoma with drug-eluting beads: doxorubicin tissue concentration and distribution in patient liver explants, J Hepatol 55(6) (2011) 1332-8.

[34] L. Weng, H.C. Le, J. Lin, J. Golzarian, Doxorubicin loading and eluting characteristics of bioresorbable hydrogel microspheres: in vitro study, Int J Pharm 409(1-2) (2011) 185-93.

[35] Y. Wang, A. Benzina, D.G. Molin, N. Akker, M. Gagliardi, L.H. Koole, Preparation and structure of drug-carrying biodegradable microspheres designed for transarterial chemoembolization therapy, J Biomater Sci Polym Ed 26(2) (2015) 77-91.

[36] N. Kilcup, E. Tonkopi, R.J. Abraham, D. Boyd, S. Kehoe, Composition-property relationships for radiopaque composite materials: pre-loaded drug-eluting beads for transarterial chemoembolization, J Biomater Appl 30(1) (2015) 93-103.

[37] M.I. Mayer, R.J. Weickum, D.A. Solimando, Jr., B.B. Fileta, M.M. Abdel-Rahim, G.V. Fant, Stability of cisplatin, doxorubicin, and mitomycin combined with loversol for chemoembolization, Ann Pharmacother 35(12) (2001) 1548-51.

[38] F. Chiadmi, J. Daroso, J. Schlatter, S. Cisternino, R. Ratiney, J.E. Fontan, Stability of doxorubicin combined with Radioselectan, a contrast agent, for chemoembolization, J Clin Pharm Ther 30(3) (2005) 255-8.

[39] K.T. Brown, R.K. Do, M. Gonen, A.M. Covey, G.I. Getrajdman, C.T. Sofocleous, W.R. Jarnagin, M.I. D'Angelica, P.J. Allen, J.P. Erinjeri, L.A. Brody, G.P. O'Neill, K.N. Johnson, A.R. Garcia, C. Beattie, B. Zhao, S.B. Solomon, L.H. Schwartz, R. DeMatteo, G.K. Abou-Alfa, Randomized Trial of Hepatic Artery Embolization for Hepatocellular Carcinoma Using Doxorubicin-Eluting Microspheres Compared With Embolization With Microspheres Alone, J Clin Oncol 34(17) (2016) 2046-53.

[40] J. Siepmann, R.A. Siegel, M.J. Rathbone, Controlled Release Society., SpringerLink ebooks - Biomedical and Life Sciences (2012), Fundamentals and applications of controlled release drug delivery, Springer : Controlled Release Society, New York, 2012.

[41] S.A. Padia, G. Shivaram, S. Bastawrous, P. Bhargava, N.J. Vo, S. Vaidya, K. Valji, W.P. Harris, D.S. Hippe, M.J. Kogut, Safety and efficacy of drug-eluting bead chemoembolization for hepatocellular carcinoma: comparison of small-versus medium-size particles, J Vasc Interv Radiol 24(3) (2013) 301-6.

[42] K.T. Brown, Fatal pulmonary complications after arterial embolization with 40-120-micro m tris-acryl gelatin microspheres, J Vasc Interv Radiol 15(2 Pt 1) (2004) 197-200.

[43] C. Spreafico, T. Cascella, A. Facciorusso, C. Sposito, L. Rodolfo, C. Morosi, E.M. Civelli, M. Vaiani, S. Bhoori, A. Pellegrinelli, A. Marchiano, V. Mazzaferro, Transarterial chemoembolization for hepatocellular carcinoma with a new generation of beads: clinical-radiological outcomes and safety profile, Cardiovasc Intervent Radiol 38(1) (2015) 129-34.

[44] A. Gholamrezanezhad, S. Mirpour, J.F. Geschwind, P. Rao, R. Loffroy, O. Pellerin, E.A. Liapi, Evaluation of 70-150-mum doxorubicin-eluting beads for transcatheter arterial chemoembolization in the rabbit liver VX2 tumour model, Eur Radiol 26(10) (2016) 3474-82.

[45] B.C. Odisio, A. Ashton, Y. Yan, W. Wei, A. Kaseb, M.J. Wallace, J.N. Vauthey, S. Gupta, A.L. Tam, Transarterial hepatic chemoembolization with 70-150 microm drug-eluting beads: assessment of clinical safety and liver toxicity profile, J Vasc Interv Radiol 26(7) (2015) 965-71.

[46] J. Namur, M. Wassef, J.M. Millot, A.L. Lewis, M. Manfait, A. Laurent, Drug-eluting beads for liver embolization: concentration of doxorubicin in tissue and in beads in a pig model, J Vasc Interv Radiol 21(2) (2010) 259-67.

[47] K. Ashrafi, Y. Tang, H. Britton, O. Domenge, D. Blino, A.J. Bushby, K. Shuturminska, M. den Hartog, A. Radaelli, A.H. Negussie, A.S. Mikhail, D.L. Woods, V. Krishnasamy, E.B. Levy, B.J. Wood, S.L. Willis, M.R. Dreher, A.L. Lewis, Characterization of a novel intrinsically radiopaque Drug-eluting Bead for image-guided therapy: DC Bead LUMI, J Control Release 250 (2017) 36-47.

[48] E. Blanco, F. Qian, B. Weinberg, N. Stowe, J.M. Anderson, J. Gao, Effect of fibrous capsule formation on doxorubicin distribution in radiofrequency ablated rat livers, J Biomed Mater Res A 69(3) (2004) 398-406.

[49] M. Lubarsky, C. Ray, B. Funaki, Embolization agents-which one should be used when? Part 2: small-vessel embolization, Semin Intervent Radiol 27(1) (2010) 99-104.

[50] M. Potente, H. Gerhardt, P. Carmeliet, Basic and therapeutic aspects of angiogenesis, Cell 146(6) (2011) 873-87.

[51] J.M. Ebos, R.S. Kerbel, Antiangiogenic therapy: impact on invasion, disease progression, and metastasis, Nat Rev Clin Oncol 8(4) (2011) 210-21.

[52] E. Sueyoshi, T. Hayashida, I. Sakamoto, M. Uetani, Vascular complications of hepatic artery after transcatheter arterial chemoembolization in patients with hepatocellular carcinoma, AJR Am J Roentgenol 195(1) (2010) 245-51.

[53] S. Ohta, N. Nitta, A. Sonoda, A. Seko, T. Tanaka, R. Takazakura, A. Furukawa, M. Takahashi, T. Sakamoto, Y. Tabata, K. Murata, Embolization materials made of gelatin: comparison between Gelpart and gelatin microspheres, Cardiovasc Intervent Radiol 33(1) (2010) 120-6.

[54] T.D. Kirchhoff, J.S. Bleck, A. Dettmer, A. Chavan, H. Rosenthal, S. Merkesdal, B. Frericks, L. Zender, N.P. Malek, T.F. Greten, S. Kubicka, M.P. Manns, M. Galanski, Transarterial chemoembolization using degradable starch microspheres and iodized oil in the treatment of advanced hepatocellular carcinoma: evaluation of tumor response, toxicity, and survival, Hepatobiliary Pancreat Dis Int 6(3) (2007) 259-66.

[55] S. Ohta, N. Nitta, S. Watanabe, Y. Tomozawa, A. Sonoda, H. Otani, K. Tsuchiya, A. Nitta-Seko, A. Yamamoto, M. Takahashi, K. Murata, Gelatin microspheres: correlation between embolic effect/degradability and cross-linkage/particle size, Cardiovasc Intervent Radiol 36(4) (2013) 1105-11.

[56] Y. Shomura, N. Tanigawa, M. Shibutani, S. Wakimoto, K. Tsuji, T. Tokuda, J. Terada, S. Kariya, H. Kojima, A. Komemushi, S. Sawada, Water-soluble polyvinyl alcohol microspheres for temporary embolization: development and in vivo characteristics in a pig kidney model, J Vasc Interv Radiol 22(2) (2011) 212-9.

[57] A. Schwarz, H. Zhang, A. Metcalfe, I. Salazkin, J. Raymond, Transcatheter embolization using degradable crosslinked hydrogels, Biomaterials 25(21) (2004) 5209-15.

[58] B.K. Kwak, H.J. Shim, S.M. Han, E.S. Park, Chitin-based embolic materials in the renal artery of rabbits: pathologic evaluation of an absorbable particulate agent, Radiology 236(1) (2005) 151-8.

[59] R.J. Owen, P.N. Nation, R. Polakowski, J.A. Biliske, P.B. Tiege, I.J. Griffith, A preclinical study of the safety and efficacy of Occlusin 500 Artificial Embolization Device in sheep, Cardiovasc Intervent Radiol 35(3) (2012) 636-44.

[60] O. Jordan, A. Denys, T. De Baere, N. Boulens, E. Doelker, Comparative study of chemoembolization loadable beads: in vitro drug release and physical properties of DC bead and hepasphere loaded with doxorubicin and irinotecan, J Vasc Interv Radiol 21(7) (2010) 1084-90.

[61] S. Louguet, V. Verret, L. Bedouet, E. Servais, F. Pascale, M. Wassef, D. Labarre, A. Laurent, L. Moine, Poly(ethylene glycol) methacrylate hydrolyzable microspheres for transient vascular embolization, Acta Biomater 10(3) (2014) 1194-205.

[62] L. Bedouet, V. Verret, S. Louguet, E. Servais, F. Pascale, A. Beilvert, M.T. Baylatry, D. Labarre, L. Moine, A. Laurent, Anti-angiogenic drug delivery from hydrophilic resorbable embolization microspheres: an in vitro study with sunitinib and bevacizumab, Int J Pharm 484(1-2) (2015) 218-27.

[63] N. Maeda, V. Verret, L. Moine, L. Bedouet, S. Louguet, E. Servais, K. Osuga, N. Tomiyama, M. Wassef, A. Laurent, Targeting and recanalization after embolization with calibrated resorbable microspheres versus hand-cut gelatin sponge particles in a porcine kidney model, J Vasc Interv Radiol 24(9) (2013) 1391-8.

[64] J.E. Bergsma, W.C. de Bruijn, F.R. Rozema, R.R. Bos, G. Boering, Late degradation tissue response to poly(L-lactide) bone plates and screws, Biomaterials 16(1) (1995) 25-31.

[65] L. Bedouet, F. Pascale, L. Moine, M. Wassef, S.H. Ghegediban, V.N. Nguyen, M. Bonneau, D. Labarre, A. Laurent, Intra-articular fate of degradable poly(ethyleneglycol)-hydrogel microspheres as carriers for sustained drug delivery, Int J Pharm 456(2) (2013) 536-44.

[66] L. Weng, D. Seelig, P. Rostamzadeh, J. Golzarian, Calibrated Bioresorbable Microspheres as an Embolic Agent: An Experimental Study in a Rabbit Renal Model, J Vasc Interv Radiol 26(12) (2015) 1887-94 e1.

[67] L. Weng, P. Rostamzadeh, N. Nooryshokry, H.C. Le, J. Golzarian, In vitro and in vivo evaluation of biodegradable embolic microspheres with tunable anticancer drug release, Acta Biomater 9(6) (2013) 6823-33.

[68] L. Weng, H.J. Tseng, P. Rostamzadeh, J. Golzarian, In vitro comparative study of drug loading and delivery properties of bioresorbable microspheres and LC bead, J Mater Sci Mater Med 27(12) (2016) 174.

[69] J.W. Choi, J.H. Park, S.Y. Baek, D.D. Kim, H.C. Kim, H.J. Cho, Doxorubicin-loaded poly(lactic-co-glycolic acid) microspheres prepared using the solid-in-oil-in-water method for the transarterial chemoembolization of a liver tumor, Colloids Surf B Biointerfaces 132 (2015) 305-12.

[70] J. Chen, S.B. White, K.R. Harris, W. Li, J.W. Yap, D.H. Kim, R.J. Lewandowski, L.D. Shea, A.C. Larson, Poly(lactide-co-glycolide) microspheres for MRI-monitored delivery of sorafenib in a rabbit VX2 model, Biomaterials 61 (2015) 299-306.

[71] J. Doucet, L. Kiri, K. O'Connell, S. Kehoe, R.J. Lewandowski, D.M. Liu, R.J. Abraham, D. Boyd, Advances in Degradable Embolic Microspheres: A State of the Art Review, J Funct Biomater 9(1) (2018).

[72] A. Momeni, E.M. Valliant, E.P. Brennan-Pierce, J.J.S. Shankar, R. Abraham, P. Colp, M.J. Filiaggi, Developing an in situ forming polyphosphate coacervate as a new liquid embolic agent: From experimental design to pilot animal study, Acta Biomaterialia 32 (2016) 286-297.

[73] A. Momeni, M.J. Filiaggi, Rheology of polyphosphate coacervates, J Rheol 60(1) (2016) 25-34.

[74] A. Momeni, M.J. Filiaggi, Degradation and hemostatic properties of polyphosphate coacervates, Acta Biomaterialia 41 (2016) 328-341.

[75] D. Bhopatkar, A.K. Anal, W.F. Stevens, Ionotropic alginate beads for controlled intestinal protein delivery: Effect of chitosan and barium counter-ions on entrapment and release, Journal of Microencapsulation 22(1) (2005) 91-100.

[76] M.J. Filiaggi, A. Momeni, Polyphosphate Glass Microspheres, Methods of Making and Uses Thereof, 2017.

[77] V. Nilles, J. Plank, Study of the retarding mechanism of linear sodium polyphosphates on alpha-calcium sulfate hemihydrate, Cement Concrete Res 42(5) (2012) 736-744.

[78] S. Awasthi, R. Sharma, Y.C. Awasthi, J.A. Belli, E.P. Frenkel, The relationship of doxorubicin binding to membrane lipids with drug resistance, Cancer Lett 63(2) (1992) 109-16.

[79] D.M. Pickup, R.J. Newport, E.R. Barney, J.Y. Kim, S.P. Valappil, J.C. Knowles, Characterisation of phosphate coacervates for potential biomedical applications, Journal of Biomaterials Applications 28(8) (2014) 1226-1234.

[80] A. Jablonska-Trypuc, G. Swiderski, R. Kretowski, W. Lewandowski, Newly Synthesized Doxorubicin Complexes with Selected Metals-Synthesis, Structure and Anti-Breast Cancer Activity, Molecules 22(7) (2017).

[81] N.A. Peppas, J.J. Sahlin, A Simple Equation for the Description of Solute Release .3. Coupling of Diffusion and Relaxation, Int J Pharmaceut 57(2) (1989) 169-172.

[82] E. Munnier, F. Tewes, S. Cohen-Jonathan, C. Linassier, L. Douziech-Eyrolles, H. Marchais, M. Souce, K. Herve, P. Dubois, I. Chourpa, On the interaction of doxorubicin with oleate ions: fluorescence spectroscopy and liquid-liquid extraction study, Chem Pharm Bull (Tokyo) 55(7) (2007) 1006-10.

[83] A. Lee, G.M. Whitesides, Analysis of Inorganic Polyphosphates by Capillary Gel Electrophoresis, Analytical Chemistry 82(16) (2010) 6838-6846.

[84] C.H. Bamford, C.F.H. Tipper, Degradation of polymers, Elsevier Scientific Pub. Co., Amsterdam ; New York, 1975.

[85] O. Warburg, F. Wind, E. Negelein, The Metabolism of Tumors in the Body, J Gen Physiol 8(6) (1927) 519-30.

[86] J.L. Wike-Hooley, A.P. van den Berg, J. van der Zee, H.S. Reinhold, Human tumour pH and its variation, Eur J Cancer Clin Oncol 21(7) (1985) 785-91.

[87] P.W. Hochachka, T.P. Mommsen, Protons and anaerobiosis, Science 219(4591) (1983) 1391-7.

[88] V. Menkin, Biochemical Mechanisms in Inflammation, Br Med J 1(5185) (1960) 1521-8.

[89] D.K. Reyes, J.A. Vossen, I.R. Kamel, N.S. Azad, T.A. Wahlin, M.S. Torbenson, M.A. Choti, J.F. Geschwind, Single-center phase II trial of transarterial chemoembolization with drug-eluting beads for patients with unresectable hepatocellular carcinoma: initial experience in the United States, Cancer J 15(6) (2009) 526-32.

[90] T. Alfrey, E.F. Gurnee, W.G. Lloyd, Diffusion in Glassy Polymers, J Polym Sci Pol Sym (12pc) (1966) 249-256.

[91] D.J. Enscore, H.B. Hopfenberg, V.T. Stannett, Effect of Particle-Size on Mechanism Controlling Normal-Hexane Sorption in Glassy Polystyrene Microspheres, Polymer 18(8) (1977) 793-800.

[92] T.L. Riss, R.A. Moravec, A.L. Niles, S. Duellman, H.A. Benink, T.J. Worzella, L. Minor, Cell Viability Assays, in: G.S. Sittampalam, N.P. Coussens, K. Brimacombe, A. Grossman, M. Arkin, D. Auld, C. Austin, J. Baell, B. Bejcek, T.D.Y. Chung, J.L. Dahlin, V. Devanaryan, T.L. Foley, M. Glicksman, M.D. Hall, J.V. Hass, J. Inglese, P.W. Iversen, S.D. Kahl, S.C. Kales, M. Lal-Nag, Z. Li, J. McGee, O. McManus, T. Riss, O.J. Trask, Jr., J.R. Weidner, M. Xia, X. Xu (Eds.), Assay Guidance Manual, Bethesda (MD), 2004.

[93] O.S. Bains, A. Szeitz, J.M. Lubieniecka, G.E. Cragg, T.A. Grigliatti, K.W. Riggs, R.E. Reid, A correlation between cytotoxicity and reductase-mediated metabolism in cell lines treated with doxorubicin and daunorubicin, J Pharmacol Exp Ther 347(2) (2013) 375-87.

[94] E. Monti, L. Paracchini, F. Piccinini, V. Malatesta, F. Morazzoni, R. Supino, Cardiotoxicity and antitumor activity of a copper(II)-doxorubicin chelate, Cancer Chemother Pharmacol 25(5) (1990) 333-6.

[95] M.J. Wood, W.J. Irwin, D.K. Scott, Photodegradation of doxorubicin, daunorubicin and epirubicin measured by high-performance liquid chromatography, J Clin Pharm Ther 15(4) (1990) 291-300.

[96] M.J.H. Janssen, D.J.A. Crommelin, G. Storm, A. Hulshoff, Doxorubicin Decomposition on Storage - Effect of Ph, Type of Buffer and Liposome Encapsulation, Int J Pharmaceut 23(1) (1985) 1-11.

[97] J.H. Beijnen, O.A.G.J. Vanderhouwen, W.J.M. Underberg, Aspects of the Degradation Kinetics of Doxorubicin in Aqueous-Solution, Int J Pharmaceut 32(2-3) (1986) 123-131.

[98] J.H. Beijnen, G. Wiese, W.J. Underberg, Aspects of the chemical stability of doxorubicin and seven other anthracyclines in acidic solution, Pharm Weekbl Sci 7(3) (1985) 109-16.

[99] K. Wassermann, Bundgaard, H., Kinetics of the acid-catalyzed hydrolysis of doxorubicin, Int J Pharmaceut 14 (1983) 73-78.

[100] T.T. Nguyen, Y.J. Lim, M.H. Fan, R.A. Jackson, K.K. Lim, W.H. Ang, K.H. Ban, E.S. Chen, Calcium modulation of doxorubicin cytotoxicity in yeast and human cells, Genes Cells 21(3) (2016) 226-40.

[101] R. Seth, S. Yang, S. Choi, M. Sabean, E.A. Roberts, In vitro assessment of copper-induced toxicity in the human hepatoma line, Hep G2, Toxicol In Vitro 18(4) (2004) 501-9.

[102] J.P. Piret, D. Jacques, J.N. Audinot, J. Mejia, E. Boilan, F. Noel, M. Fransolet, C. Demazy, S. Lucas, C. Saout, O. Toussaint, Copper(II) oxide nanoparticles penetrate into HepG2 cells, exert cytotoxicity via oxidative stress and induce pro-inflammatory response, Nanoscale 4(22) (2012) 7168-84.

[103] A. Yamamoto, R. Honma, M. Sumita, Cytotoxicity evaluation of 43 metal salts using murine fibroblasts and osteoblastic cells, J Biomed Mater Res 39(2) (1998) 331-40.

[104] J.L. Pariente, L. Bordenave, R. Bareille, C. Ohayon-Courtes, C. Baquey, M. Le Guillou, In vitro cytocompatibility of radio-opacifiers used in ureteral endoprosthesis, Biomaterials 20(6) (1999) 523-7.

[105] B. Kopp, D. Zalko, M. Audebert, Genotoxicity of 11 heavy metals detected as food contaminants in two human cell lines, Environ Mol Mutagen 59(3) (2018) 202-210.

[106] H. Tao, Y. Man, X. Shi, J. Zhu, H. Pan, Q. Qin, S. Liu, Inconceivable Hypokalemia: A Case Report of Acute Severe Barium Chloride Poisoning, Case Rep Med 2016 (2016) 2743134.

[107] M. Matsuura, M. Inamori, A. Nakajima, Y. Komiya, Y. Inoh, K. Kawasima, M. Naitoh, Y. Fujita, A. Eduka, N. Kanazawa, S. Uchiyama, R. Tani, K. Kawana, S. Ohtani, H. Nagase, Effectiveness of therapeutic barium enema for diverticular hemorrhage, World J Gastroenterol 21(18) (2015) 5555-9.

[108] M. Syed, C. Skonberg, S.H. Hansen, Effect of some organic solvents on oxidative phosphorylation in rat liver mitochondria: Choice of organic solvents, Toxicol In Vitro 27(8) (2013) 2135-41.

[109] G. Ellison, J.V. Straumfjord, Jr., J.P. Hummel, Buffer capacities of human blood and plasma, Clin Chem 4(6) (1958) 452-61.

[110] B.E. Kim, T. Nevitt, D.J. Thiele, Mechanisms for copper acquisition, distribution and regulation, Nat Chem Biol 4(3) (2008) 176-85.

[111] D. Denoyer, S. Masaldan, S. La Fontaine, M.A. Cater, Targeting copper in cancer therapy: 'Copper That Cancer', Metallomics 7(11) (2015) 1459-76.

[112] G.F. Hu, Copper stimulates proliferation of human endothelial cells under culture, J Cell Biochem 69(3) (1998) 326-35.

[113] G. Khan, S. Merajver, Copper chelation in cancer therapy using tetrathiomolybdate: an evolving paradigm, Expert Opin Investig Drugs 18(4) (2009) 541-8.

[114] B.S. Bhoelan, C.H. Stevering, A.T. van der Boog, M.A. van der Heyden, Barium toxicity and the role of the potassium inward rectifier current, Clin Toxicol (Phila) 52(6) (2014) 584-93.

[115] D. Newton, G.E. Harrison, C. Kang, A.J. Warner, Metabolism of injected barium in six healthy men, Health Phys 61(2) (1991) 191-201.

[116] I.O.f. Standardization, Biological evaluation of Medical devices, Tests for *in vitro* cytotoxicity, IHS, Switzerland, 2009.

Appendix A: Coacervates and Water Content

This appendix describes studies to assess the nature of the water associated with coacervates in order to better understand the impact of freeze drying procedures required for drug loading.

Materials and Methods

Coacervate was analyzed with thermogravimetry/differential scanning calorimetry (TGA-DSC) to confirm the presence of two levels of water in its matrix, as described by Pickup et al [79]. 1mL of Barry coacervate was synthesized, as described in section 3.2.2. The coacervate was transferred into a capless vial, and placed in a desiccator for a period of 24 hours to allow for some of the superficial water to evaporate, as described by Pickup et al [79]. 32.2mg of coacervate was then transferred into a platinum/rhodium (90%Pt/10%Rh) crucible, and analyzed with TGA-DSC. The temperature was increased 10°C/min, from 25°C to 900°C.

Results and Discussion

TGA revealed two distinct phases of mass loss, the first occurring at approximately 100°C, and the second around approximately 200°C (Figure A.1). DSC showed corresponding endothermic peaks at these temperatures. These results indicate that two distinct levels of water in coacervate. Water that was loosely associated with the polymer matrix evaporated easily at 100°C. Structural water was more tightly associated with the coacervate matrix, and remained bound until a temperature of approximately 200°C, at which time it also evaporated.

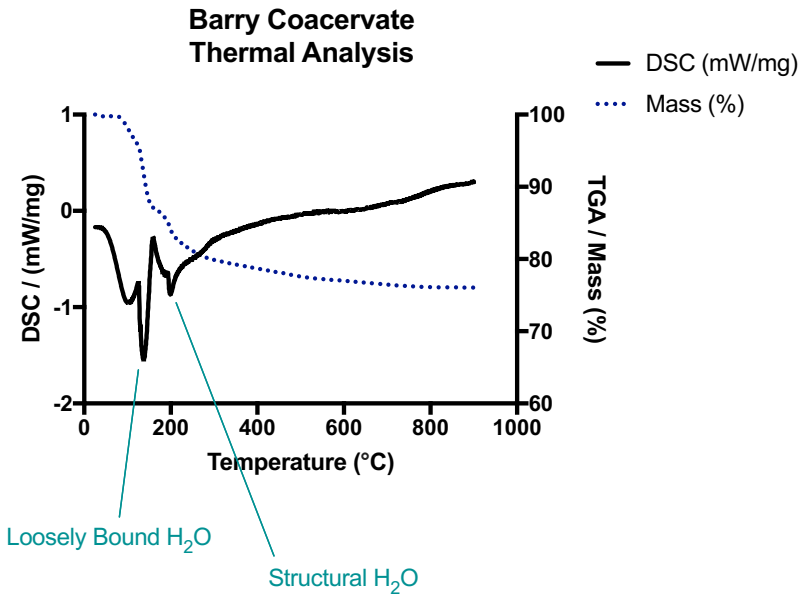

Figure A.1 TGA-DSC analysis of Barry coacervate. DSC data is plotted on the left Y-axis (mW/mg) in the solid black line. TGA is plotted on the right Y-axis (Mass %), in the dotted blue line.

Appendix B: Cu-DOX Complexing

This appendix is included to demonstrate the importance of adjusting the pH of elution media before measuring the DOX concentration of the sample. Cu^{2+} is known to form complexes with DOX at neutral pH, altering the 480nm absorbance of the sample; decreasing the pH is known to dissociate these complexes [80].

Materials and Methods

50μM and 5μM DOX solutions were prepared at pH 7.4 (0.1M TBS) and pH 6.5 (0.1M ACES). A 1M Cu^{2+} solution was prepared in ddH_2O from $CuCl_2{\cdot}(H_2O)_2$ (Alfa Aesar). Each DOX solution was divided into 4 aliquots of 2mL. Volumes of 1M Cu^{2+}, 1M HCl, and additional buffer (TBS or ACES) were added as described in Table B.1 to create solutions with 0, 100:1, and 1000:1 Cu^{2+}: DOX molar ratios at pH 7.4, 6.5 and 2. All TBS solutions had a final volume of 2.043μL. All ACES solutions had a final volume of 2.075μL. pH was measured using an Accumet AB 15/15+ bench-top pH meter (Fisher Scientific). The 480nm absorbance of each sample was measured as described in section 3.2.3. Absorbance measurements were analyzed to determine if decreasing the pH of the solution to 2 was sufficient to dissociate Cu^{2+}-DOX complexes and restore the 480nm absorbance to that of DOX with no Cu^{2+} in solution. Differences were analyzed statistically using one-way ANOVAs, with Bonferroni multiple comparisons testing. The threshold for significance was $p < 0.05$.

Results and Discussion

At pH 6.5 and 7.4, the presence of Cu^{2+} significantly altered the 480nm absorbance of the solution (Figure B.1). With 5μM DOX, the presence of Cu^{2+} increased the 480nm absorbance; this is the result of the tail end of the Cu^{2+}-DOX complex, which peaks at 577nm [80]. With 50μM DOX, Cu^{2+} decreased the 480nm absorbance of the solution. This decrease was caused by the shift in the peak absorbance to 577nm; at the higher concentration of DOX the initial absorbance at 480nm is greater than the tail of the 577nm Cu^{2+}-DOX peak [80]. In all cases, decreasing the pH of the solution to 2 restored the absorbance to values measured without Cu^{2+} in solution. No significant differences were

found between DOX pH 2 and Cu:DOX pH 2 samples. These results prove that decreasing the pH of elution media to 2 was sufficient to reliably measure the concentration of DOX in solution.

Table B.1 Volumes added to 2mL aliquots of DOX solutions.

Sample Number	Buffer	[DOX] (μM)	Volume 1M Cu^{2+} (μL)	Volume 1M HCl (μL)	Volume Buffer (μL)	Cu:DOX Molar Ratio	pH
1	TBS	50	0	0	43	0	7.4
2	TBS	5	0	0	43	0	7.4
3	TBS	50	0	33	10	0	2
4	TBS	5	0	33	10	0	2
5	TBS	50	10	0	33	100:1	7.4
6	TBS	50	10	33	0	100:1	2
7	TBS	5	10	0	33	1000:1	7.4
8	TBS	5	10	33	0	1000:1	2
9	ACES	50	0	0	75	0	6.5
10	ACES	5	0	0	75	0	6.5
11	ACES	50	0	65	10	0	2
12	ACES	5	0	65	10	0	2
13	ACES	50	10	0	65	100:1	6.5
14	ACES	50	10	65	0	100:1	2
15	ACES	5	10	0	65	1000:1	6.5
16	ACES	5	10	65	0	1000:1	2

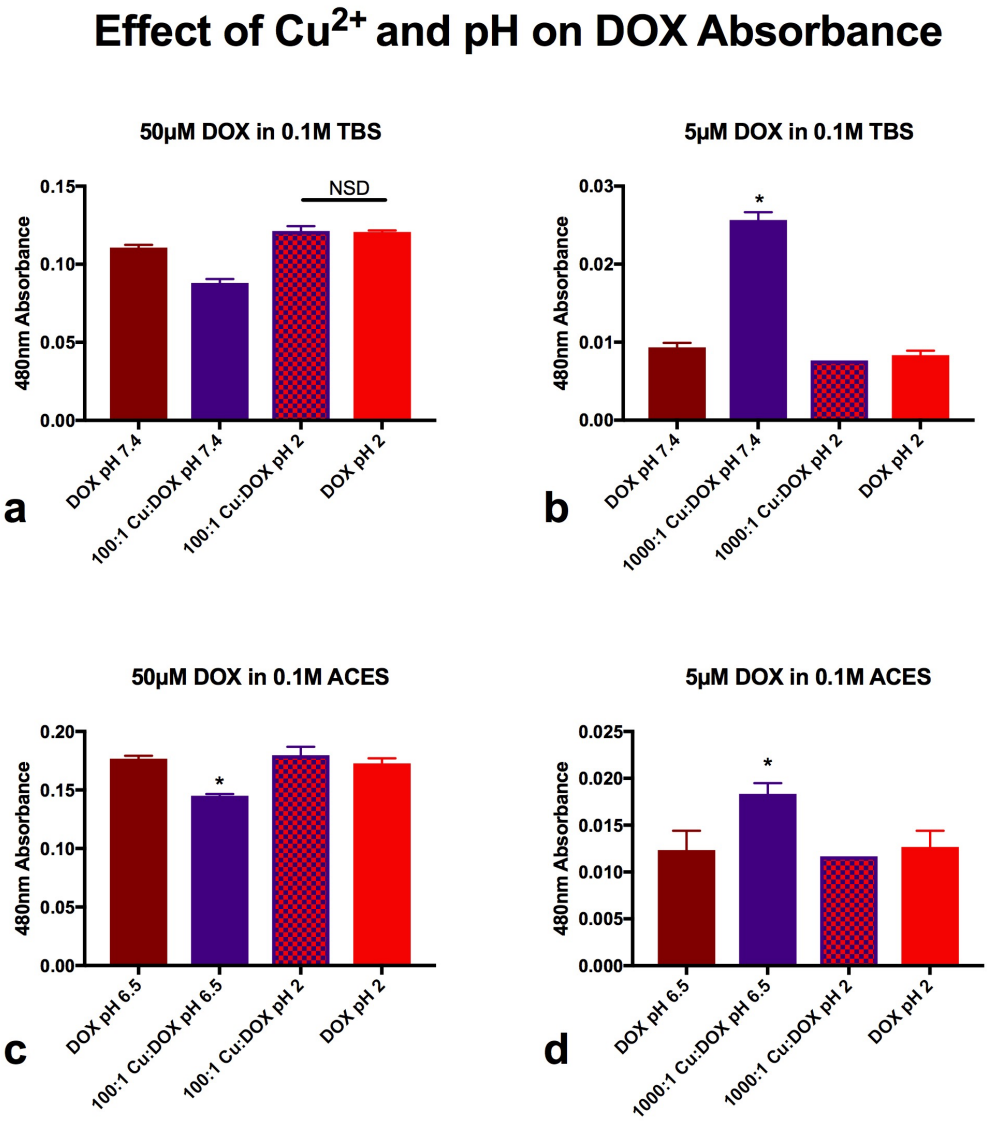

Figure B.1 The impact of Cu^{2+} and pH on DOX absorbance solutions were prepared as described in Table 8.1, average 480nm absorbance was plotted with error bars representing standard deviation (n = 3). (a) "NSD" indicates the only non-significant difference between 2 groups ($p < 0.05$). (b-d) * indicates one group that significantly differed from all other groups ($p < 0.05$).

Appendix C: DOX Chromophore Stability

A preliminary study was conducted to verify the short-term stability of DOX in 2% HCl solutions. This acidity was needed to dissociate Cu^{2+}-DOX complexes, and so it was critical to verify that DOX would not be degraded under these conditions.

Materials and Methods

10mg of DOX was dissolved in 100mL ddH_2O to yield a 0.1mg/mL solution that was then serial diluted to concentrations of 0.05mg/mL, 0.01mg/mL, and 0.001mg/mL. 10mL aliquots of each solution were taken. 200µL of 12M HCl was added to each solution, and the 480nm absorbance was measured immediately, as described in section 3.2.3. The absorbance was then measured again 1 hour, 2.5 hours, and 24 hours thereafter to determine the rate of DOX chromophore degradation.

Results and Discussion

DOX degraded minimally over the time points measured (Figure C.1). The greatest degradation occurred in the 0.001mg/mL solution, which lost 31.6 ± 11.7% of its concentration after 24 hours. The most experimentally relevant time point was 1 hour, as all DOX absorbance measurements were taken within approximately 30 minutes of sample acidification in all reported experiments. After 1 hour, the 0.001mg/mL sample lost 15.8 ± 16.4% of its concentration. The incredibly high standard deviation in these measurements was attributed to proximity to the detection limit of the instrument. All other samples showed negligible degradation over these time points. Taking into account the high variability in this measurement and the negligible degradation observed at the other concentrations, it was determined that acidifying DOX samples using this method was an appropriate for DOX elution studies.

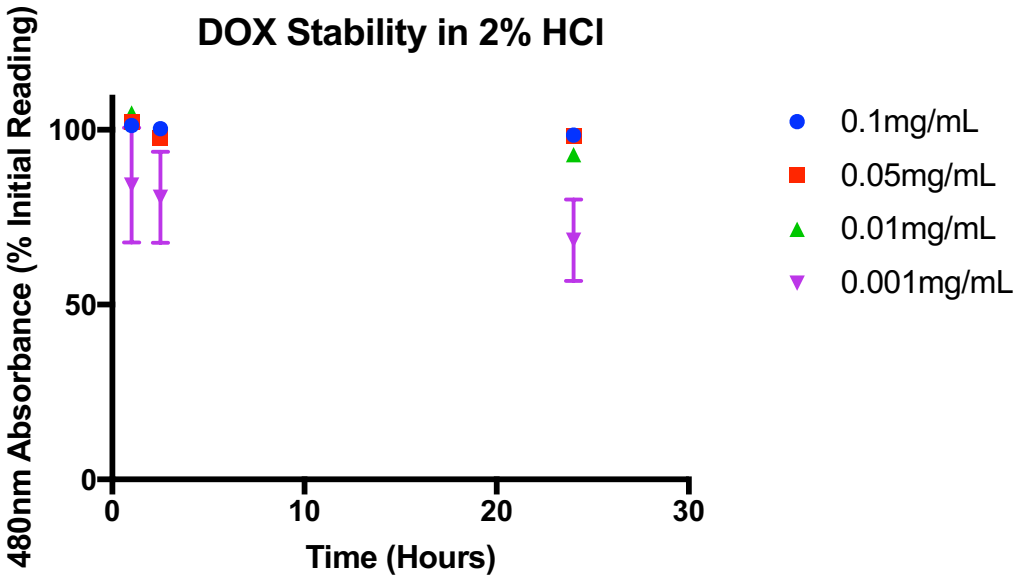

Figure C.1 480nm absorbance readings of acidified DOX standard solutions, expressed as a percentage of the initial absorbance reading of the sample. Error bars represent standard deviation (n = 3).

Appendix D: pH-Mediated DOX Release (Protocol Development)

A preliminary elution study was conducted to establish a protocol for degradation/elution studies. The volume of elution media was a variable under consideration. The volume needed to be larger enough to provide sink conditions, and provide a sufficient buffering capacity to maintain constant pH. 5mL of elution media was chosen in this initial attempt, but was found in retrospect not to provide sufficient buffering capacity. The results of this preliminary elution study are included in support of the proposed mechanisms of DOX release in section 4.3.

Materials and Methods

1% DOX Calvin PGMs were synthesized as described in section 3.2. A degradation study was performed, as described in section 4.2. Four different elution media were used in this study: 0.1M tris (pH 7.4), 0.1M TBS (pH 7.4), 0.1M ACES (pH 6.5), 0.1M ABS (pH 6.5). 5mL of elution media was used, and was refreshed at 4 hours, 1 day, 3 days, 7 days, 14 days, 21 days, and 28 days. At each time point, the elution media was analyzed for DOX concentration and pH, as described in section 4.2.

Results and Discussion

The results of this elution study support the conclusions made in chapter 4. When acidic degradation products overwhelmed the buffering capacity of tris and TBS, DOX was released (Figure D.1a). In fact, the release of DOX was proportional to the acidity of the media. In ACES and ABS, the buffering capacity was overwhelmed to a lesser extent, and so minimal deviation from the expected linear release profile was observed (Figure D.1b). Overall, these results strongly support the theory that DOX release is dependent on the pH of the elution media.

Additionally, the theory surrounding the impact of elution media osmolarity was supported. With both buffers, more DOX was released in elution media that did not contain NaCl (Figure D.1).

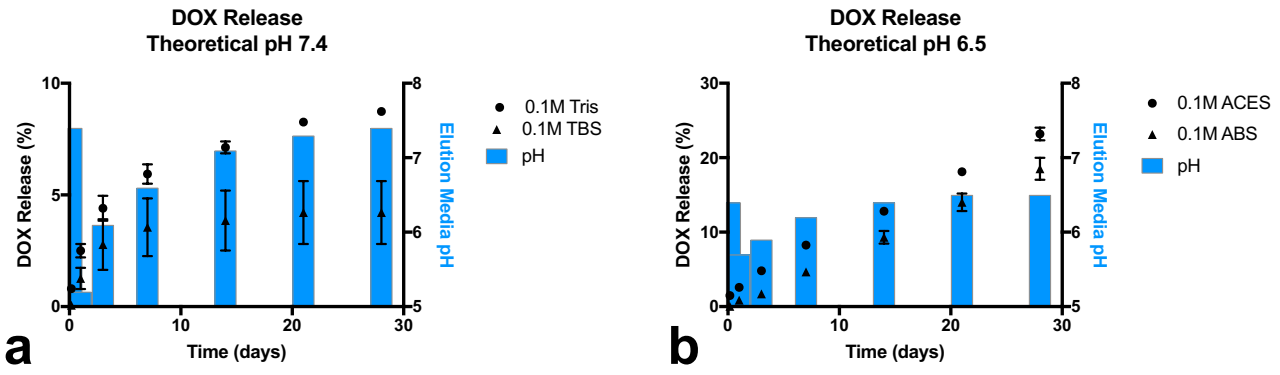

Figure D.1 Cumulative DOX release from 1% DOX Calvin PGMs. PGMs were degraded in 5mL of elution media at theoretical pH values of 7.4(a), and 6.5(b). The cumulative release of DOX is plotted on the left y-axis (black points), with error bars representing standard deviations (n = 3). The average pH of the elution media was plotted on the right y-axis (blue bars).